BOND CHARACTERISTICS
OF
EPOXY COATED REINFORCING BARS

by

David W. Johnston and Paul Zia

Technical Report Documentation Page

1. Report No.	2. Government Accession No.	3. Recipient's Catalog No.
FHWA/NC/82-002		

4. Title and Subtitle	5. Report Date
"BOND CHARACTERISTICS OF EPOXY COATED REINFORCING BARS"	August, 1982
	6. Performing Organization Code
7. Author(s)	8. Performing Organization Report No.
David W. Johnston and Paul Zia	ERSD 110-79-4
9. Performing Organization Name and Address	10. Work Unit No. (TRAIS)
Center for Transportation Engineering Studies Department of Civil Engineering North Carolina State University Raleigh, North Carolina 27650	11. Contract or Grant No. HRP 79-4
	13. Type of Report and Period Covered
12. Sponsoring Agency Name and Address North Carolina Department of Transportation Raleigh, North Carolina and Federal Highway Administration Raleigh, North Carolina	Final Report
	14. Sponsoring Agency Code

15. Supplementary Notes

16. Abstract

The objective of this study was to evaluate the flexural bond characteristics of epoxy coated reinforcing bars in comparison to uncoated bars under static and fatigue loadings.

Comparative tests were conducted between reinforcing bars with epoxy coated, normal mill scale and blast cleaned surface conditions. Both #6 and #11 bars were included. Forty flexural bond specimens of the beam end type were tested in static and fatigue loadings. Three embedment lengths were used in the tests. In addition, six slab specimens were tested to evaluate the effect of epoxy coating on concrete crack spacing and crack width.

Behavior is assessed in terms of influence on crack spacing, crack width, bond strength and bond fatigue. Suggestions for design criteria modification are proposed.

17. Key Words	18. Distribution Statement
Reinforced concrete, epoxy coated rebars, bond, development, bond fatigue, cracking, fatigue	Unlimited

19. Security Classif. (of this report)	20. Security Classif. (of this page)	21. No. of Pages	22. Price
None	None	176	

Form DOT F 1700.7 (8-72) Reproduction of completed page authorized

BOND CHARACTERISTICS OF EPOXY COATED REINFORCING BARS

By

David W. Johnston
Associate Professor

and

Paul Zia
Professor and Head
Department of Civil Engineering

Research Project ERSD-110-79-4

Final Report

in cooperation with
North Carolina Department of Transportation
and
The United States Department of Transportation
Federal Highway Administration

CENTER FOR TRANSPORTATION ENGINEERING STUDIES
Department of Civil Engineering
North Carolina State University at Raleigh

August 1982

The contents of this report reflect the views of the authors who are responsible for the facts and the accuracy of the data presented herein. The contents do not necessarily reflect the official views or policies of the North Carolina Department of Transportation or the Federal Highway Administration. This report does not constitute a standard, specification or regulation.

ABSTRACT

The objective of this study was to evaluate the flexural bond characteristics of epoxy coated reinforcing bars in comparison to uncoated bars under static and fatigue loadings.

Comparative tests were conducted between reinforcing bars with epoxy coated, normal mill scale and blast cleaned surface conditions. Both #6 and #11 bars were included. Forty flexural bond specimens of the beam end type were tested in static and fatigue loadings. Three embedment lengths were used in the tests. In addition, six slab specimens were tested to evaluate the effect of epoxy coating on concrete crack spacing and crack width.

Behavior is assessed in terms of influence on crack spacing, crack width, bond strength and bond fatigue. Suggestions for design criteria modification are proposed.

ACKNOWLEDGMENTS

The research documented in this report has been sponsored by the North Carolina State Department of Transportation and Highway Safety in cooperation with the United States Department of Transportation, Federal Highway Administration.

A technical liaison committee including Mr. Landis Temple and Mr. Pat Strong of the North Carolina Department of Transportation and Mr. Devohn Rhame of the Federal Highway Administration coordinated the research project. The area of investigation was originally suggested by Mr. Craig A. Ballinger of the Federal Highway Administration.

Several industry suppliers generously provided materials used in fabrication of test specimens for the project. These included Rosson-Richards Corp., Florida Steel Corp., Lone Star Cement Corp., Arnold Stone Co., Master Builders, Inc., and Dayton Sure Grip and Shore Corp. Valuable advice on concrete materials was provided by Mr. Ken Hall, formerly of Materials and Test Unit, NCDOT.

Able assistance was provided by Mr. Habib Akbar and Mr. Ping-Lang Sue, Graduate Research Assistants in the Department of Civil Engineering.

All of the above have been most helpful in the formulation, guidance and conduct of the research reported herein. Thanks are also due to Dr. W. G. Mullen, Coordinator of the Highway Research Program under which the study was originally initiated.

TABLE OF CONTENTS

TABLE OF CONTENTS (cont.)

LIST OF FIGURES

LIST OF TABLES

LIST OF SYMBOLS

b = width of concrete section, in.

cr = subscript indicating cracking

d = depth to tension reinforcement, in.

d_b = diameter of the reinforcing bar, in.

f'_c = compressive strength of concrete, psi.

f_f = fatigue stress range, ksi.

f_{min} = algebraic minimum fatigue stress level, tension positive, compression negative, ksi.

f_s = stress in reinforcing bar, psi

f_{su} = rupture stress of steel reinforcement, psi

f_y = yield stress of tension reinforcement, ksi

f_{yt} = yield stress of transverse reinforcement, psi

h = height of rolled on transverse deformation, in.

ℓ_d = required development length, in.

ℓ_{db} = basic development length, in.

r = base radius of rolled on deformation, in.

s = spacing of transverse reinforcement, in.

u = subscript indicating ultimate failure

A_b = area of an individual bar, in.^{2}

A_{tr} = area of transverse reinforcement crossing plane of splitting, in.^{2}

B = subscript or superscript indicating blast cleaned specimen

C = concrete compression force, kips

C_c = thickness of concrete cover measured from extreme tension fiber to center of bar, in.

C_s = the smaller of the cover to the center of bar measured along a line through the layer of bars or half the center to center distance of bars in the layer, in.

E = subscript or superscript indicating epoxy coated specimen

E_g = modulus of elasticity of steel reinforcing, psi.

K = smaller of $C_c + K_{tr}$ or $C_s + K_{tr}$ but $K \leq 3d_b$, in.

K_{tr} = $A_{tr} f_{yt} / 1500\ s$ but $K_{tr} \leq d_b$, in.

L = length of embedment, in.

M = subscript of superscript indicating mill scale specimen

M_n = calculated nominal moment capacity, ft-k.

P = deck slab load, kips

P_{mn} = deck slab load corresponding to calculated nominal moment capacity, kips

P_{vn} = deck slab load corresponding to calculated nominal shear capacity, kips

R, R_v = reaction force, kips

T = tensile force applied to the reinforcing bar, kips.

V = shear force, kips.

V_c = calculated shear capacity contributed by the concrete, kips.

V_n = calculated nominal shear capacity, kips

δ = slip of the reinforcing bar, in.

ϕ = capacity reduction factor

Σ_o = sum of the perimeters of the reinforcing bars, in.

μ = average bond stress, psi.

1. INTRODUCTION

1.1 Background

The use of epoxy coated reinforcement has increased rapidly in recent years as a means of combating corrosion. Applications have included reinforcement in concrete bridge decks and parking deck slabs where corrosion problems have been encountered due to use of deicing salts. In these cases, No. 5 and No. 6 bars have seen the most widespread use. However, bar sizes 3 through 11 are being epoxy coated and used for virtually all reinforcement in some bridges located in marine environments. It has been estimated that over 100 million pounds of reinforcing bar have been coated between 1975 and 1980.

In order to investigate the possibilities of a nonmetallic coating for reinforcing bars, the Federal Highway Administration sponsored research by Clifton, Beeghly and Mathey (1) at the National Bureau of Standards. The research involved 47 different coating materials of which 36 were epoxies. Evaluation of the coatings was based upon chemical resistance, cured coating film integrity, physical durability, electrochemical resistance, and bond of the coated bars in concrete. Largely as a result of the NBS study, approximately 5 epoxy formulations have been approved for use on Federal Aid Highway Construction.

Evaluation of bond in the NBS study was based upon bond strength and bond creep tests. The bond strength tests included 23 epoxy coated (10 different epoxies with a range of coating thickness) and five uncoated No. 6 deformed reinforcing bars. Pull out bond specimens with one bar embedment length were subject to static loading. The creep

tests included 18 epoxy coated (9 epoxies in duplicates with a range of coating thicknesses) and four uncoated No. 6 deformed reinforcing bars. The creep specimens had one embedment length and were loaded in a manner similar to the pullout test. As a result of the tests, certain of the epoxies were judged acceptable in comparative performance with the uncoated bars.

Among the conclusions of the NBS study was a recommendation that additional tests of flexural members be carried out to confirm results of the pullout tests. Increasing use of epoxy coated reinforcement has added impetus to study not only flexural bond as recommended but also the influence of bar size, embedment length, fatigue loading, and the effect of the coating on concrete crack spacing and crack width.

The basic differences between a pullout test and one type of flexural bond test are shown in Figures 1.1 and 1.2 respectively. In practical situations, a bar under tension is almost always in a concrete tension zone. However, in the pull-out test, the concrete is in compression, and the detrimental influence of concrete cracking is not present. As shown in Figure 1.2, the flexural bond test arrangement places the bar being loaded in a flexural tension zone. Furthermore, the effect of possible cover splitting is approximately modeled.

1.2 Objective and Scope of Research

The objective of the research described herein was to further evaluate the bond characteristics of epoxy coated reinforcing bars in comparison to uncoated bars under static and fatigue loadings. A range of variable parameters were included in the evaluation to determine if

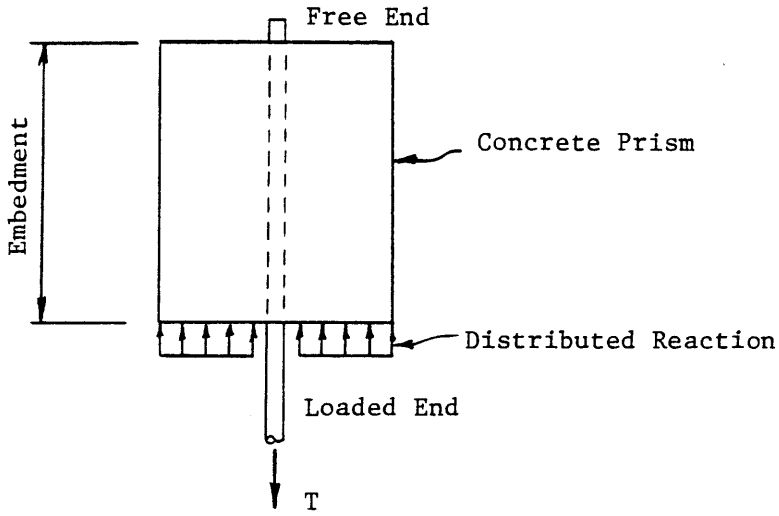

Figure 1.1 Pull-out Type Bond Test

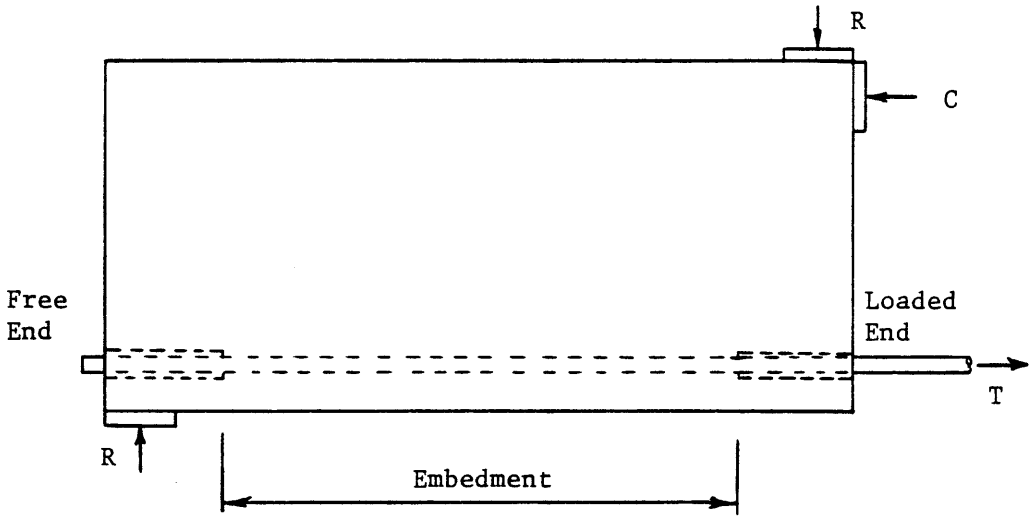

Figure 1.2 Beam End Flexural Bond Test

significant bond strength differences exist between coated and uncoated bars.

To evaluate the flexural bond characteristics of epoxy coated bars, comparative tests were made principally with uncoated (normal mill scale) and epoxy coated bars. Two basic types of flexural bond tests were conducted. The first type was for an evaluation of crack width and crack spacing in flexural specimens. The second type was for an evaluation of bar load versus bar slip relationships and strength.

The effect of epoxy coating on crack width and crack spacing was examined by testing specimens of concrete bridge deck slabs under flexure and shear loadings. Six specimens were tested, three with coated and three with uncoated No. 6 bars.

Bar load versus bar slip relationships were examined by testing 40 beam end specimens similar to Figure 1.2. The variable parameters in the tests included the following:

1. Rebar Surface Condition
    a) Mill Scale (normal)
    b) Epoxy Coated
    c) Blast Cleaned
2. Loading Condition
    a) Static (monotonic)
    b) Fatigue (cyclic)
3. Reinforcing Bar Size
    a) No. 6
    b) No. 11

4. Bar Embedment Length

   (a) 8", 13", 18" for #6 bar

   (b) 16", 24", 30", for #11 bar

Constants for the tests include reinforcing steel grade and production heat, concrete mix, epoxy coating type and thickness (within specifications) and concrete cover.

The comparative behavior of the test specimens is analyzed and discussed. Based upon the results, suggestions for design criteria modification are proposed.

2. REVIEW OF LITERATURE

2.1 Previous Bond and Fatigue Research on Epoxy Coated Reinforcement

The study conducted at the National Bureau of Standards by Clifton, Beeghly and Mathey (1) constitutes the primary source of research information on behavior of epoxy coated reinforcement. Summaries of this research have also been published on specific topics including bond (2), creep (3) and corrosion protection (4).

In the NBS study, evaluation of both bond strength and bond creep was based upon a pull-out type specimen with a 10 in. x 10 in. x 12 in. concrete prism. The test bars were located concentric with the longitudinal axis so that the length of embedment was 12 in. To minimize splitting, the concrete was reinforced with a cylindrical cage of 2 in. x 2 in. - 12/12 welded wire fabric. Instrumentation included one dial gage to measure free end slip and two dial gages to measure loaded end slip versus applied load. No. 6 deformed bars with two different deformation patterns meeting requirements of ASTM A 615-72 Grade 60 were utilized.

The NBS bond strength tests were conducted on 34 pullout specimens. These included 5 uncoated (mill scale) bars, 23 epoxy coated bars (10 different epoxy coatings and a range of coating thicknesses), and 6 specimens with polyvinyl chloride coatings. The concrete compressive strengths varied from about 5700 to 6600 psi. Load on the bar was gradually increased until either bond failure occurred or the steel stress considerably exceeded the yield strength in which case the test was halted. Bond failures only occurred for specimens with epoxy coated

bars having coating thicknesses of about 25 mils and with polyvinyl chloride coated bars. Bond failure did not occur in any one of the uncoated bar specimens nor in any of the 19 epoxy coated specimens with coating thickness between 1 and 11 mils that were judged acceptable based upon bond strength.

Bond strength was evaluated using slip criteria. The critical bond stress was taken as the lower value of average bond stress corresponding to a loaded-end slip of 0.01 in. or a free end slip of 0.002 in. Average bond stress, μ, is computed from the formula

$$\mu = \frac{f_s A_s}{\Sigma_o L} = \frac{T}{\Sigma_o L} \qquad (2.1)$$

where f_s = the stress in the reinforcing bar; T = the load or tensile force applied to the bar; A_s = the nominal cross-sectional area of the bar; Σ_o = the nominal perimeter of the bar; and L = the length of embedment. The average value of applied load corresponding to the critical bond strength in the 19 pullout specimens with bars having epoxy coatings 1 mil - 11 mils thick was 6% less than for the pullout specimens containing uncoated (mill scale) bars.

The NBS bond creep tests were reported after loading for 45 days in the original report (1) and after 2 years by Clifton, Mathey and Anderson (3). The 24 specimens tested included 4 uncoated (mill scale) bars, 2 polyvinyl chloride coated bars and 18 epoxy coated bars. The 18 epoxy coated bars included 9 different epoxy coatings on duplicate specimens with a thickness range from 1 to 11 mils. Approximately

one half of the specimens were loaded to a bar stress of 15 ksi and the remaining half to 30 ksi. Loaded end and free end slips were measured versus time. A creep ratio was defined as

$$CR = \frac{\text{Slip of coated bar}}{\text{Average slip of uncoated bar}} \text{ or } \frac{\delta_E}{\delta_M} \qquad (2.2)$$

and a pullout bond stress ratio based upon slip criteria was defined as

$$BR = \frac{\text{Pullout bond stress for uncoated bar}}{\text{Pullout bond stress for coated bar}} \text{ or } \frac{\mu_M}{\mu_E} \qquad (2.3)$$

Reinforcing bars with 6 of the epoxy coating materials were judged by the authors to have adequate bond strengths and creep resistance. For these six, the pullout test bond stress ratio for the loaded end ranged from 1.01 to 1.15 and for the free end ranged from 0.858 to 1.01. For the same six materials, the creep test slip ratio for the loaded end ranged from 0.635 to 1.42 and for the free end ranged from 1.00 to 1.67.

Hawkins (5) conducted fatigue tests which included one slab reinforced with epoxy coated bars. The tests were designed to evaluate bar fatigue in concrete, not bond fatigue. The slabs were 50 in. wide and 5 in. thick with a span of 48 in. Reinforcement consisted of No. 5 Grade 60 bars, all from the same heat, spaced at 6 in. centers. Three slabs were tested, one with normal mill scale bars, one with galvanized bars and one with epoxy coated bars. The applied loading induced a calculated flexural stress range of about 26 ksi with a minimum stress about 7% of the maximum. For the mill scale bar, first fracture occurred at 1.50×10^6 cycles and failure at 2.14×10^6 cycles. For the

galvanized bar, first fracture occurred at 0.48×10^6 cycles and failure at 0.814×10^6 cycles. However, for the specimen containing epoxy coated bars, failure had not occurred after 3.0×10^6 cycles. Thus, the stress range was increased to 28 ksi and loading continued for another 3.0×10^6 cycles without failure. Hawkins concluded that epoxy coating bars would increase the potential fatigue life of a bridge deck. He also recommended that the bar stress range caused by moments in bridge decks be limited to 21 ksi for uncorroded mill scale or epoxy coated bars, 19 ksi for uncoated galvanized bars, and 17 ksi for mill scale or galvanized corroded bars.

2.2. Epoxy Coating Specifications

Based upon results of the NBS study (1), FHWA acceptance requirements for epoxy coating materials and project specifications for coating and acceptance of coated bars were developed. After several years of use, these requirements evolved into ASTM A 775-81, "Standard Specifications for Epoxy-Coated Reinforcing Bars" (6).

Requirements for acceptance of the epoxy coating material include tests for chemical resistance, resistance to applied voltage, chloride permeability, adhesion of coating, bond strength to concrete, abrasion resistance, impact and hardness. The bond strength to concrete is evaluated using two coated and two uncoated, uncleaned No. 6 bars in pullout tests with concrete prisms identical to those used in the NBS study (1). The critical bond strength is determined as the smaller of the stress corresponding to a free end slip of 0.002 in. or a stress corresponding to a loaded end slip of 0.010 in. For acceptance of the coating, the

mean critical bond strength for coated bar is required to be not less than 80% of the mean strength for uncoated bars. A bond creep test is also sometimes required. For acceptance based upon bond creep, the slip-ratio of coated bars to uncoated bars shall not be greater than 1.3 for free end slip nor greater than 1.6 for loaded end slip.

Prior to coating, the specification requires the surface of the reinforcing bars to be cleaned by abrasive blast cleaning to near-white metal. The coating is to be applied by an electrostatic spray process and cured in accordance with recommendations of the manufacturer. Acceptance of the coated bar is based upon evaluations of the coating thickness, continuity and adhesion to the bar. Coating thickness is required by ASTM 775-81 to be 5 to 12 mils. (Some project specifications have required that thickness be 7 $\pm$ 2 mils or 8 + 2 mils). Thickness tests are required on a minimum of two bars of each size from each production shift. A minimum of 15 measurements are taken approximately evenly spaced along the test bar. At least 90% of the measurements are to be within the specification limits for acceptance. The maximum amount of coating damage due to fabrication is limited to 2% of the surface area of each bar. Damaged areas larger than 0.1 in.^{2} must be repaired with a compatible patching material.

In the case of bars utilized in this study, the coating (Scotchkote 213) manufacturer recommendations for coating application included pre-heating the bar to an optimum temperature at entrance to the coating station of 450^{o}F to 463^{o}F. Other recommendations included provisions for cooling, curing, support and handling of the bar immediately after coating is applied. An automated production line was utilized by the

reinforcing bar coater. After blast cleaning, the bars were first flame heated by passing through a gas furnace. Then the grounded bar was immediately passed through an electrostatic spray chamber. Therein, positively charged epoxy powder was attracted to the bar and melted upon contact. After passing out of the chamber, the coated bar was air and water spray cooled and then passed through a holiday detector.

2.3 Design Provisions for Bond and Fatigue

Neither ACI 318-77 (7) nor the 1977 AASHTO Standard Specifications for Highway Bridges (8) has unique provisions for design with epoxy coated bars. For bond and development of reinforcement, design practice has generally assumed no difference between epoxy coated reinforcement and normal mill scale reinforcement.

ACI and AASHTO provisions for development of straight deformed bars in tension are essentially the same. Basic development length for #11 bars and smaller is given by the equation

$$\ell_{db} = 0.04\, A_b f_y / \sqrt{f'_c} \qquad (2.4)$$

but not less than $0.0004\, d_b f_y$

where A_b = Area of an individual bar, $in.^2$

f_y = Yield strength of the reinforcing, psi

f'_c = Compressive strength of concrete, psi

d_b = Diameter of the reinforcing, in.

This basic length is further modified by multiplication factors, such as 1.4 for the "top reinforcement" effect, to determine the required development length, ℓ_d. The development length is required to be not less than 12 in. except for development of shear reinforcement. Equation 2.4 was developed based upon a strength criteria that the bar stress must reach 1.25 f_y in order for the anchorage to perform satisfactorily.

ACI Committee 408 (9) has suggested revised code provisions which would also consider cover thickness and transverse reinforcement parameters. Under the proposed provisions, basic development length would be given by the equation

$$\ell_{db} = \frac{5500\ A_b}{\phi K \sqrt{f'_c}} \qquad (2.5)$$

where

ϕ = capacity reduction factor = 0.8

K = smaller of $C_c + K_{tr}$ or $C_s + K_{tr}$ but $K \leq 3d_b$, in.

$K_{tr} = A_{tr} f_{yt}/1500s$ but $K_{tr} \leq d_b$, in.

A_{tr} = area of transverse reinforcement crossing plane of splitting, in.^{2}

f_{yt} = yield strength of transverse reinforcement, psi

s = spacing of transverse reinforcement, in.

C_c = thickness of concrete cover measured from extreme tension fiber to center of bar, in.

C_s = the smaller of the cover to the center of bar measured along a line through the layer of bars or half the center to center distance of bars in the layer, in.

A more detailed definition of the above parameters is given in the committee report (9). The rationale for the suggested provisions has been presented by Jirsa, Lutz and Gergely (10). Introduction of the capacity reduction factor, $\phi = 0.8$, in the denominator is intended to assure a basic development length which will develop the reinforcement to 1.25 f_y. Provisions for modification factors and a minimum development length of 12 in. are also included.

Neither ACI 318-77 nor the 1977 AASHTO Standard Specification for Highway Bridges has provisions for bond fatigue. AASHTO (8) does limit concrete and reinforcement fatigue stresses (except for concrete deck slabs with primary reinforcement perpendicular to traffic). For reinforcement stresses, the stress range caused by live load and impact is limited to

$$f_f = 21 - 0.33 f_{min} + 8(r/h) \qquad (2.6)$$

where

f_f = stress range, ksi

f_{min} = algebraic minimum stress level, tension positive, compression negative, ksi

r/h = ratio of base radius to height of rolled on transverse deformation; when actual value is not known, use 0.3.

A report (11) by ACI Committee 215 has presented considerations for design of concrete structures subjected to fatigue loading. The report did not contain specific recommendations for limiting bond fatigue stresses but fatigue of deformed bars was considered. As a lower bound, the committee recommended that the stress range on straight

deformed reinforcement that may be imposed on minimum stress levels of 0.40 f_y shall not exceed 20,000 psi. A more detailed analysis was dictated when these values were exceeded.

Hawkins (12) has reviewed existing information on bond fatigue and reported results of additional tests. He concluded that the information provided by the data was inadequate for a proper quantitive characterization of bond fatigue strength. It was surmised that for repeated loadings the bond strength depends primarily on the maximum bond stress induced during the loading cycle and that shear effects strongly influenced bond fatigue strength. He concluded that if inclined cracking does not develop, the maximum reduction in the ultimate bond strength due to repeated loading is probably about 40 percent.

3. EXPERIMENTAL PROGRAM

3.1 Scope of Test Program

A primary objective of the test program was to prepare companion specimens that were essentially identical except for having bars with normal mill scale surface embedded in some and epoxy coated bars embedded in others. A limited number of specimens were also prepared with bars in a blast cleaned but not coated condition. Two primary specimen configurations were utilized.

The first was the slab specimens for crack width, crack spacing and strength comparisons. This set of specimens was labeled series SC and is summarized in Table 3.1. The only variable was mill scale versus epoxy coated bars, and 3 replicate specimens were fabricated with each.

The second was the beam end specimens for comparative evaluation of bar load versus bar slip. Two types of loading were applied to various specimens. The statically (monotonic) loaded specimens were labeled series BS and the number of specimens for each variable considered are listed in Table 3.2. Beam end specimens subjected to fatigue (cyclic) loading were labeled series BF, and they are listed in Table 3.3.

A specimen labeling system was utilized as in the following example:

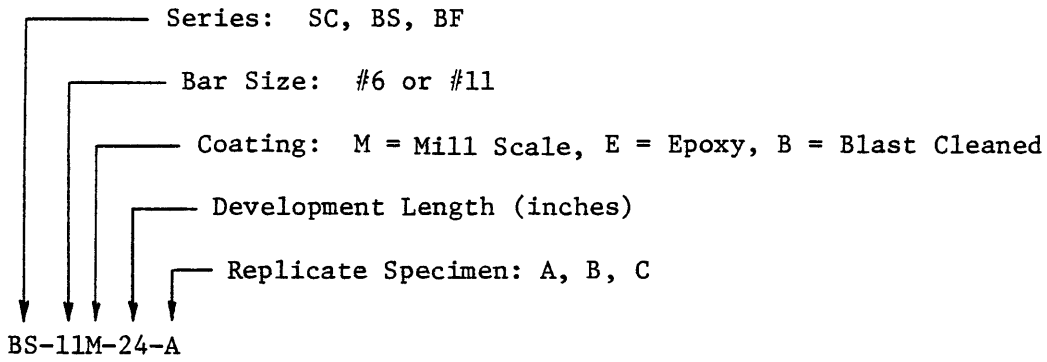

3.2 Slab Cracking Specimens (Series SC)

Since a primary use of epoxy coated bars is in bridge deck slabs, these specimens were designed to duplicate a typical deck section. Although NCDOT designs vary somewhat, a typical stringer bridge with cast-in-place concrete deck has stringers at 8 feet on center and a 8 1/2 in. thick deck, as shown in Figure 3.1a. Normally, only the top bars are epoxy coated. This includes both negative moment bars and perpendicular temperature bars. Thus, the negative moment region over a girder is the primary area of interest. A maximum negative moment over a girder would be generated by wheel loads located at mid-span of the slab between girders, producing the shear and moment diagram shown in Figure 3.1b. With a point of inflection occurring 2 feet from the girder, it was possible to duplicate the general loading condition with a segment of simply supported slab subjected to a mid-span load underneath, as shown in Figure 3.1c.

Examination of several deck designs indicated fairly typical use of bar sizes, bar spacing and bar supports, as shown in specimen sections of Figure 3.2. The top cover is normally specified to be 2 1/2 in. minimum, primarily for corrosion protection of the reinforcing. However,

Table 3.1 - Deck Slab Specimens for Crack Width, Crack Spacing and Strength Comparisons (Series SC)

Bar Size	Coating	No. of Specimens
#6	Mill	3
#6	Epoxy	3

Total = 6

Table 3.2 - Beam End Specimens for Static Tests (Series BS)

		No. of Specimens of Each Coating		
Bar Size	Embedment	Mill	Epoxy	Blast
#6	8"	2	2	-
#6	13"	2	2	1
#6	18"	2	2	-
#11	16"	2	2	-
#11	24"	2	2	1
#11	30"	2	2	-

Total = 26

Table 3.3 - Beam End Specimens for Fatigue Tests (Series BF)

		No. of Specimens of Each Coating		
Bar Size	Embedment	Mill	Epoxy	Blast
#6	8"	1	1	-
#6	13"	1	1	1
#6	18"	1	1	-
#11	16"	1	1	-
#11	24"	1	1	1
#11	30"	1	1	-

Total = 14

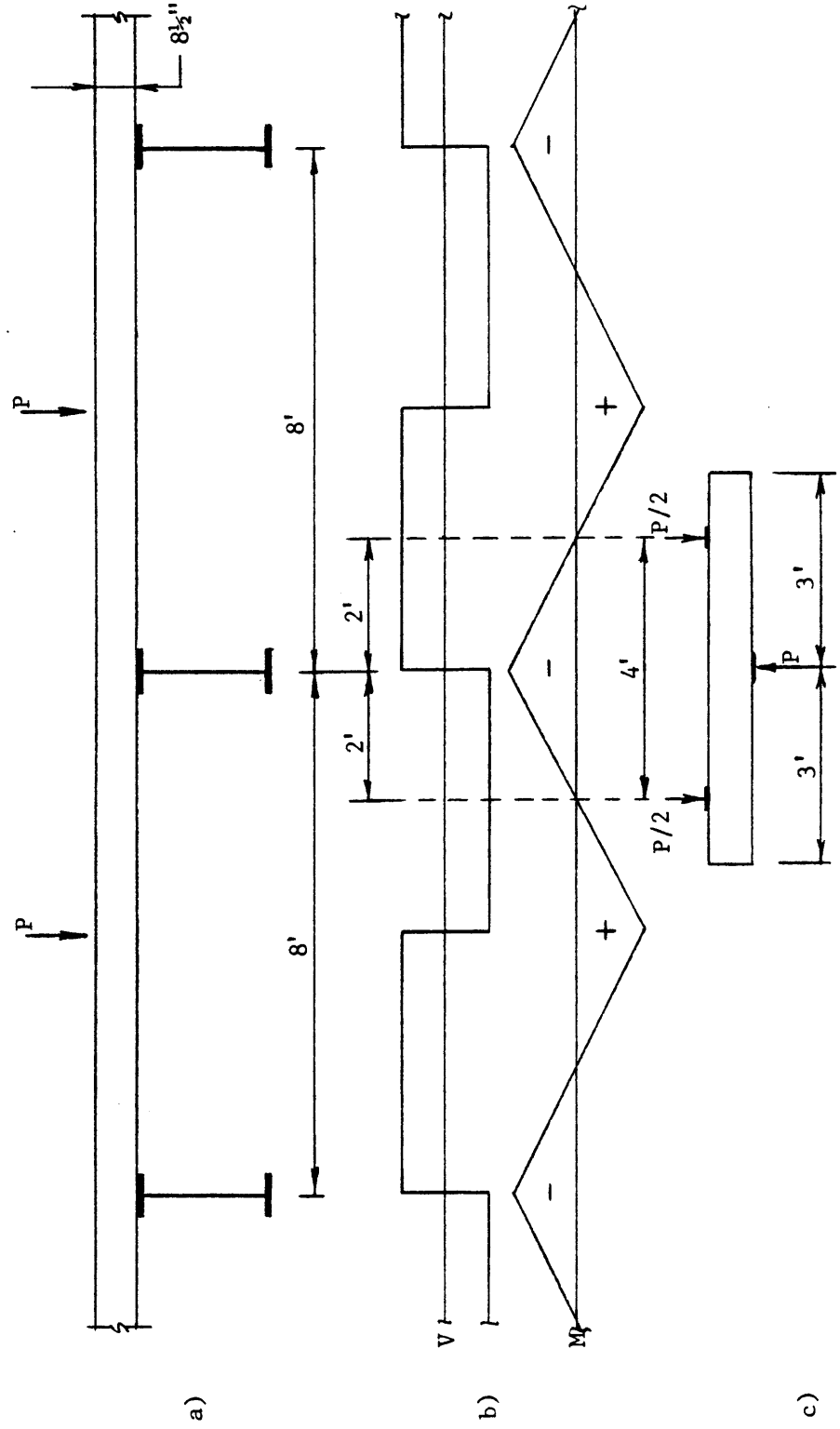

Figure 3.1 Evolution of Deck Slab Specimen

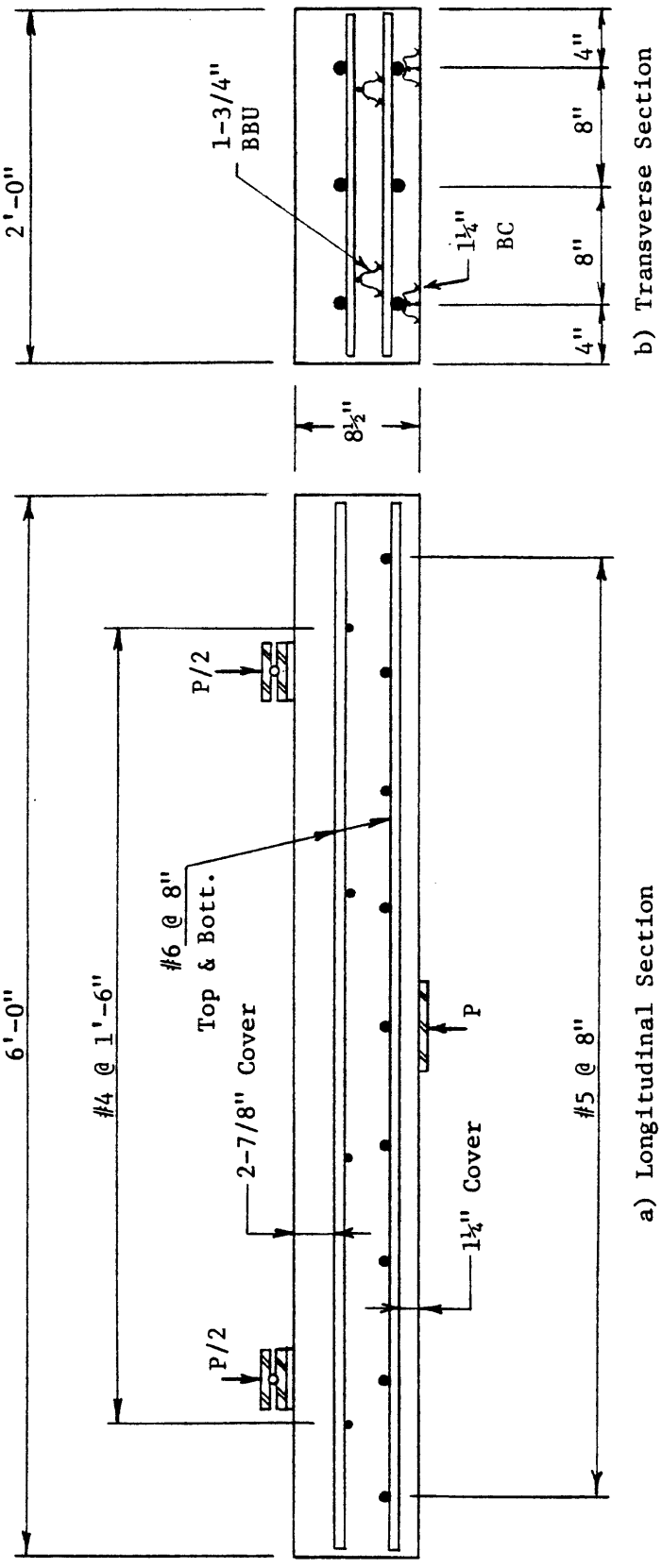

Figure 3.2 Slab Specimen Details (Series SC-6x-35-x)

specified bar supports and bar diameters would normally result in more than the minimum cover. The actual top cover in the fabricated specimens was 2 7/8 in. As in typical designs with epoxy coated bars, both the No. 6 and No. 4 top bars were epoxy coated in specimens SC-6E-35-A, B & C. For all slab specimen designations, the 35 refers to the 35 inches of development from the point of maximum moment to the end of the No. 6 bars.

3.3 Beam End Specimens (Series BS and BF)

A conceptual derivation of the beam end test specimen is shown in Figure 3.3. The objective is to place the bar in a flexural tension zone typical of most beams (Figure 3.3a). A half beam specimen can be used to duplicate the condition, as shown in Figure 3.3b. For the test program, this half beam or beam end was inverted as shown in Figure 3.3c. The inversion did not change the loading condition; yet, it made access to key areas of the specimen much easier for crack examination and gage readings.

Details of the beam end specimens used in both the static and fatigue tests are shown in Figures 3.4, 3.5 and 3.6. Design of the specimens was based upon several criteria related to typical bridge construction. Cover of approximately 2 in. for No. 11 bars in beam members and 2 1/2 in. for No. 6 bars in slabs would be representative of actual use. Stirrups were designed to meet ACI 318 minimums and requirements for the anticipated loads. At the same time, the resulting top transverse reinforcement was 0.22 $in.^2/ft.$ for the No. 6 bar specimens, which is comparable to deck transverse reinforcement (0.15 $in.^2/ft.$). The No. 11 specimens had 0.44 $in.^2/ft$, which is

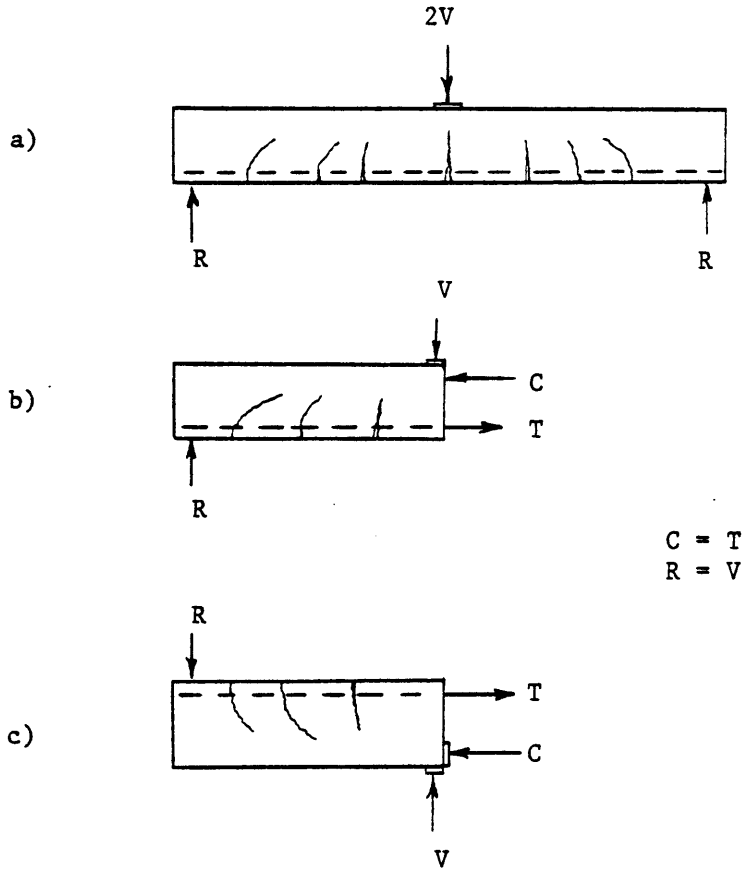

Figure 3.3 Evolution of Beam End Specimen

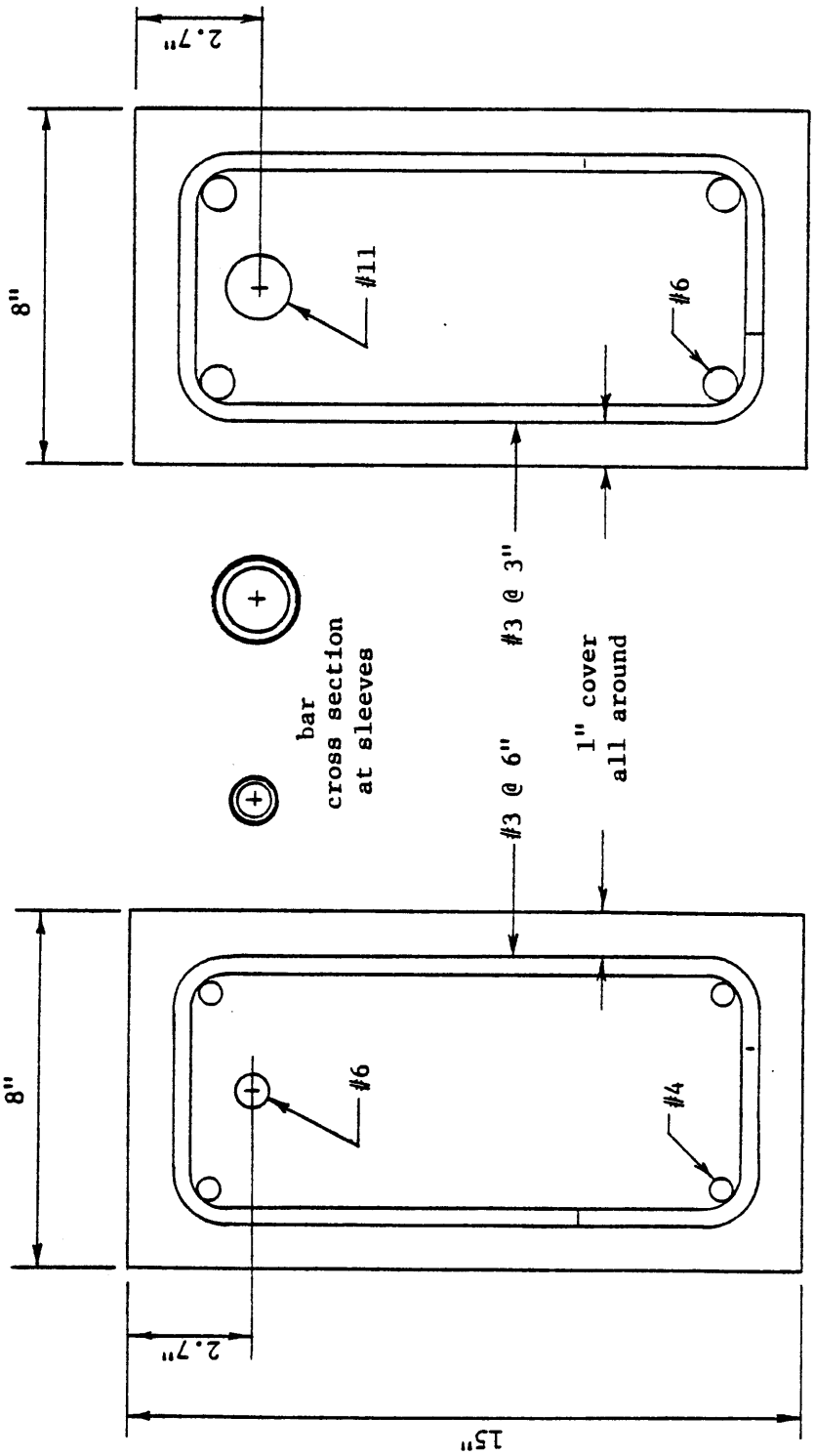

b) Section of #11 Specimens
Series Bx-11x-x-x

a) Section of #6 Specimens
Series Bx-6x-x-x

Figure 3.4 Beam End Specimen Cross Section Details

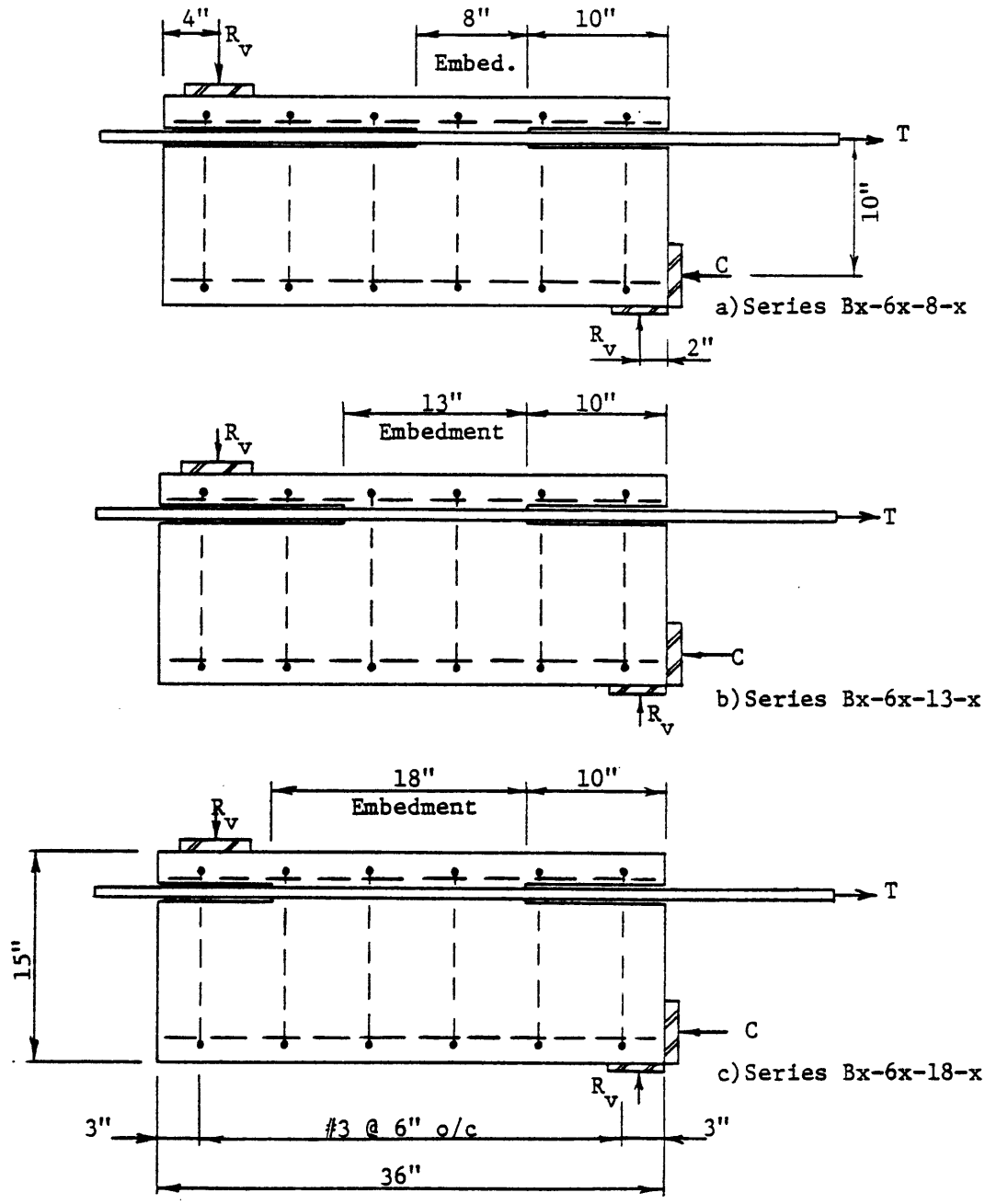

Figure 3.5 Beam End Specimen Details with No. 6 Bars

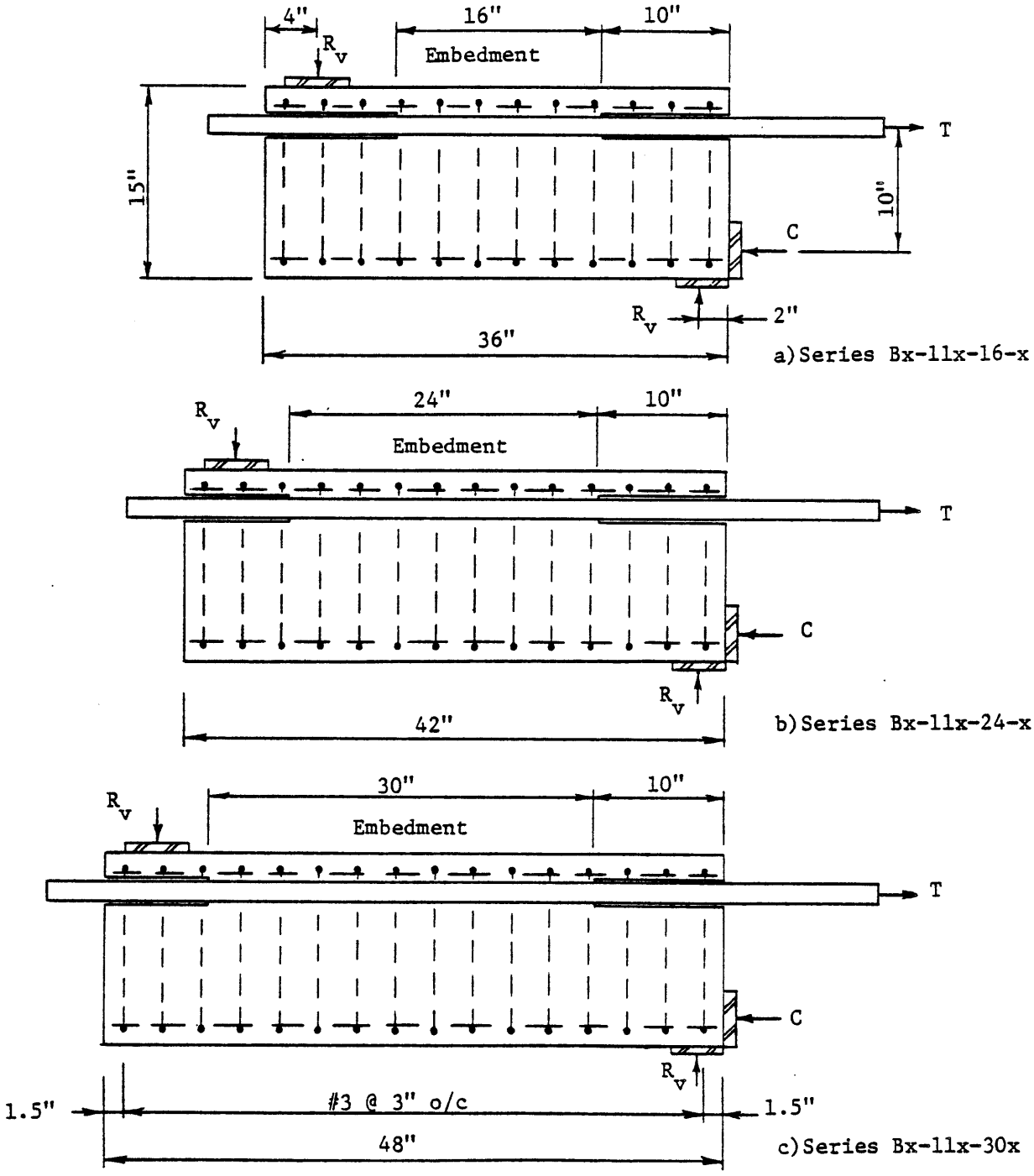

Figure 3.6 Beam End Specimen Details with No. 11 Bars

comparable to the higher stirrup areas in larger members. Stirrups were fabricated as closed ties with lapped 90^{o} hooks. The lapped hooks were always located at the bottom of the specimen (remote from the test bar) and alternated from one side to the other. The specimen cross section dimensions were the same to minimize formwork and simplify the test rig.

Embedment lengths were selected based upon previous research (13) on similar bond specimens with No. 6 and No. 11 bars. The embedment length was varied in part by changing the length of PVC pipe (ASTM D-2241) sleeves which were slipped onto the bar at each end. By providing the sleeve at the free end of the bar, the clamping force of the vertical reaction was circumvented. The sleeve at the loaded end was provided to avoid local popout of the concrete surface in the vicinity of the slip gages. Nominal 3/4" pipe with 0.93 in. I. D. and 1.05 in. O. D. was used around No. 6 bars. Nominal 1 1/2 in. pipe with 1.75 in. I. D. and 1.90 in. O. D. was used around No. 11 bars. The bars were centered in the sleeves, and a clay-like rope caulking was used to seal the interspace at each end of the embedded length.

The cages in all specimens were fabricated using normal reinforcing with mill scale. Only the test bar surface condition varied. Thus, bond performance in comparative tests was a function only of the test bar surface. Secondary magnifying effects which could occur with simultaneous transverse bar surface variations were eliminated.

3.4 Reinforcing Steel Properties

Reinforcing steel used in the specimens, both the test bars and supplementary reinforcing, were produced to meet ASTM A615-72 Grade 60

(nominal). All bars of a given size were produced from the same heat of steel, whether coated or uncoated. The stress-strain curves and other properties for the No. 6 and No. 11 test bars are shown in Figure 3.7. In general, the yield stress for the No. 6 bars was noted to be very consistent at 63.6 ksi. The yield stress of the No. 11 bars averaged 63.0 ksi but ranged from approximately 62.5 to 64.0 ksi. No relation appeared to exist between the variation in No. 11 bar yield and the coated vs. uncoated condition.

3.5 Reinforcing Surface Condition and Coating

The reinforcing steel test bars were utilized in three basic surface conditions: mill scale, epoxy coated and blast cleaned as shown in Figures 3.8 and 3.9.

The mill scale surface is the condition of a typically produced bar. The bars were not heavily rusted but did have occasional rust spots along and between the deformations. Previous research (14, 15) has indicated that rusting of reinforcing increases the bond slightly and is acceptable in construction if the bar area is not significantly reduced. For purposes of the comparative tests, it was decided that the normal mill scale condition should not be heavily rusted. Thus, any differences in bond which might be encountered would not be exaggerated by increased bond of the uncoated bars due to extensive pitting of the surface.

Coating of the reinforcing bars involves several stages, as detailed in Section 2.2. The primary stages are blast cleaning, preheating, electrostatic spray coating, and curing. Some of the test

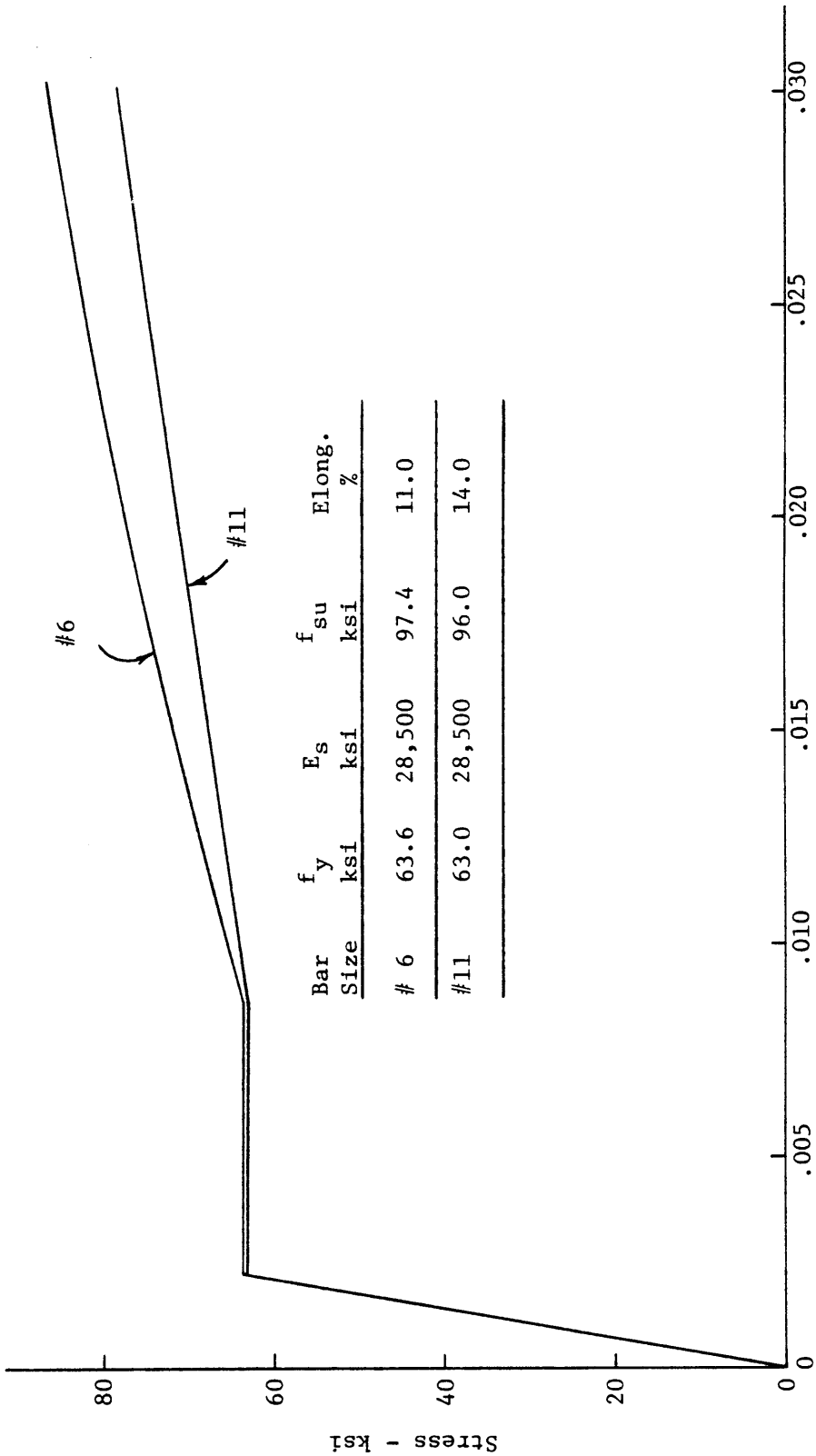

Bar Size	f_y ksi	E_s ksi	f_{su} ksi	Elong. %
# 6	63.6	28,500	97.4	11.0
#11	63.0	28,500	96.0	14.0

Figure 3.7 Mechanical Properties of Reinforcing Steel

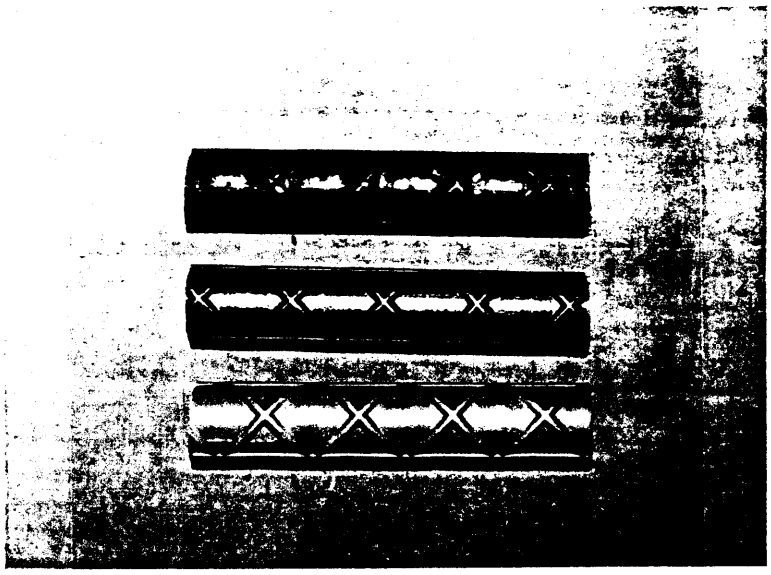

Figure 3.8 Surface Condition of No. 6 Reinforcing Bars

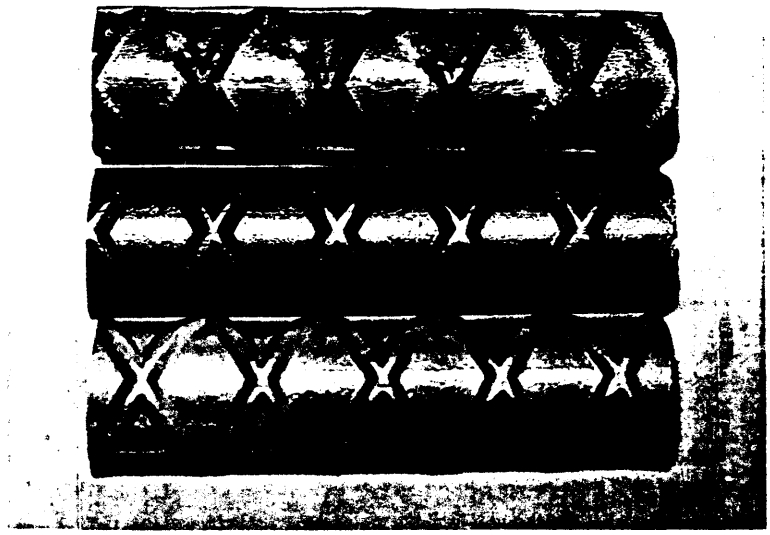

Figure 3.9 Surface Condition of No. 11 Reinforcing Bars

bars were left in the blast cleaned condition. The purpose of testing the blast cleaned bars was an effort to determine if removal of the mill scale alone had a significant effect on bond or bond fatigue.

The epoxy coating utilized was Scotchkote 213. To assure as much uniformity as possible, the full length bars were selected from the middle of larger commercial production runs. The test bars were saw cut from the longer lengths, avoiding any touched up or blemished areas.

Coating thickness was measured using a Nordson dry film thickness gage as shown in Figure 3.10. For calibration purposes, standard samples of nonmagnetic coatings on mild steel were borrowed from the National Bureau of Standards. After calibration for 8 mils thickness, a series of 10 consecutive readings were taken on each of several standard samples to evaluate gage accuracy and operator precision over a broad range of thickness. Resulting readings averaged 3.39 mils on a 3.25 standard, 5.25 on 5.40, 7.71 on 7.67, 7.96 on 8.00, 15.1 on 15.3 and 20.7 on 20.7.

Correction factors defining effects of the bar preparation process were determined as the difference between the average of 10 gage readings on a cleaned but uncoated reinforcing bar of the size and lot coated and the average of 5 gage readings on a smooth mild steel plate. The correction factor, 0.16 mils for the No. 6 bars and 0.29 mils for the No. 11 bars, was subtracted from subsequent gage readings on coated bars.

The coating thickness was measured on the body of the bar between deformations and ribs. For acceptance purposes, coating thickness would

normally be measured at scattered locations along the length of selected samples. However, for the test program recorded measurements (defined as the average of three individual readings on adjacent areas between deformations) were taken between each deformation along both sides of the bar for the full embedment length. Recorded measurements were taken to the nearest 0.1 mils. Results of the thickness measurements are presented in Table 3.4.

Dimensions of the reinforcing bar deformations are given in Table 3.5 in comparison to ASTM A615-72 requirements. The bars had two longitudinal side ribs and a smaller third rib to designate grade 60.

Prior to casting, the pulling end of the bars used in the beam end specimens was machined to accept Howlitte grip couplers, as shown in Figure 3.11. The No. 6 bar was turned to 0.757 in. diameter and the No. 11 to 1.382 in. diameter.

3.6 Concrete Properties

Since a major use of epoxy coated reinforcement is in concrete bridge decks, the concrete mix was designed to meet the North Carolina Department of Transportation Standard Specifications for Class AA concrete. These specifications require a minimum cement content of 715 lbs/cu. yd., a maximum slump of 3 in., a maximum water cement ratio of 0.425, an air content = 6% $\pm$ 1.5% and a minimum compressive strength of 4500 psi at 28 days. The relatively high cement content is in part to enhance corrosion protection. With the high cement content and good aggregates, it is not unusual in practice to attain strengths in excess of 6000 psi, and this was also the case in the test

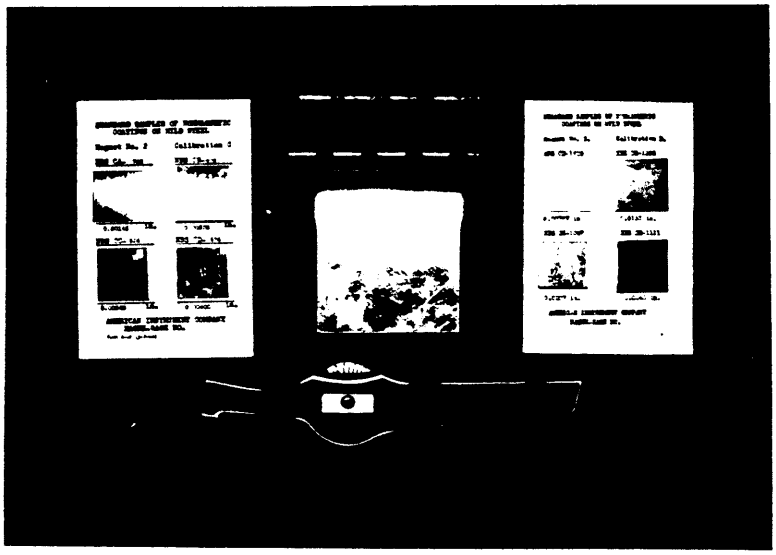

Figure 3.10 Dry Film Coating Gage and Standards

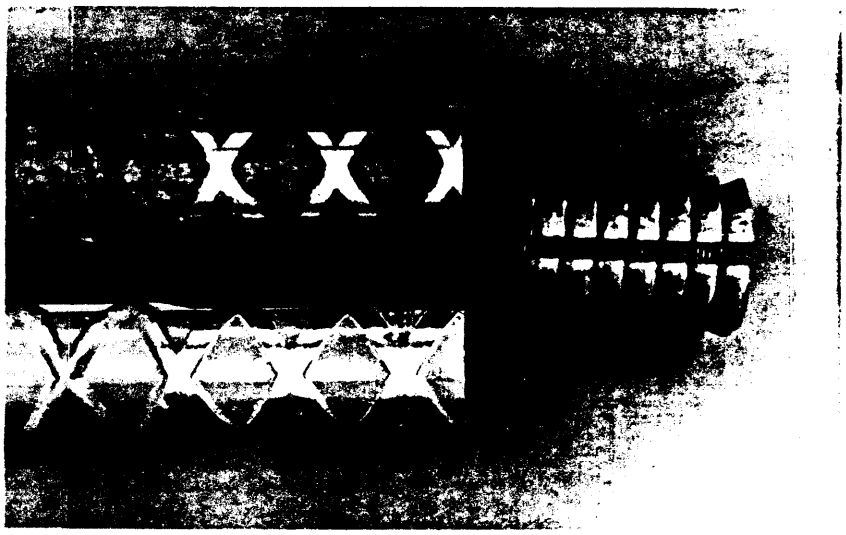

Figure 3.11 Bar Ends Machined to Accept Grip Couplers

Table 3.4 Epoxy Coating Thickness in Mils

Specimen	Individual Bar Mean	Standard Deviation	Group Mean	Group Mean
SC- 6E-35-A (1)	8.53	1.09		
(2)	11.05	1.43	9.07	
(3)	7.62	0.89		
SC- 6E-35-B (1)	8.18	1.15		All
(2)	10.15	1.24	9.08	SC
(3)	8.90	1.06		9.11
SC- 6E-35-C (1)	9.60	1.23		
(2)	8.28	1.38	9.18	
(3)	9.67	1.42		
BS- 6E- 8-A	9.13	1.12	8.61	
BS- 6E- 8-B	8.09	1.06		
BS- 6E-13-A	7.81	0.83	7.82	All BS & BF No. 6 8.56
BS- 6E-13-B	7.84	1.04		
BS- 6E-18-A	7.82	0.88	8.99	
BS- 6E-18-B	10.16	1.41		
BS-11E-16-A	9.89	1.16	8.88	
BS-11E-16-B	7.47	1.35		
BS-11E-24-A	8.64	1.07	8.71	All BS & BF No. 11 8.16
BS-11E-24-B	8.78	1.04		
BS-11E-30-A	6.74	0.92	8.12	
BS-11E-30-B	9.50	0.95		
BF- 6E- 8-A	7.18	0.96		
BF- 6E-13-A	8.16	0.75	8.65	
BF- 6E-18-A	9.72	1.44		
BF-11E-16-A	7.09	1.28		
BF-11E-24-A	7.38	1.02	7.61	
BF-11E-30-A	8.09	0.87		

1 mil = 0.001 inches

program. The concrete mix per cubic yard was as follows:

Cement (Type I)	715 lbs./cu. yd.
Coarse Aggregate (Garner Quarry)	1889 lbs./cu. yd.
Fine Aggregate (Senter Pit)	1032 lbs./cu. yd.
Water	288 lbs./cu. yd.
Air Entraining (AE-10)	0.75 oz./sk
Water Reducer (Pozzilith 300 N)	3 oz./sk

All cement for the specimens came from a single lot which was stored under low humidity conditions. Although the specimens were cast over a period of several months, no strength variation as a function of cement age could be detected. The resulting concrete slump varied from 1.5 to 2.5 inches, and the air content ranged from 5.0 to 6.5 percent.

Since concrete strength was not a planned variable, effort was made to follow consistent batching, mixing and fabrication practice. Standard 6 x 12 cylinders, consolidated by rodding in cardboard molds, were taken for compression and splitting tests. It was the intention to test both the cylinders and the test specimens at an age of 28 days. This approach was maintained for the slab specimens (Series SC) and the beam end static specimens (Series BS). However, test equipment problems delayed initiation of the fatigue tests (Series BF); thus, the fatigue specimens and accompanying cylinders were tested at later ages.

Results of the concrete strength tests are presented in Table 3.6. The individual cylinder strengths from a given batch varied practically as much as the range of all cylinders from a given series. Thus, a listing of average specimen strength versus specimen series coating

Table 3.5 Reinforcing Bar Deformations

	Average Spacing (in.)	Average Height (in.)	Average Gap (in.)
No. 6 ASTM	0.525 max	0.038 min	0.286 max
No. 6 Mill	0.499	0.045	0.115
No. 6 Blast	0.499	0.046	0.114
No. 6 Epoxy	0.499	0.046	0.125
No. 11 ASTM	0.987 max	0.071 min	0.540 max
No. 11 Mill	0.631	0.097	0.145
No. 11 Blast	0.631	0.097	0.144
No. 11 Epoxy	0.631	0.097	0.156

Table 3.6 Concrete Compressive and Splitting Tensile Strengths

Specimen Series	Age (days)	Avg. Compressive Strength (psi)	Avg. Splitting Strength (psi)
SC- 6M	28	6050	529
SC- 6E	28	6684	480
BS- 6M	28	6390	507
BS- 6E	28	6562	528
BS- 6B	28	5716	522
BS-11M	28	6480	506
BS-11E	28	6562	527
BS-11B	28	5716	522
BF- 6M	37	6254	516
BF- 6E	37	6302	466
BF- 6B	37	6493	469
BF-11M	41	7041	473
BF-11E	44	6979	543
BF-11B	41	6996	531

type best indicates the influence of concrete strength for evaluating relative bond characteristics. The splitting strengths were not always consistent with the compressive strengths as in the case of series SC-6M relative to SC-6E. Also, the unusually low strength of the batch for specimens BS-6B-13-A and BS-11B-24-A (in each case the only specimens of the series BS-6B and BS-11B) could not be explained. Otherwise, the strengths were reasonably comparable.

3.7 Specimen Fabrication

Reinforcing bar mats and cages were pre-assembled with tie wire and then placed on bar supports providing the desired cover. The formwork for the slab cracking specimens (Figure 3.12) and beam end specimens (Figure 3.13) was constructed of 1/2 in. A/C fir plywood on 2 x 2 and 2 x 4 studs. By providing ample rigidity, only external clamps and tie rods were necessary. Tight form tolerances were maintained in order to facilitate specimen alignment in the test frame.

Test bars in the beam end specimens projected through holes in the end bulkheads. The holes were drilled for a tight fit around the PVC sleeves. After passing through the sleeves, the bars were centered, suspended and tied to the form externally. Then the sleeves were sealed as previously described. Lifting hooks were installed near each end of the slab specimens. For the beam end specimens, two lifting hooks were located at mid-length of the top side by hooking around cage bars.

Concrete was placed in the oiled forms and vibrated internally. Particular care was taken in the beam end specimens to avoid direct contact between the vibrator and the test bar or sleeves. The specimens

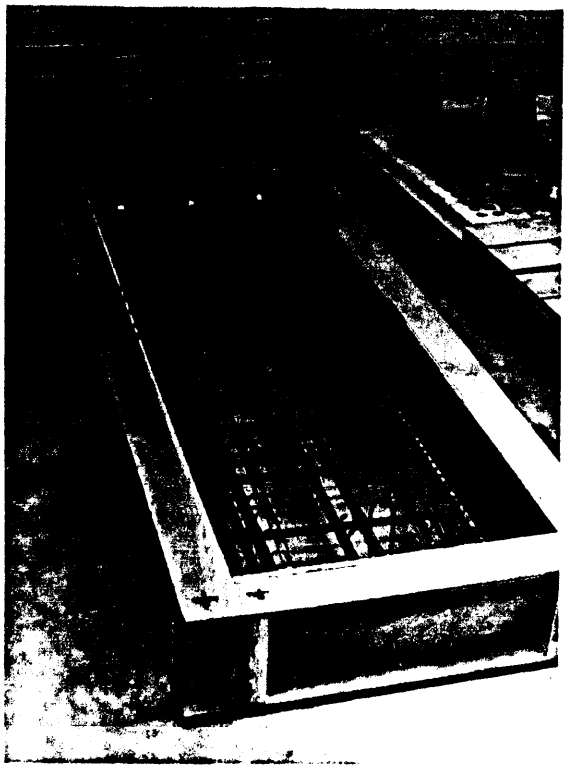

Figure 3.12 Slab Specimen Formwork and Reinforcing

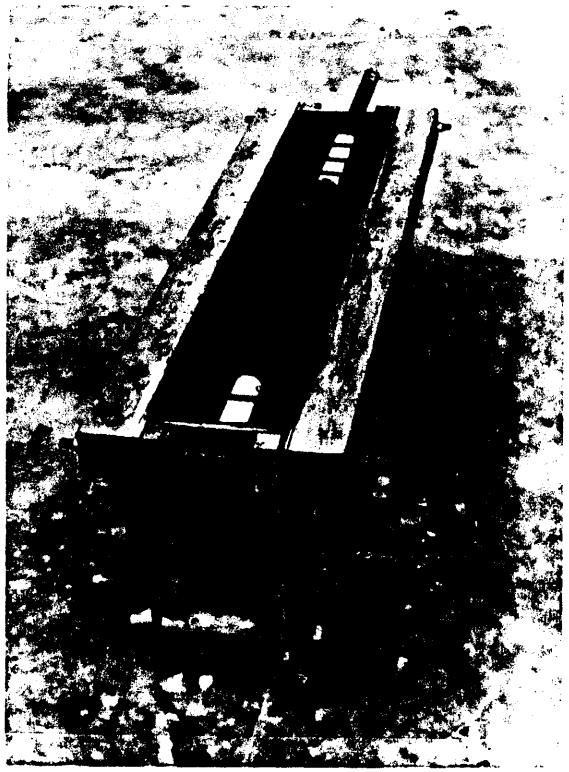

Figure 3.13 Beam End Specimen Formwork and Reinforcing

were screeded and then lightly troweled to improve crack visibility later. Following casting, the specimens and cylinders were covered with polyethylene and allowed to cure overnight.

The specimens and cylinders were stripped the next day. Curing procedures attempted to duplicate NCDOT requirements for bridge deck concrete. Deck slabs must be moist cured for 7 days while the cylinders from the pour are maintained in a moist environment until testing at 28 days. Thus, immediately after stripping, the test specimens were rewetted and wrapped in polyethylene for 6 additional days moist curing. The cylinders were generally moist cured until testing of the specimens. A few cylinders were wrapped with a few test specimen castings and then allowed to dry after the 7 day period. No significant difference in 28 day cylinder strength was found in comparison with others from the same batch that were moist cured for 28 days.

Prior to testing, the specimens were coated with a lime and cement whitewash to aid crack detection during the test.

3.8 Slab Test Equipment and Procedures

The test frame and general loading arrangement for the slab crack tests (series SC) is shown schematically in Figures 3.14 and 3.15. Additional views of the test set-up are shown in Figures 3.16 and 3.17. Gages were used to collect data on specimen deflection, crack width and bar slip.

Vertical deflections were measured using 10 dial gages with minimum divisions of 0.001 in. All deflection gages were mounted

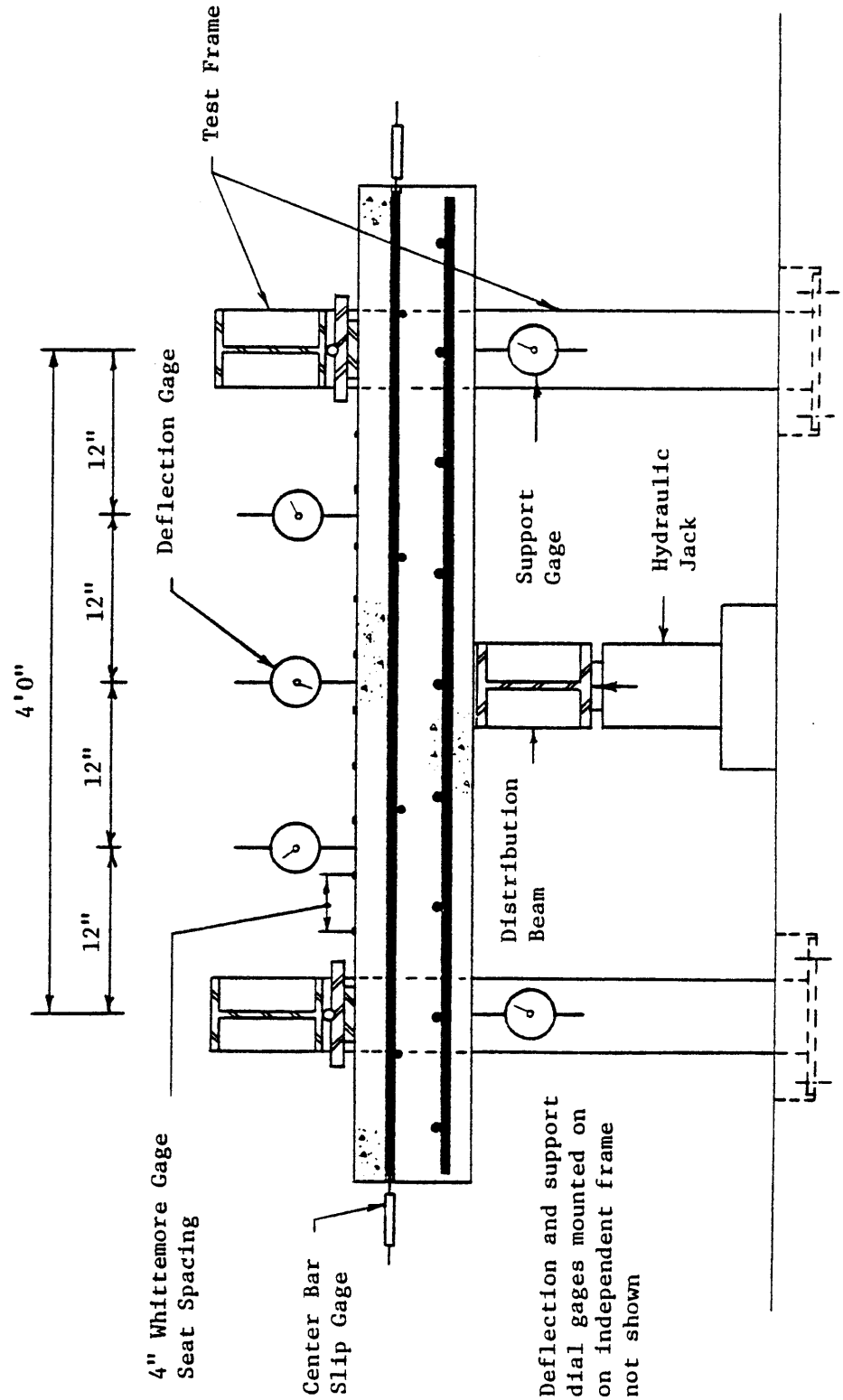

Figure 3.14 Side Elevation of Slab Specimen Test Arrangement

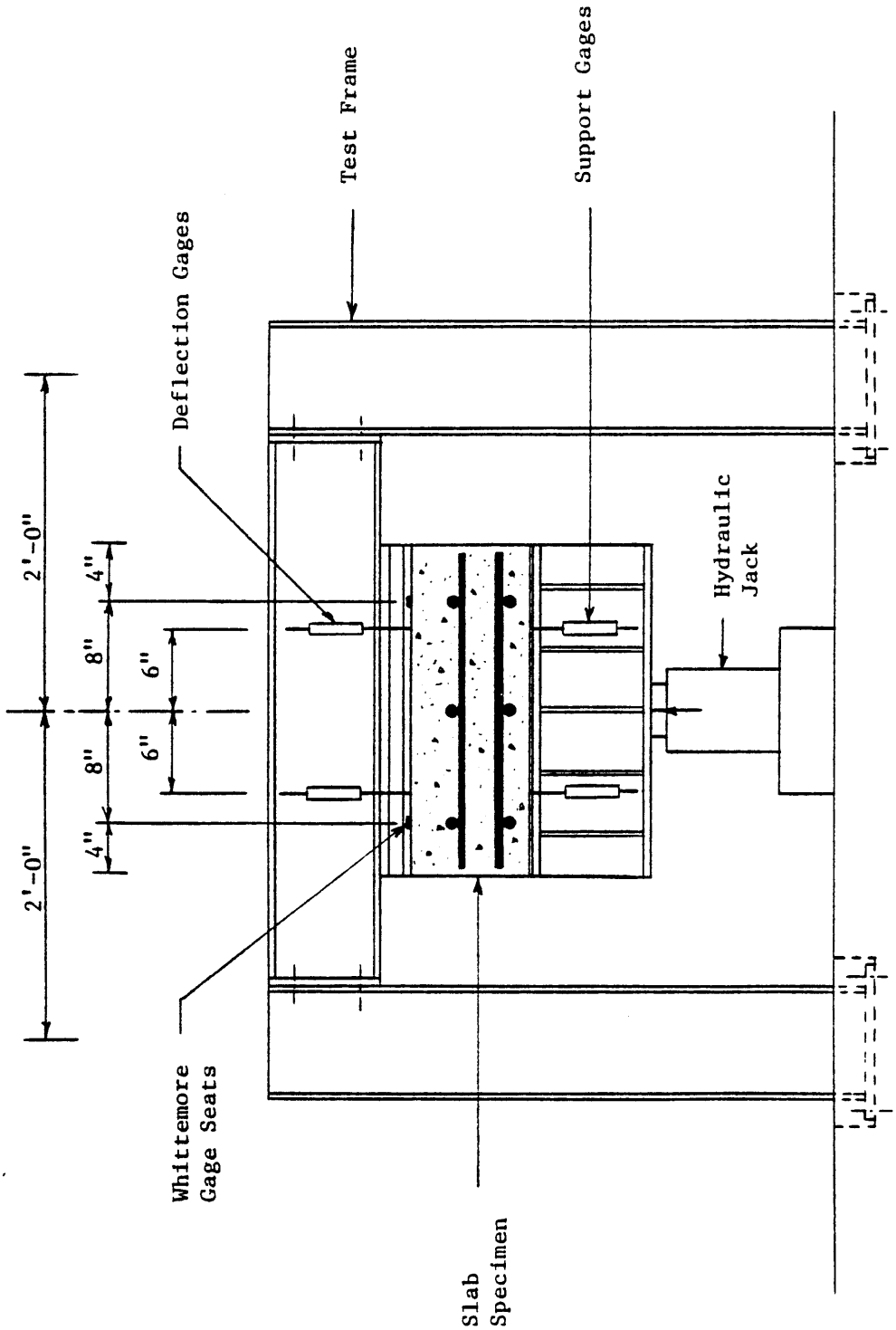

Figure 3.15 End Elevation of Slab Specimen Test Arrangement

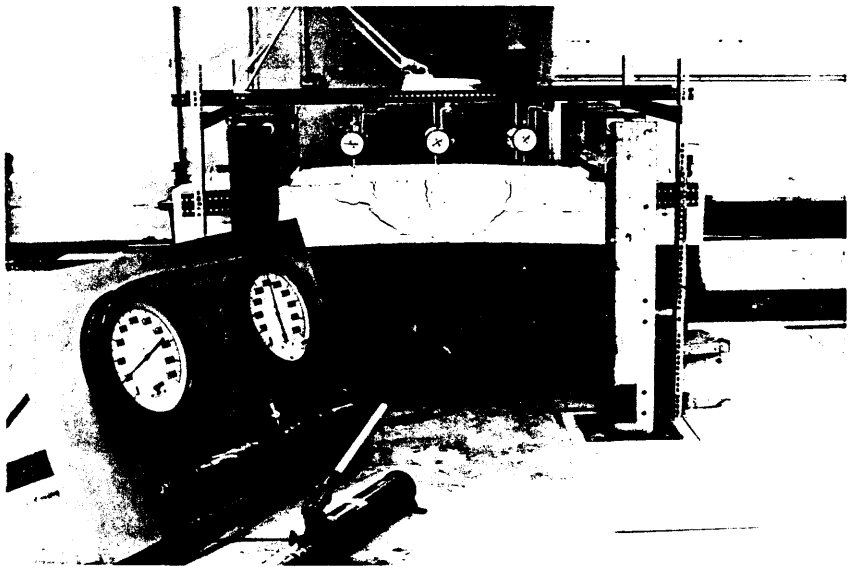

Figure 3.16 Photograph of Slab Specimen Test Set-up

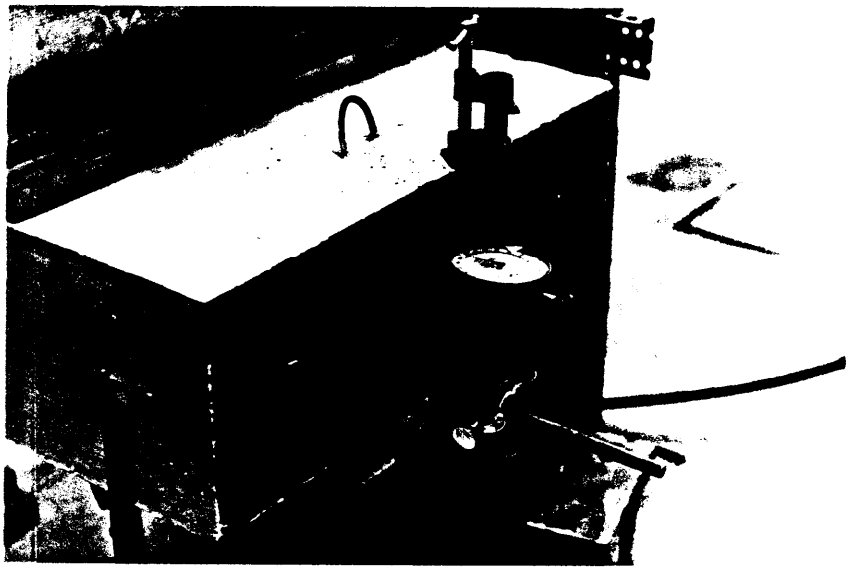

Figure 3.17 Slab Specimen Bar End Slip Gage

on an independent frame so that measurements were relative to the rigid floor. The gages were aligned in two rows of 5 each located 6 inches from the front and back edges of the specimen. Of the 10 gages, 4 measured support displacement, 2 measured midspan deflection, and 2 measured deflections at each quarter span.

In order to measure crack widths, Whittemore gage points were glued at 4 inch centers longitudinally on the tension face in two rows 4 inches from each edge. A Whittemore extensometer with 0.0001 in. dial divisions was used to measure the tension face elongation between each set of points. To facilitate comparison of crack spacings, a grid of lines at 2 inch centers was drawn on the tension face prior to the test.

Although measurement of bar end slip was not intended as the primary purpose of these tests, the end slips of the center top bars were measured. Dial gages having 0.0001 inch divisions were mounted as shown in Figure 3.17.

Load was slowly applied by means of a hydraulic jack in increments of 3,000 lbs. After application of each increment, the load was held until deflections stabilized and then all gage readings were recorded. Total time for each test required approximately 4 hours.

3.9 Static Bond Test Equipment and Procedures

The test frame and general loading arrangement for the beam end static bond tests (Series BS) is shown schematically in Figures 3.18 and 3.19. Additional views of the test setup are shown in Figures 3.20 thru 3.23.

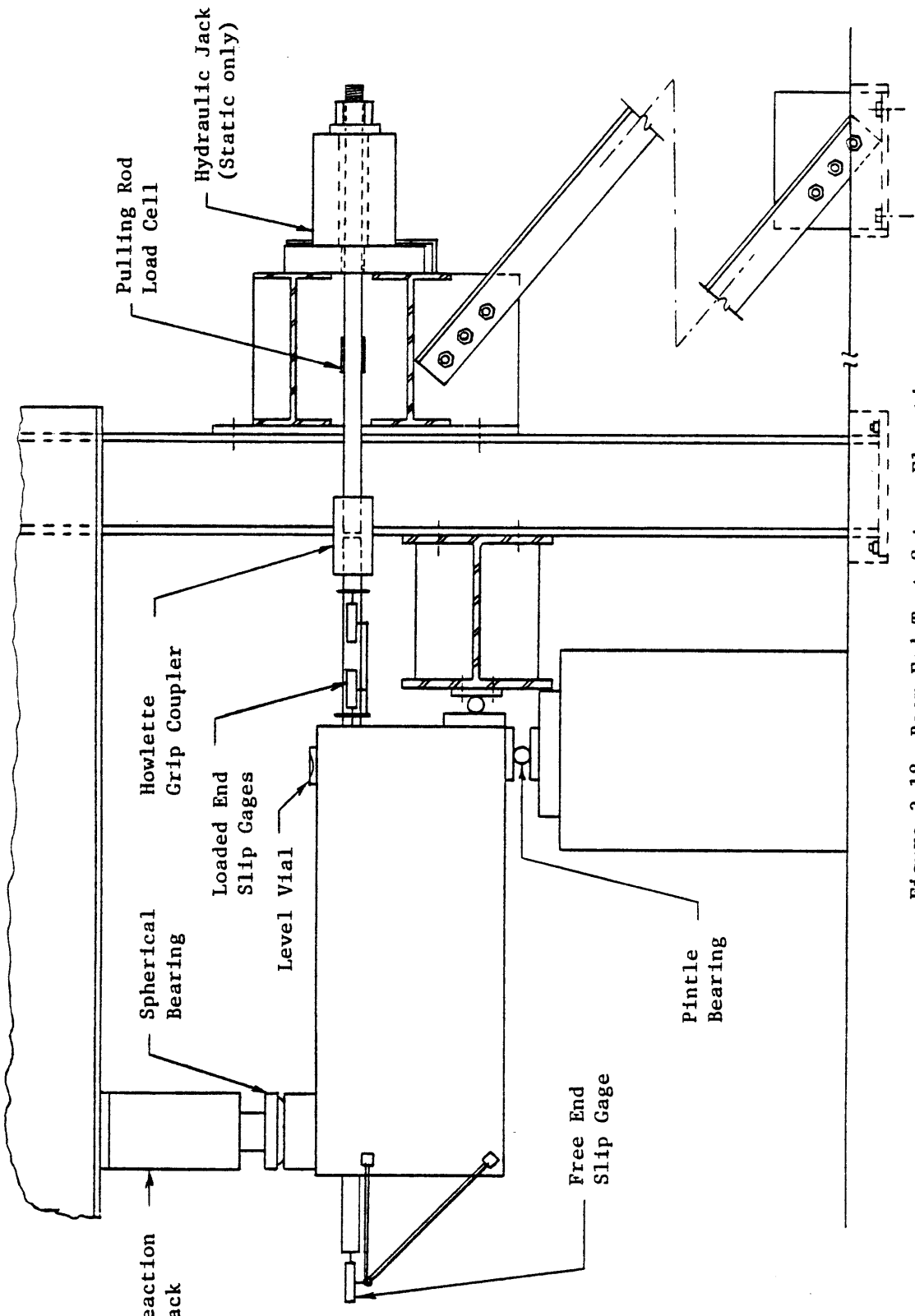

Figure 3.18 Beam End Test Set-up Elevation

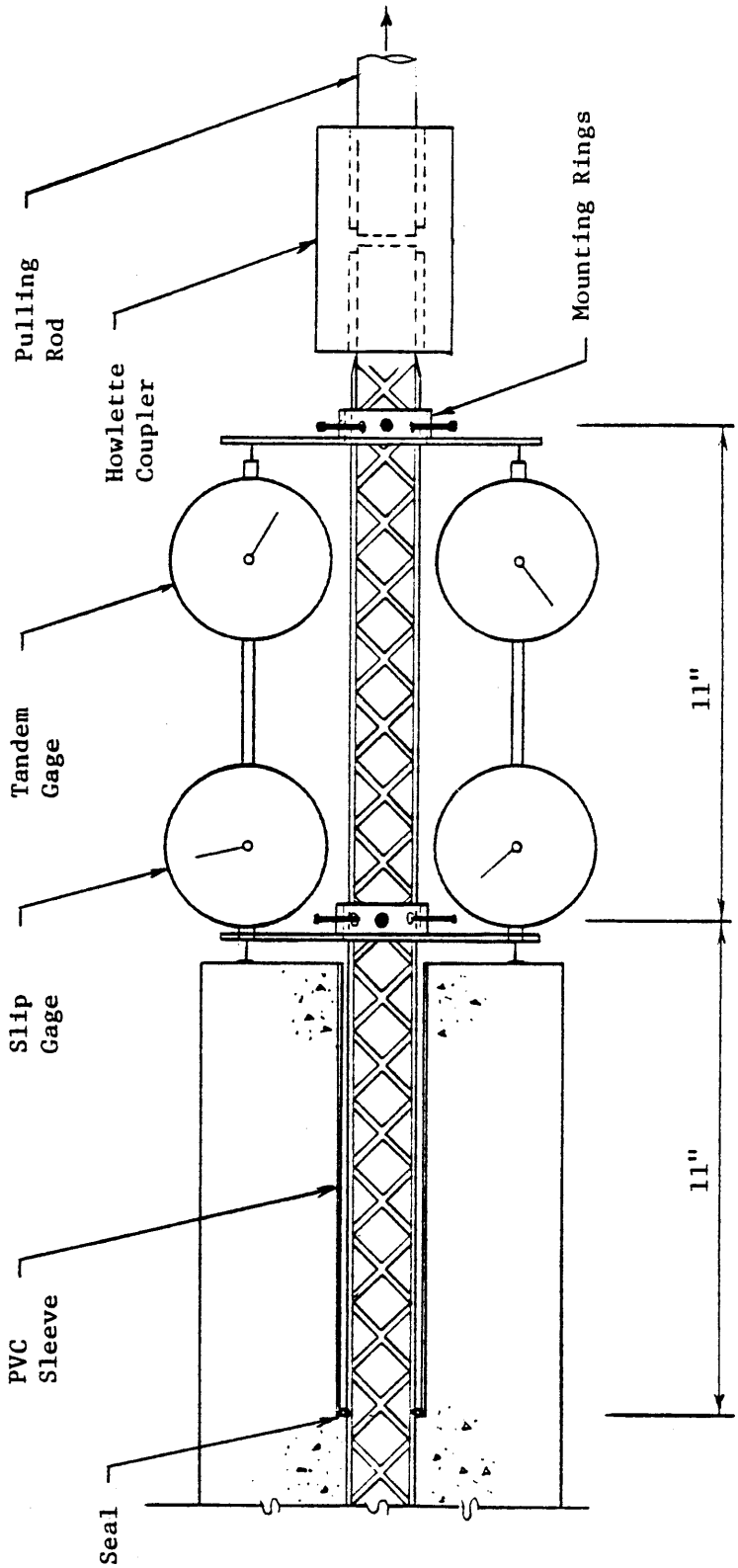

Figure 3.19 Loaded End Slip Gages

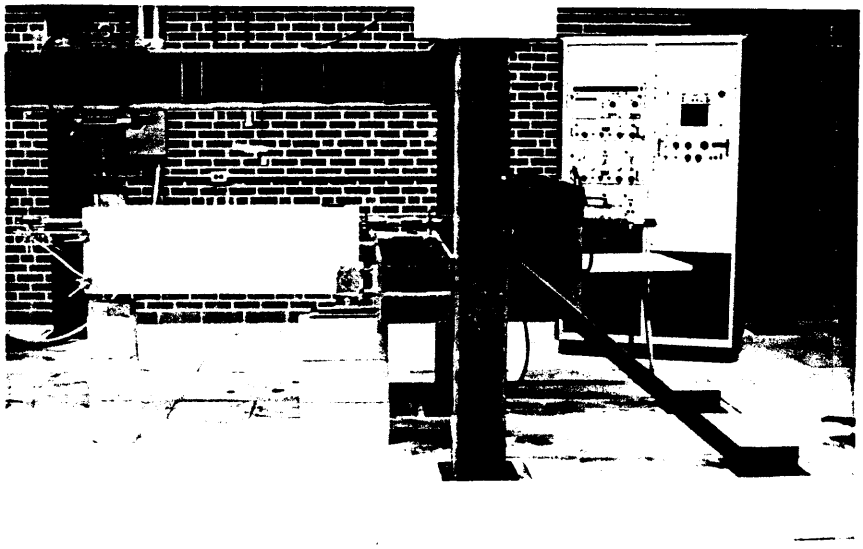

Figure 3.20 General View of Beam End Specimen Static Test Set-up

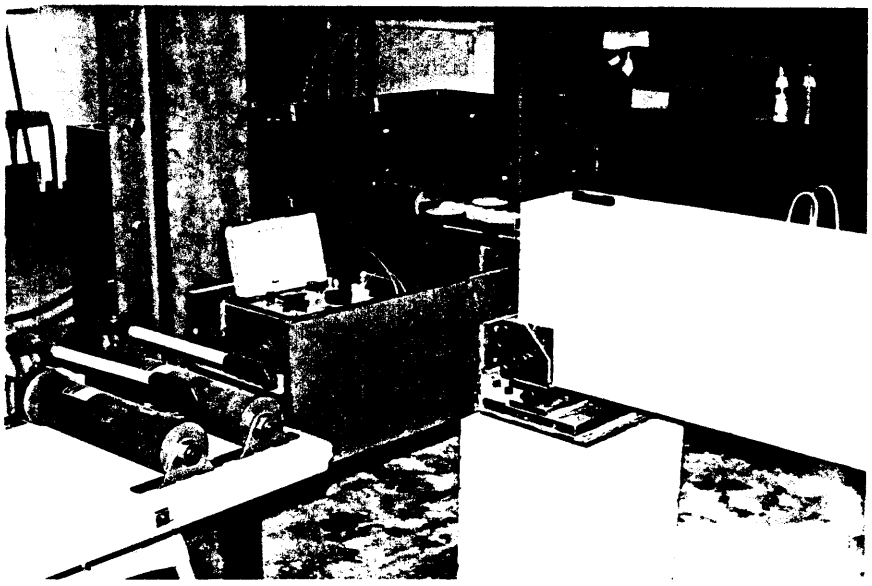

Figure 3.21 Beam End Specimen Instrumentation

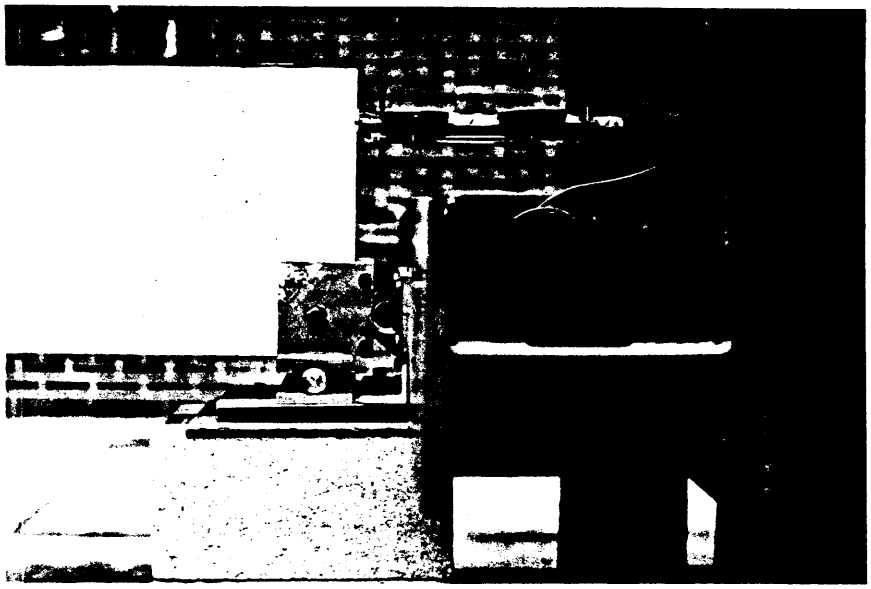

Figure 3.22 Loaded End Slip Gages, Pintle Bearing and Level Vial

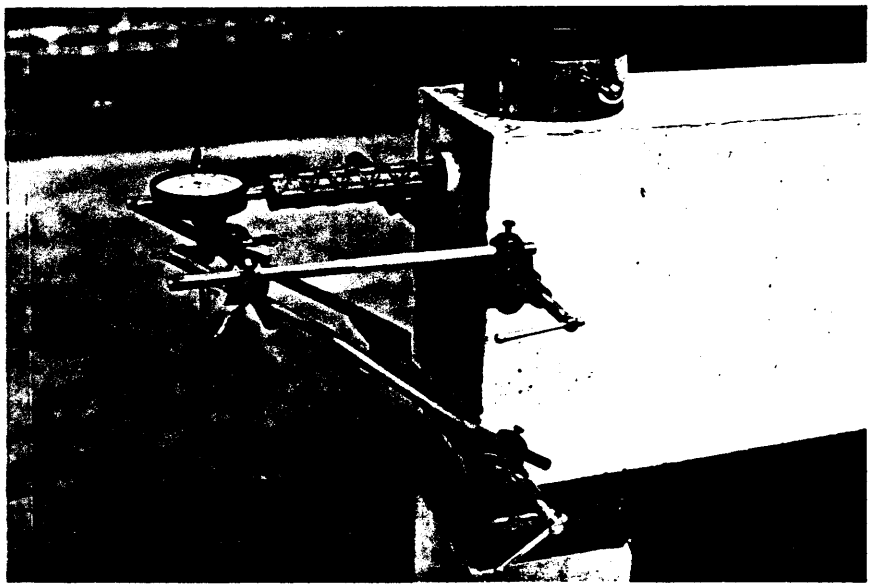

Figure 3.23 Free End Slip Gages

Under the static test mode, the objective was to slowly increase the load applied to the embedded test bar while monitoring slip at the loaded and free ends of the bar. In order to apply the load, the reinforcing bar was axially attached to a 160 ksi smooth prestressing rod of equal diameter by use of a Howlette grip coupler. The threaded end of the prestressing rod was passed through a 120 kip center hole jack and anchored with a nut. Due to the high comparative strength of the pulling rod, it remained below its yield when the reinforcing bars were loaded well above their 60^{+} ksi yield point. Thus the pulling rod was instrumented with electrical resistance strain gages to act as a load cell.

The vertical and horizontal reaction bearings at the specimen loaded end were independent pintle pin bearings, which facilitated alignment and assured consistent reaction force location. The vertical reaction at the specimen free end consisted of a spherical bearing and a second hydraulic jack which served a dual function. First, the jack could be adjusted to provide reaction at the proper vertical elevation and thus facilitate initial alignment of the specimen. Second, as load was applied to the embedded bar, the reaction jack could be extended to maintain proper rotational alignment of the specimen. During the test, cracking of the concrete causes natural curvature of the specimen. The specimen was initially leveled and a sensitive bubble level placed on the specimen at the loaded end. As loading was increased, the concrete face of the loaded end was maintained perpendicular to the bar pulling direction by not allowing rotation of the loaded end. This was accomplished by extending the vertical reaction jack to compensate, in effect,

for specimen deflection over its "half length." Simultaneously, deflections of the test frame were accommodated in the same manner.

Bar slips were measured using 0.0001 inch dial gages. At the free end, the gage was mounted on the concrete with the probe against the end of the reinforcing bar. At the loaded end, two gages were attached to the bar using a ring and set screws, with the probes against the concrete face. A second pair of gages, mounted in tandum with the slip gages, measured bar elongation over a gage length equal to distance between the slip gages and the beginning of the bonded length. Net slip could then be determined as the difference between the two sets of movements.

Loads were generally applied in increments of 2 kips (4.5 ksi) to the No. 6 bars and in increments of 7.5 kips (4.8 ksi) to the No. 11 bars until yielding occurred. Thereafter, the increments of increase were reduced somewhat. Loading was terminated either upon pullout, in the case of short embedment specimens, or upon reaching 125 to 140% of bar yield in the case of long embedment lengths.

Loads were held at each increment until slip movements stabilized. After application of each increment, slip measurements were recorded and initiation or progress of concrete cracking was marked on the specimen surface. The test duration varied somewhat but generally was approximately 3 hours.

3.10 Bond Fatigue Test Equipment and Procedures

For the bond fatigue tests, the static test frame was modified by replacing the hydraulic jack used to load the test bar with a 50 kip actuator, as shown in Figures 3.24 and 3.25. Instrumentation remained essentially the same as for the static bond test except the

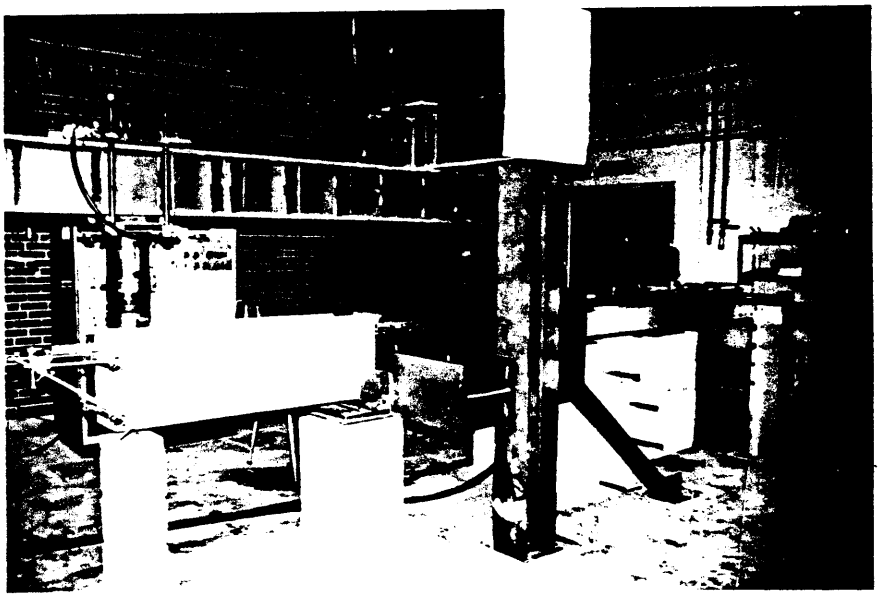

Figure 3.24 General View of Beam End Specimen Fatigue Test Set-up

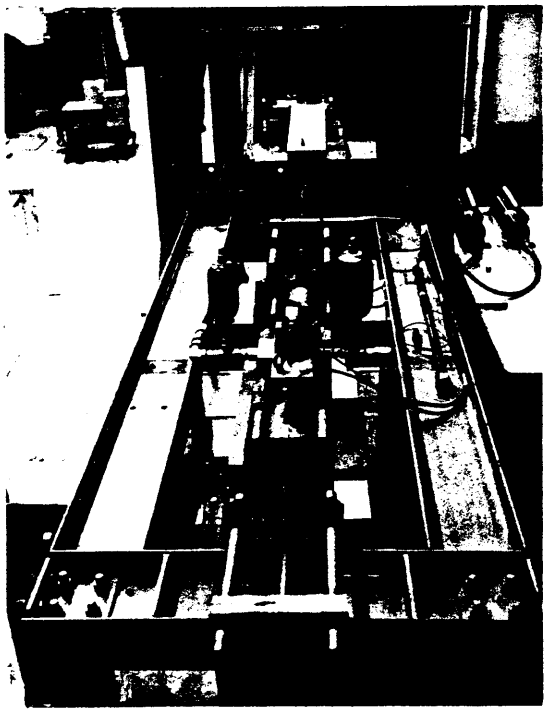

Figure 3.25 Fatigue Load Actuator

load was controlled through an actuator mounted electronic load cell. The pull rod load cell was used for confirmation of the load.

The loading pattern involved cycling from a low level of tension load in the bar to a higher tension level. The low level was chosen to be representative of dead load stresses while the high level was representative of total service load stresses. A sine wave loading function was utilized with a frequency of 1.0 cps for the first 10 cycles, 1.5 cps from 10 to 1000 cycles and 2.5 to 2.7 cps thereafter. Total cycles, up to 1,400,000, varied, but companion specimens were generally subjected to identical loading histories. Details of the loading magnitudes and number of cycles are presented with the test results in Chapter 6.

During the course of the fatigue tests, the loaded end and free end bar slips were monitored. Readings were taken, as a minimum, after 1, 10, 100, 1000, 10,000 and 50,000 cycles and at approximately 100,000 cycle intervals thereafter. In the case of the No. 11 bar specimens, the readings were taken more frequently.

After completion of the desired number of loading cycles, the specimen was subjected to a monotonic static loading until failure. Concrete crack propagation and bar slips were monitored versus applied load.

4. PRESENTATION AND ANALYSIS OF RESULTS FOR SLABS

4.1 Introduction

In this chapter, results of the slab specimen tests are presented and analyzed. The slab specimens with normal mill scale bars were designated SC-6M-35-A, B and C while those with epoxy coated bars were designated SC-6E-35-A, B and C. All specimens were subjected to a static midspan loading, as previously described, which was gradually increased until failure occurred. While the general behavior of all specimens was basically similar, some differences were noted. Thus, comparative performance of the specimens is considered in terms of cracking and deformations, ultimate strength and bar anchorage.

4.2 Cracking and Deformation

Initial cracking behavior in all slab specimens was similar. The first crack to occur was a flexural crack located approximately at midspan, the point of maximum bending moment. The midspan loads corresponding to initiation of the first crack are given in Table 4.1. The average cracking load, P_{cr}^{M}, of the mill scale bar specimens was 4% higher than the average cracking load, P_{cr}^{E}, of the epoxy coated bar specimens. On an average, the concrete modulus of rupture was 614 psi for the mill scale bar specimens and 590 psi for the epoxy coated bar specimens. This difference was consistent with splitting strengths, although contrasting with the differences in compressive strength as noted in Chapter 3.

Table 4.1 Cracking and Ultimate Strengths of Slab Cracking (SC) Specimens

Specimen	Cracking Load, P_{cr}			Ultimate Load, P_u		
	P_{cr} (kips)	$P_{cr}^{avg.}$ (kips)	P_{cr}^{M}/P_{cr}^{E}	P_u (kips)	$P_u^{avg.}$ (kips)	P_u^{M}/P_u^{E}
SC-6M-35-A	13.5	14.8	1.04	63.0	60.5	1.04
SC-6M-35-B	14.5			58.5		
SC-6M-35-C	16.5			60.0		
SC-6E-35-A	14.0	14.2		58.5	58.0	
SC-6E-35-B	13.5			57.0		
SC-6E-35-C	15.0			58.5		

Cracking patterns for the slab specimens are shown in photographs compiled in the Appendix Figures 10.1 and 10.3 through 10.8. As loading increased, two additional flexural cracks developed with one on each side of the midspan crack. The distance between these principal tension face cracks varied but was generally on the order of 8 inches. No significant difference in spacing could be detected as a function of coated versus uncoated bars.

As the loading approached the failure load, the crack widths increased and other secondary scattered flexural cracks occurred. At or shortly before failure, some of the specimens developed diagonal tension cracks typical of shear failures. Two specimens, SC-6M-35-C and SC-6E-35-C primarily exhibited shear failures although in significant flexural distress as well. The other four specimens primarily exhibited flexural failures with compression zone concrete crushing after significant steel yielding although some evidence of shear distress was also apparent. Nevertheless, the mode of failure (shear versus flexure) did not appear to be related to coated versus uncoated bar condition.

Load versus deflection curves are presented in Figure 4.1 for midspan deflection and in Figure 4.2 for average quarter span deflection. In terms of deflections, three observations can be made. First, after cracking, the stiffness decreased slightly, as would be expected. Second, below a load of approximately 35 to 40 kips, very little difference can be detected between the specimens. Third, above P = 35 to 40 kips, individual results are mixed; however, the average deflection of the epoxy coated bar specimens is somewhat greater, 6% at P = 45 kips and 20% at

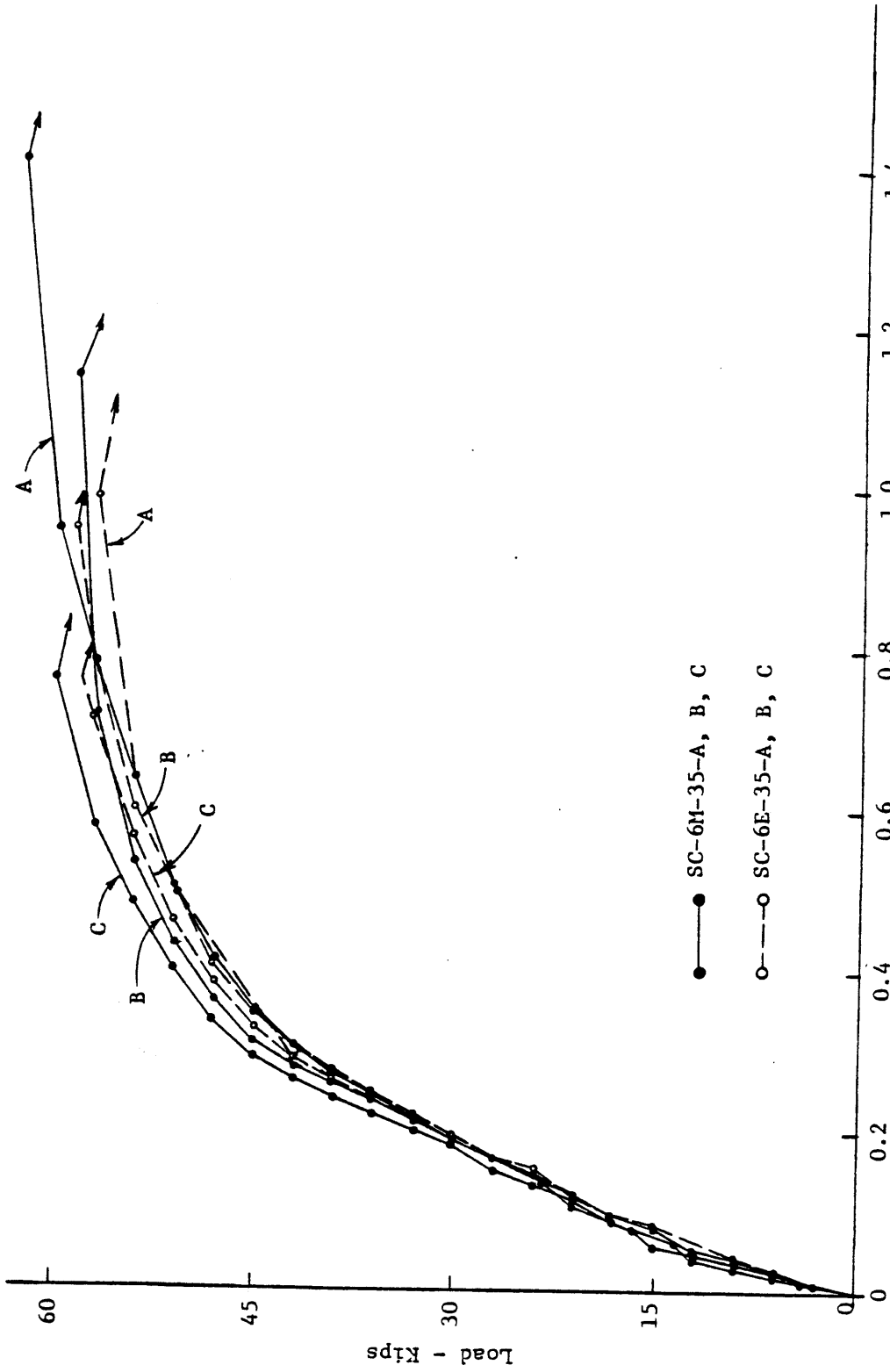

Figure 4.1 Slab Load versus Midspan Deflection

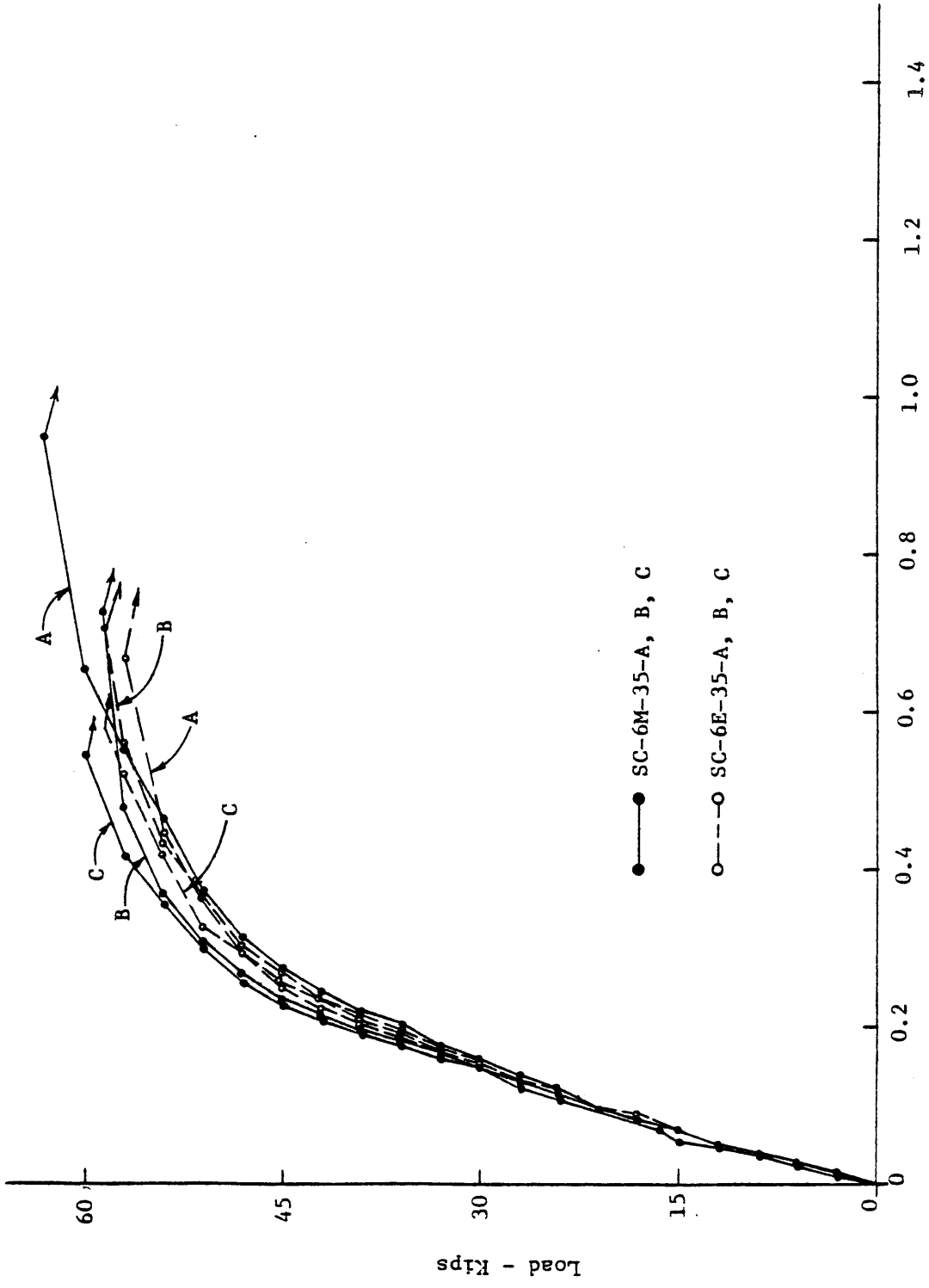

Figure 4.2 Slab Load versus Average ¼ Span Deflection

P = 54 kips, than the average deflection of the mill scale bar specimens.

The elongation of the tension face of the concrete slabs was measured using a Whittimore extensometer, as described in Section 3.8. The measurements were made between points spaced longitudinally at 4" on center initially. The accumulation of these extensions over a 3 foot length centered at midspan represented the tension face elongation due primarily to the crack openings and, to a much lesser extent, the uncracked concrete tensile strain between cracks. A comparison of these elongations versus load is presented in Figure 4.3. The elongations were generally greater for the specimens with epoxy coated bars, averaging 20% greater at both a load of 45 kips and a load of 54 kips. There is of course a direct relation between these surface elongations, bending deformations and the deflections of the slab presented in Figures 4.1 and 4.2, and the comparative performance was reasonably consistent.

4.3 Ultimate Strength

A comparison of midspan ultimate load, P_u, corresponding to specimen failure is presented in Table 4.1. The mill scale bar specimens (SC-6M) averaged 4% higher strength than the specimens with epoxy coated bars (SC-6E). Several factors should be considered in evaluating this strength difference where the failures were a mixture of flexure and shear failures.

The flexural strength of a reinforced section is primarily a function of the steel provided. For all specimens, the number, size

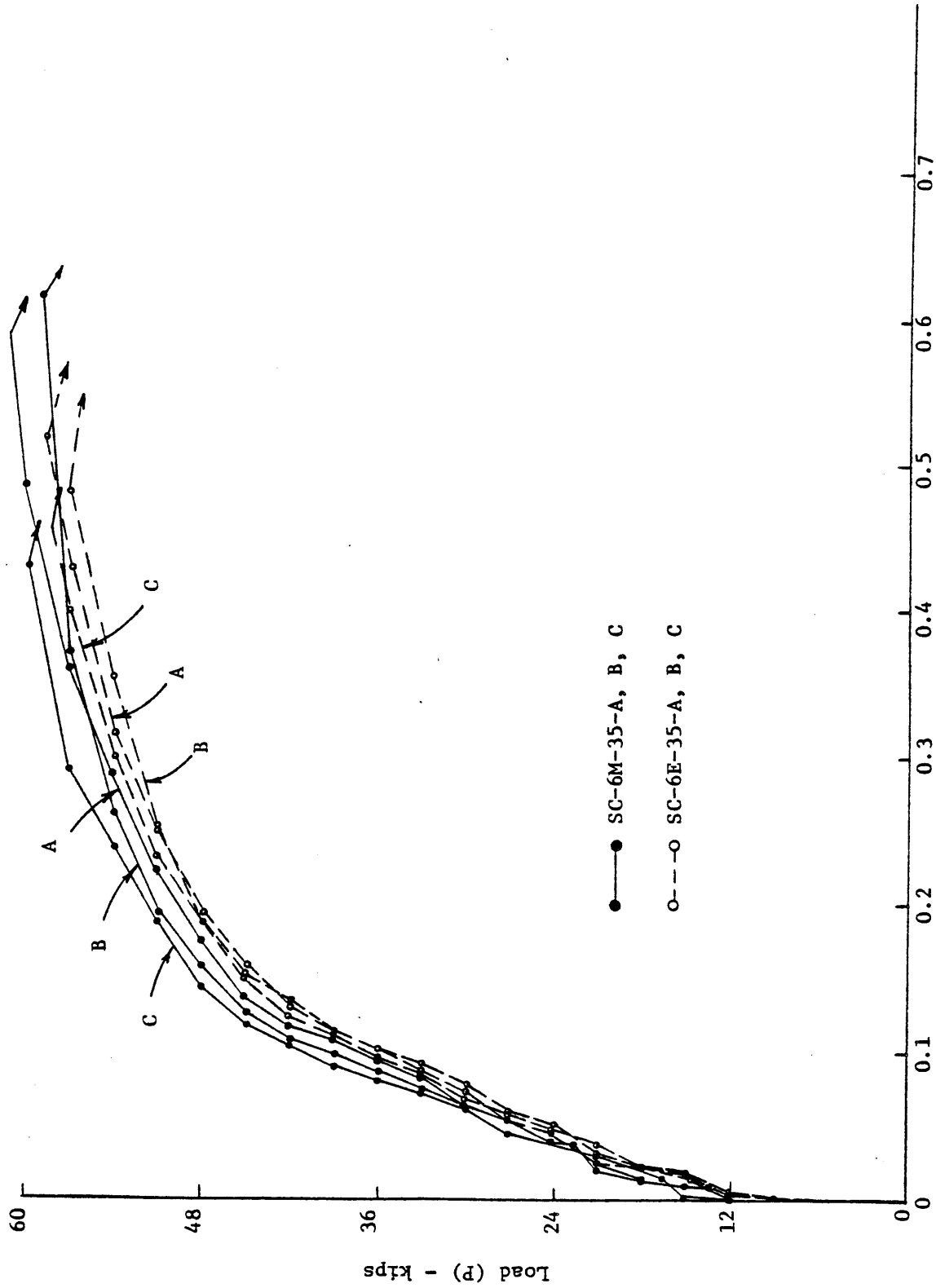

Figure 4.3 Slab Load versus Tension Face Elongation

and location of bars was essentially identical. The strength of the No. 6 bars was the same whether coated or uncoated. Thus, bar strength does not appear to be the source of the difference. The flexural strength is also a function of the concrete compressive strength; however, comparatively large increases in compressive strength normally produce only a small increase in flexural strength. The concrete mixes were the same for all specimens, but the cylinder compressive strengths were higher for the epoxy coated bar specimens. Since the epoxy coated bar slab specimens had slightly lower strength than the mill scale bar specimens, this difference is not attributable to concrete compressive strength differences. Indeed, the opposite would have been expected.

Many factors contribute to the shear strength of a section subjected to bending and shear. Among these, concrete tensile strength has a major influence. Usually, concrete tensile strength is directly related to compressive strength. However, for the SC-6M specimens, the compressive strength was lower while the splitting strengths were higher when compared to the SC-6E specimens. Thus, clear conclusions are more difficult. This disparity may have been due to problems in sampling or other reasons. Since the slab modulus of rupture and the cylinder splitting strength were slightly higher for the SC-6M specimens, this may have contributed to the slightly greater ultimate strengths of the SC-6M specimens versus the SC-6E specimens.

A comparison of calculated versus test ultimate strengths is presented in Table 4.2. Nominal ultimate strengths, without capacity

Table 4.2 Comparison of Calculated versus Test Ultimate Strengths for Slab Cracking (SC) Specimens

Condition	Material Strength (psi)	Calculated				Test
		M_n (ft-k)	P_{mn} (k)	V_n (k)	P_{vn} (k)	P_u (k)
Design Min.	f_y=60000 f'_c= 4500	31.8	31.8	16.9	33.8	-
Mill Scale	f_y=63600 f'_c= 6050	34.3	34.3	19.6	39.2	60.5
Epoxy Coated	f_y=63600 f'_c= 6684	34.5	34.5	20.6	41.2	58.0

reduction factor (ϕ), were calculated for bending, M_n, and for shear, V_n. These strengths were then converted to equivalent midspan loads, P_{mn} and P_{vn}, respectively. For bending, the ACI rectangular stress block was assumed, and for shear, the strength was assumed based upon

$$V_n = V_c = 2\sqrt{f'_c}\ bd.$$

Three material property condition sets were considered in the comparisons. The Design Min. condition refers to NCDOT minimum specification requirements used for design while Mill Scale and Epoxy Coated refer to actual material properties for the specimens. In each case, the ultimate strength from the test is substantially higher than the calculated nominal ultimate strengths. This is to be expected since the strain hardening range of steel strength is ignored in calculation, and the shear strength representation is conservatively approximate. Analysis revealed that the reinforcing was near its rupture strength at failure.

Several observations can be made from the results. First, the calculated capacities based upon design minimums are approximately equal for bending and shear, which confirms the validity of the test model. Second, the calculated nominal ultimate capacity of the deck slab specimens is in the range of 31 to 35 kips of load. Working levels of load would normally be approximately 40 to 60% of the nominal strength or 13 to 20 kips. In both these ranges, the load-deflection response of mill scale and epoxy coated specimens was approximately equal, as shown in Figures 4.1 and 4.2.

4.4 Bar Anchorage

The slab longitudinal reinforcing was extended 11.5 inches beyond the support to provide anchorage, as shown in Figure 3.2a. Slip of the center top bar was measured by dial gages clamped to each end of the concrete section. The average slip for the SC-6M and SC-6E specimens is presented in Figure 4.4. In both cases, the recorded slips were well below the usual free end critical slip limit of 0.002 in. However, the slip of the epoxy coated reinforcement was greater than for the mill scale reinforcement. Also, slip initiated at a lower load level for the epoxy coated bars than for the mill scale bars.

It is probable that the larger slip of the epoxy coated reinforcement contributed to the larger deflections and wider cracks observed in the SC-6E specimens. The resulting larger strains and rotations of the SC-6E specimens could also contribute to slightly earlier cracking of concrete and failure at a lower load level.

4.5 Conclusions from Slab Cracking Tests

For specimens and loadings representative of concrete bridge deck slabs, the following comparative conclusions can be made between mill scale and epoxy coated reinforcing:

1. No difference was found in terms of crack spacing for the short span specimens.
2. At working stress levels and even up to yield of of the reinforcement, little difference was noted in terms of deflection or crack widths. Deflection and crack widths of the epoxy coated bar specimens may have been slightly but not significantly larger.

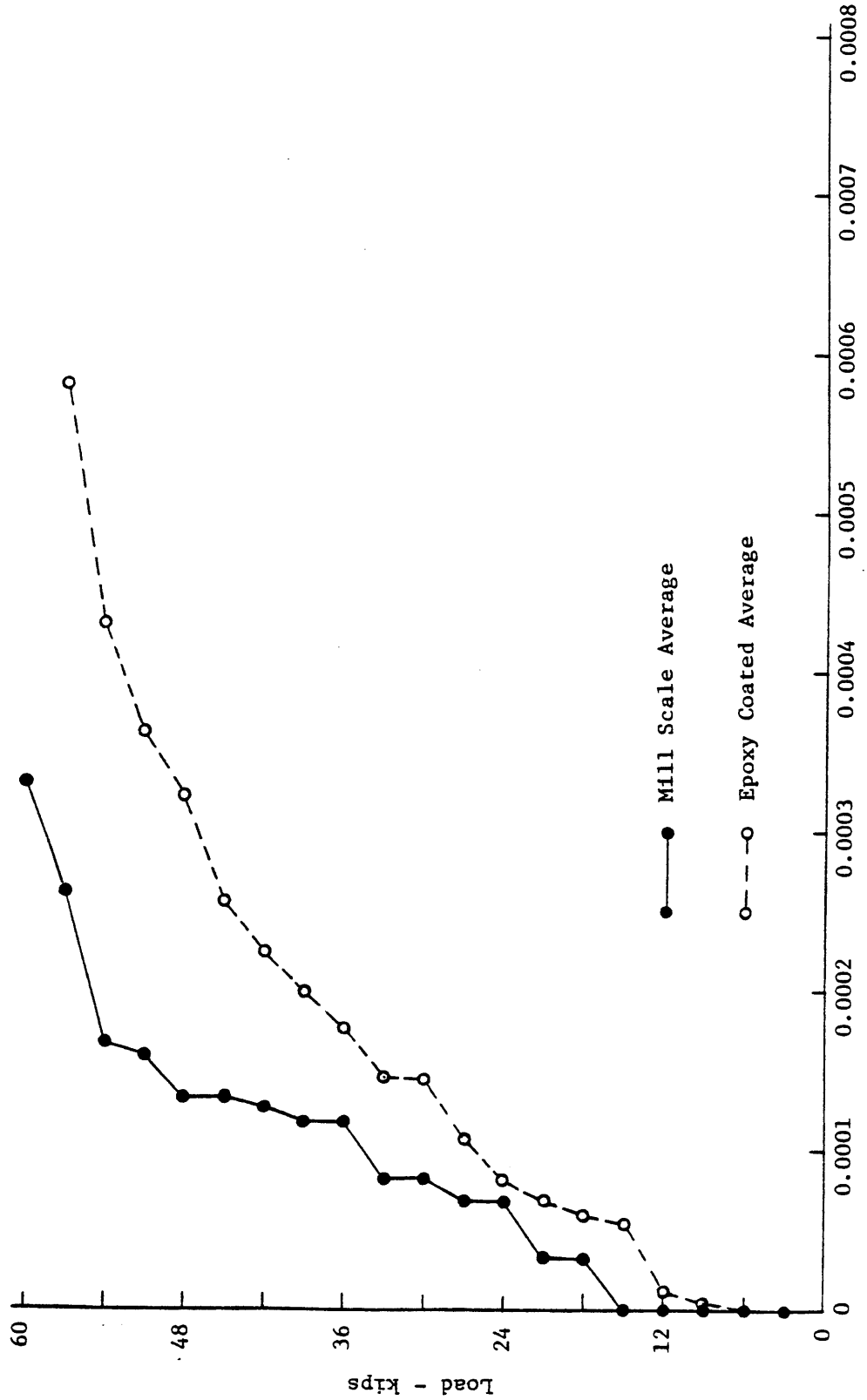

Figure 4.4 Slab Load versus Center Bar End Slip

3. At post yield load levels, the epoxy coated bar specimens exhibited greater deflection and larger crack widths.
4. The mill scale bar specimens failed at a load level averaging 4% higher than the epoxy coated bar specimens.

5. PRESENTATION AND ANALYSIS OF RESULTS FOR BEAM END STATIC TESTS

5.1 Introduction

In this chapter, results of the beam end specimen static bond tests (Series BS) are presented and analyzed. The principal variables for this series of tests were bar surface condition (mill scale, epoxy coated or blast cleaned), embedment length and bar size (No. 6 or No. 11). Neither concrete maturity and strength nor epoxy coating type and thickness were intended variables. A total of 26 specimens were included in the BS series.

Comparative performance of the specimens is considered in terms of general behavior, specimen cracking, load-slip relationships and strength under various criteria.

5.2 Specimen Behavior and Cracking

5.2.1 General Behavior

Load was gradually applied to the bar in increments until either the bar began to pull out of the specimen or until the bar stress reached 1.25 to 1.40 times the yield stress of the bar, as indicated in Table 5.1. Pull out was indicated when the free end of the bar moved rapidly and at the same rate as the loaded end.

During the tests, the specimen was repeatedly examined for cracks. The bar tension load increment at which each crack became visible was marked adjacent to the crack and this process repeated to mark crack progress at each subsequent increment. Cracking patterns for the beam end static specimens are shown in photographs compiled in Appendix Figures 10.2 and 10.9 through 10.34.

Table 5.1 Beam Static Specimen Loads and Stresses at End of Test

Specimen	Bar Force (k)	Bar Stress (ksi)	Bond Stress (psi)	Note*
BS- 6M- 8-A	33.0	75.0	1750	t
BS- 6M- 8-B	33.5	76.1	1777	P>Y
BS- 6E- 8-A	28.0	63.6	1485	P>Y
BS- 6E- 8-B	29.0	65.9	1538	P>Y
BS- 6M-13-A	33.0	75.0	1077	t
BS- 6M-13-B	38.0	86.4	1241	t
BS- 6E-13-A	37.0	84.1	1208	t
BS- 6E-13-B	38.0	86.4	1241	t
BS- 6B-13-A	38.0	86.4	1241	t
BS- 6M-18-A	36.0	81.8	849	t
BS- 6M-18-B	38.0	86.4	896	t
BS- 6E-18-A	38.0	86.4	896	t
BS- 6E-18-B	38.0	86.4	896	t
BS-11M-16-A	99.8	64.0	1408	P>Y
BS-11M-16-B	97.5	62.5	1376	P>Y
BS-11E-16-A	88.5	56.7	1249	P<Y
BS-11E-16-B	80.0	51.3	1129	P<Y
BS-11M-24-A	120.0	76.7	1129	t
BS-11M-24-B	119.0	76.3	1119	t
BS-11E-24-A	117.5	75.3	1105	t
BS-11E-24-B	110.0	70.5	1034	P>Y
BS-11B-24-A	120.0	76.9	1128	P>Y
BS-11M-30-A	120.0	76.9	903	t
BS-11M-30-B	120.0	76.9	903	t
BS-11E-30-A	120.0	76.9	903	t
BS-11E-30-B	120.0	76.9	903	t

*P<Y = Test ended when bar pulled out at load below yield.

P>Y = Test ended when bar pulled out at load above yield.

t = Test terminated at force and stresses indicated (Usually above 1.25 f_y).

Two primary types of cracking were noted. The first was flexure-shear cracking where a transverse crack first appeared on the top (tension) face and migrated under increasing load vertically down the two side faces. The influence of shear gradually changed the crack slope until it was approximately 45 degrees. This type of cracking is typical of negative moment regions of continuous beams near supports. Alternately, if the section is envisioned turned over, it is similar to flexure-shear cracking in simply supported beams.

The second type of cracking was bond splitting where a longitudinal crack formed in the cover of the top face directly above the test bar. This type of cracking began at the loaded end of the embedment length and migrated toward the free end. The splitting was due to wedging action of bar deformations against the concrete as the bar became mobilized. At both ends of the splitting crack, two diagonal cracks often appeared on the top face in the unbonded regions. These secondary diagonal cracks resulted from local shear stresses in the unbonded region. The shear stresses were induced by lateral movement of the cover in the bonded region due to the wedging action of bar interlock.

A tabulation of the loads at which splitting cracks were first noted is presented in Table 5.2. A ratio of the average bond stress for the mill scale bar, μ_M, to the average bond stress of the epoxy coated bar, μ_E, or the blast cleaned bar, μ_B, is tabulated to compare splitting cracking in specimens of equal embedment length. A similar ratio for bar force, T, is tabulated to compare loads at flexural cracking. This table and the photographs in the Appendix will serve as reference in the following evaluation of the effects of blast cleaning, epoxy coating, embedment length and bar size.

Table 5.2 Beam Static Specimen Splitting and Flexural Cracking Loads

Specimen	Splitting Load				Flexural Cracking Load		
	Bar Force (k)	Bar Stress (ksi)	Bond Stress (psi)	$\frac{\mu_M}{\mu_{E,B}}$	Bar Force (k)	Bar Stress (ksi)	$\frac{T_M}{T_{E,B}}$
BS- 6M- 8-A	*	-	-		29.0	65.9	
BS- 6M- 8-B	33.5	76.1	1777	1.18	29.0	65.9	1.04
BS- 6E- 8-A	28.0	63.6	1485		28.0	63.6	
BS- 6E- 8-B	29.0	65.9	1538		28.0	63.6	
BS- 6M-13-A	*	-	-		14.0	31.8	
BS- 6M-13-B	*	-	-	-	*	-	-
BS- 6E-13-A	*	-	-		*	-	
BS- 6E-13-B	*	-	-		22.0	50.0	
BS- 6B-13-A	*	-	-	-	36.0	81.8	-
BS- 6M-18-A	*	-	-		*	-	
BS- 6M-18-B	*	-	-	-	*	-	-
BS- 6E-18-A	*	-	-		*	-	
BS- 6E-18-B	*	-	-		*	-	
BS-11M-16-A	82.5	52.9	1164		67.5	43.4	
BS-11M-16-B	60.0	38.5	846	1.26	52.5	33.7	1.07
BS-11E-16-A	60.0	38.5	846		60.0	38.5	
BS-11E-16-B	52.5	33.7	741		52.5	33.7	
BS-11M-24-A	90.0	57.7	847		72.5	46.5	
BS-11M-24-B	75.0	48.1	705	1.57	52.5	33.7	1.28
BS-11E-24-A	60.0	38.5	564		60.0	38.5	
BS-11E-24-B	45.0	28.8	423		37.5	24.0	
BS-11B-24-A	75.0	48.1	705	1.10	52.5	33.7	1.19
BS-11M-30-A	90.0	57.7	677		52.5	33.7	
BS-11M-30-B	75.0	48.1	564	1.57	37.5	24.0	1.20
BS-11E-30-A	52.5	33.7	395		45.0	28.8	
BS-11E-30-B	52.5	33.7	395		30.0	19.2	

*Indicates no cracking at termination of test ($T > 1.25\ f_y$)

5.2.2 Effect of Blast Cleaning

Two specimens with blast cleaned bars were tested, BS-6B-13-A and BS-11B-24-A. Both flexural and splitting cracking occurred in the No. 11 blast cleaned bar specimen and the comparison mill scale specimens of the same embedment length, BS-11M-13-A and B. Neither type of cracking was noted in specimen BS-6B-24-A nor the comparison specimens BS-6M-24-A and B. Hence the data is rather limited. On an average, splitting and flexural cracking occurred at lower loads for the blast cleaned specimen. However, the loads at splitting and at flexural cracking were the same for BS-11B-24-A and BS-11M-24-B while the cracking loads for specimen BS-11M-24-A were higher. By comparison, the blast cleaned concrete cylinder splitting strength (Table 3.6) was slightly higher and the compressive strength slightly lower than for the mill scale specimens.

5.2.3 Effect of Epoxy Coating

Specimens with epoxy coated bars developed splitting cracks at significantly lower load levels and flexural cracking at somewhat lower load levels than comparable specimens with mill scale bars, as shown in Table 5.2. This relative performance could not be related to concrete cylinder compression or cylinder splitting strengths, which varied only slightly. Thus, the earlier cracking is attributed to the effect of the epoxy coating. It is possible that the adhesion component of bond is reduced by the coating. This would cause wedging action to be mobilized earlier and splitting to occur at a lower load. The reason for flexural cracking at a lower load is less clear. Possibly the flexural stresses were aggravated by local wedging stresses.

Since the epoxy coated bar specimens cracked at a lower load, the crack widths were larger than for comparison mill scale specimens at a given load. For these short specimens, no conclusions could be reached in regard to effect of the coating on flexural crack spacing.

No correlation was noted between epoxy coating thickness and cracking load; however, coating thickness was not an intended variable and the range of thicknesses was relatively small.

5.2.4 Effect of Embedment Length

Results of the No. 11 bar specimen tests presented in Table 5.2 indicate that embedment length had little effect on load at first splitting. For both mill scale and epoxy coated bars, splitting was primarily related to the bar force. Local bond stresses and wedging at the loaded end are responsible for initiating splitting. Thus, average bond stress is not a good indicator of splitting.

Results of the No. 6 bar specimens were too scattered to draw conclusions. Significant splitting cracking only occurred in the specimens with 8 in. embedment length. Even though the specimens with 13 and 18 in. embedment lengths were subjected to higher loads, bending moments and shears, the extent of flexural cracking was much less. Again it is possible that local effects of wedging and transfer of force in the 8 in. embedment specimens contributed to triggering flexural cracks.

5.2.5 Effect of Bar Size

Although there was much more cracking in the No. 11 bar specimens than the No. 6 bar specimens, it cannot be concluded that bar size in

general or bar size related to epoxy coating was the cause. Cover thickness and transverse reinforcement also varied, and each has considerable effect on splitting and bond strength (10). Furthermore, concrete cross section was the same for both bar sizes to reduce formwork. Thus, more extensive flexure and shear cracking would be expected and did occur in the No. 11 bar specimens, which were subjected to greater loads than the No. 6 bar specimens.

5.3 Load-Slip Behavior

5.3.1 General Behavior

Both loaded end and free end slips of the embedded reinforcing bar were measured using instrumentation and procedures previously described in section 3.9. The load-slip curves for the static beam end specimens (Series BS) are presented in Figures 5.1 through 5.12. Each set of curves corresponds to a single bar size and embedment length. The load axis is scaled to show both the bar stress and the average bond stress. Scales on the slip axis were selected so that the magnitudes of the traditional slip criteria, loaded end net slip = 0.010 inches and free end slip = 0.002 inches, would be equal.

Loaded end slip general behavior can be summarized in three phases based upon review of Figures 5.1, 3, 5, 7, 9 and 11. The first was below 10 to 20 ksi bar stress where initial slip was at a lower rate but gradually increasing. This initial higher resistance to slip may have been due to adhesion bond which was gradually broken at the loaded end. The second occurred above 10 to 20 ksi bar stress where slip increased nearly linearly in relation to load. In this phase, both

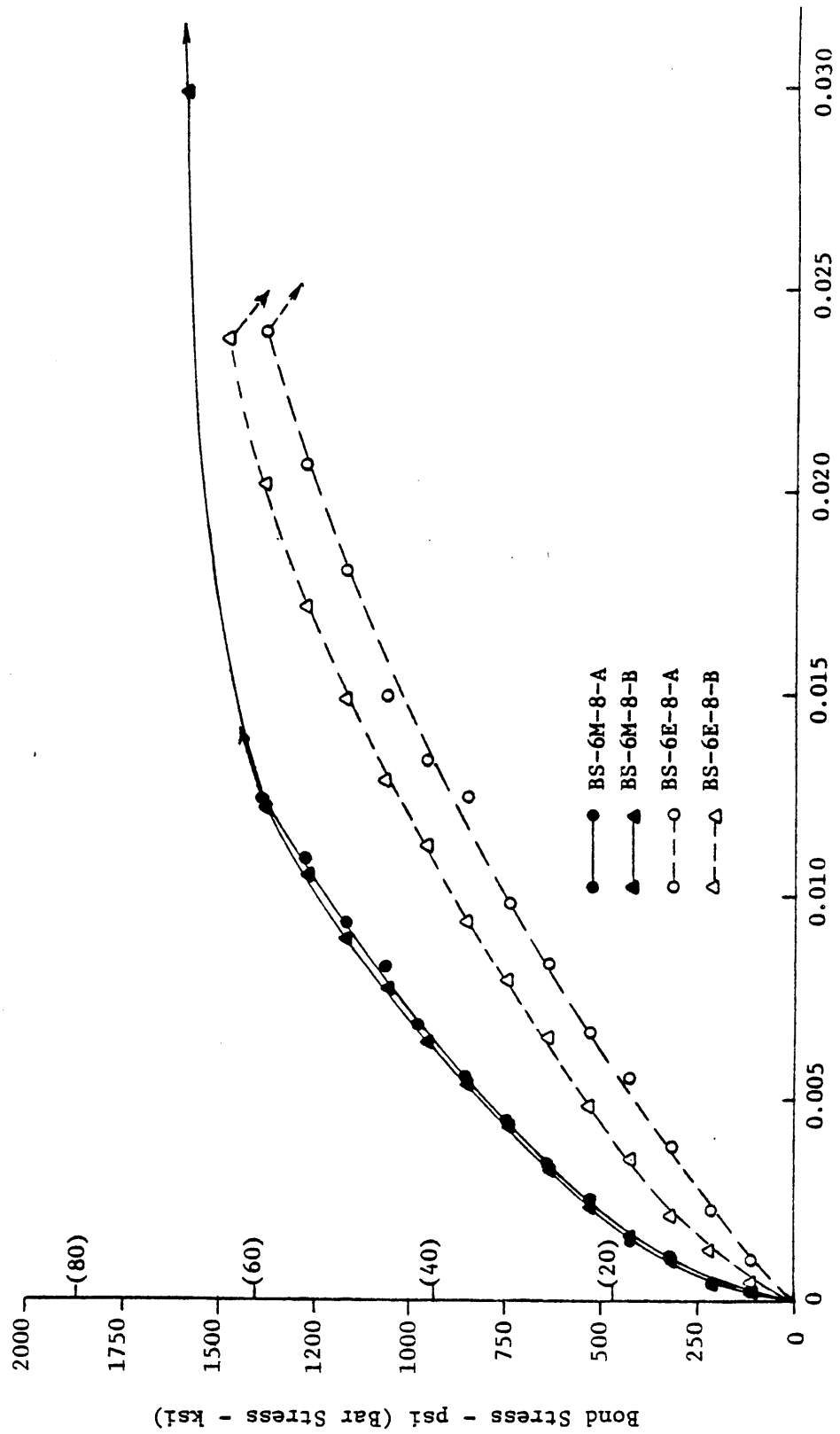

Figure 5.1 Bond Stress versus Loaded End Slip for Series BS-6x-8

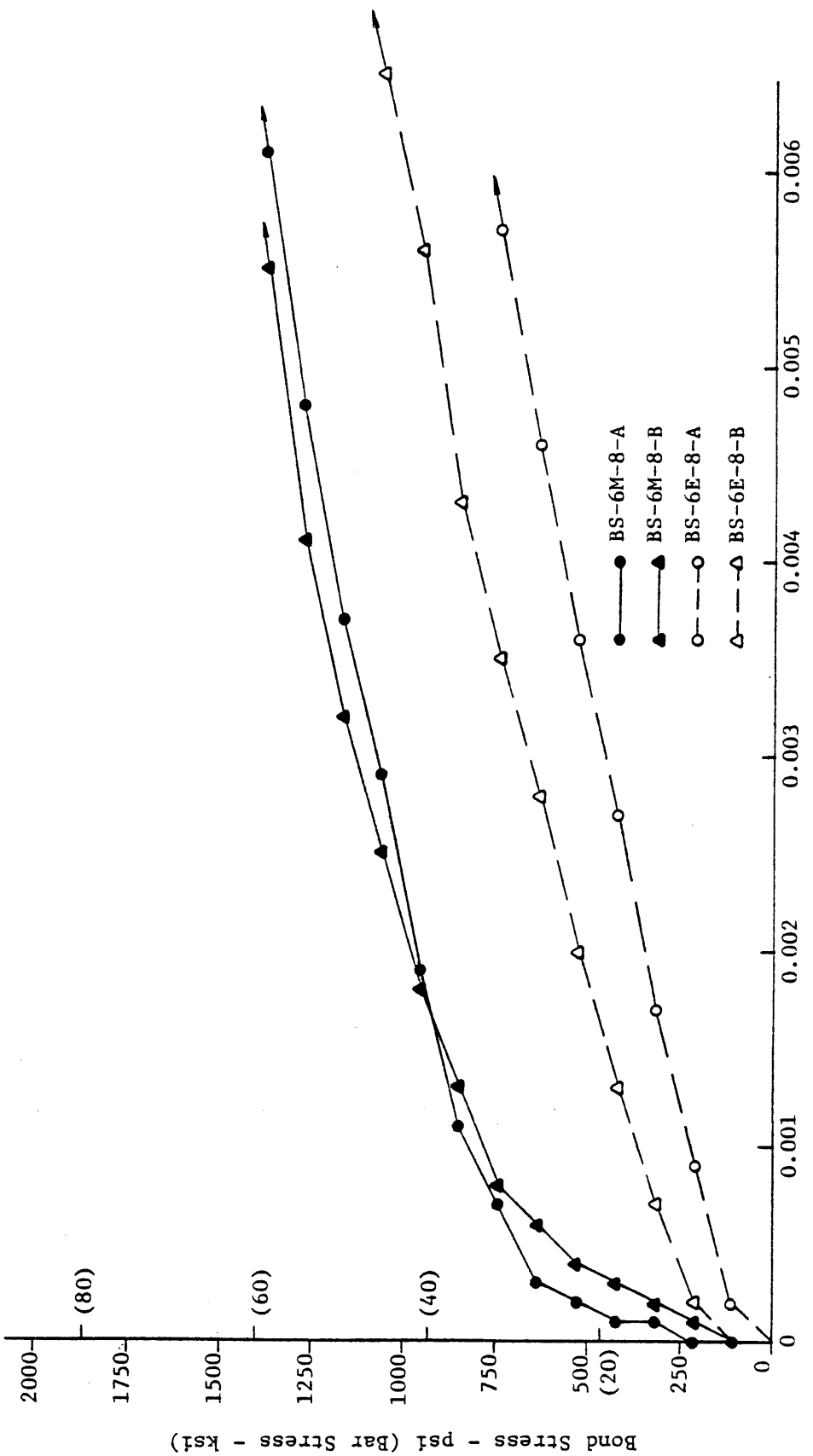

Figure 5.2 Bond Stress versus Free End Slip for Series BS-6x-8

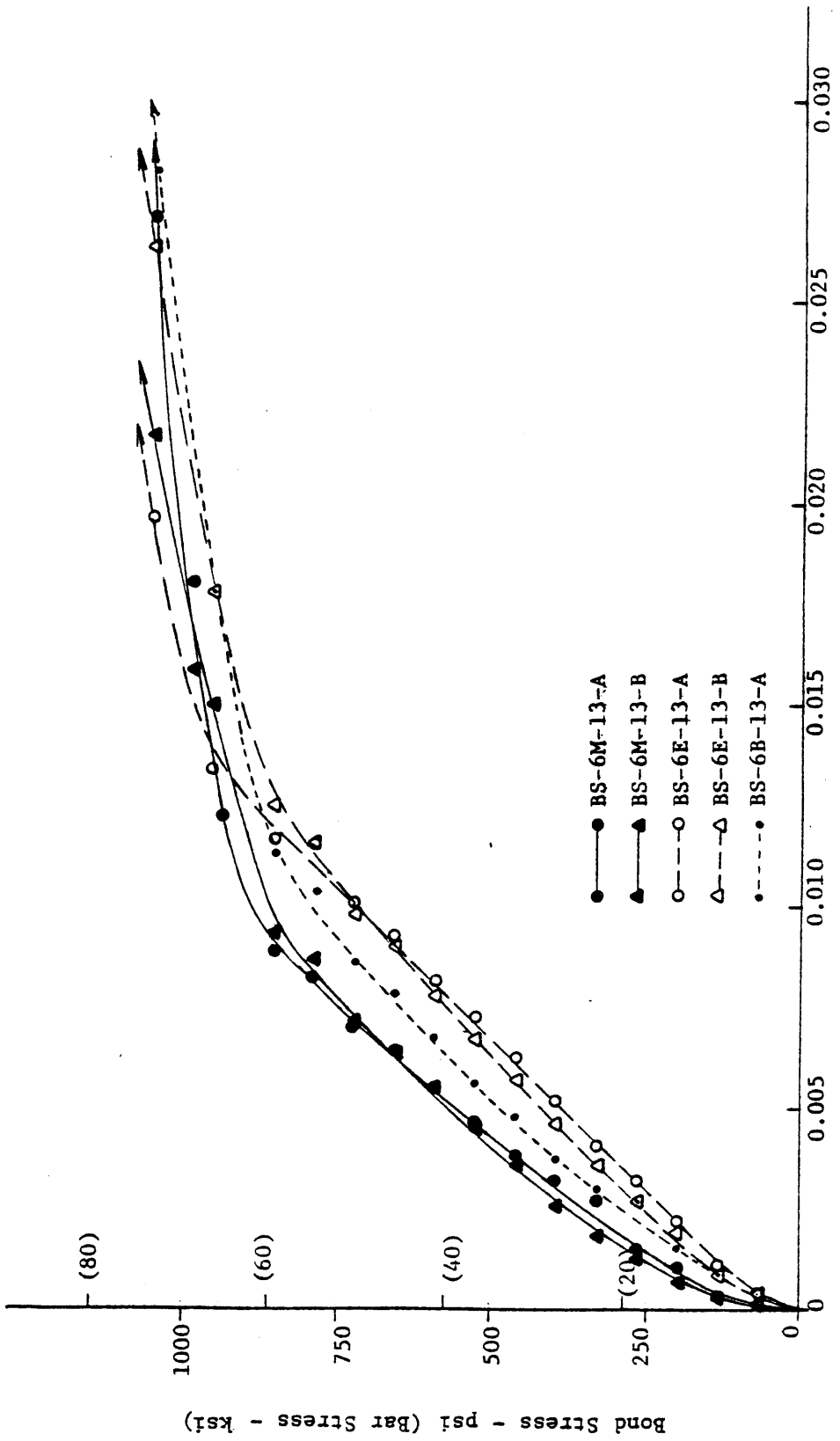

Figure 5.3 Bond Stress versus Loaded End Slip for Series BS-6x-13

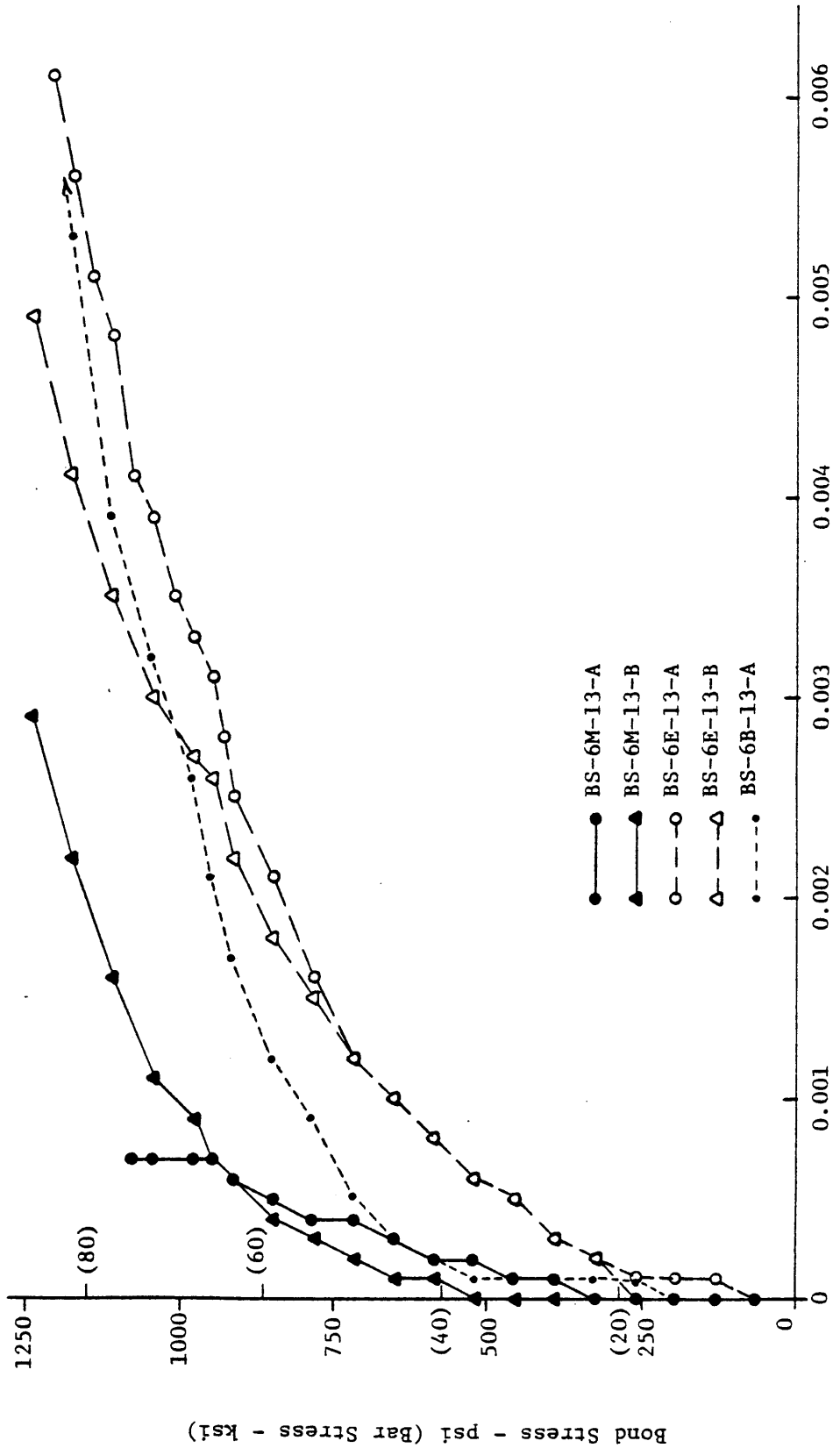

Figure 5.4 Bond Stress versus Free End Slip for Series BS-6x-13

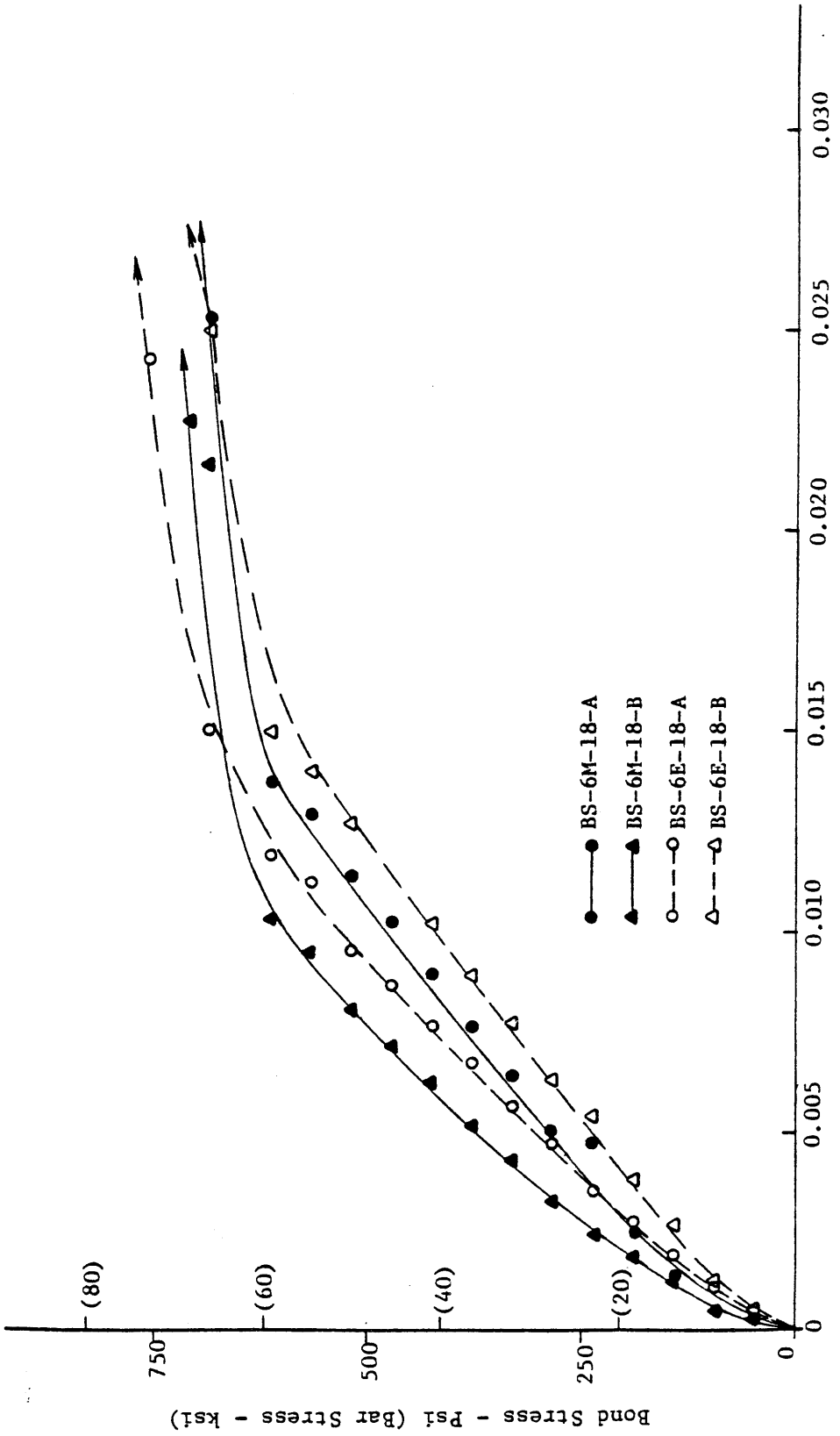

Figure 5.5 Bond Stress versus Loaded End Slip for Series BS-6x-18

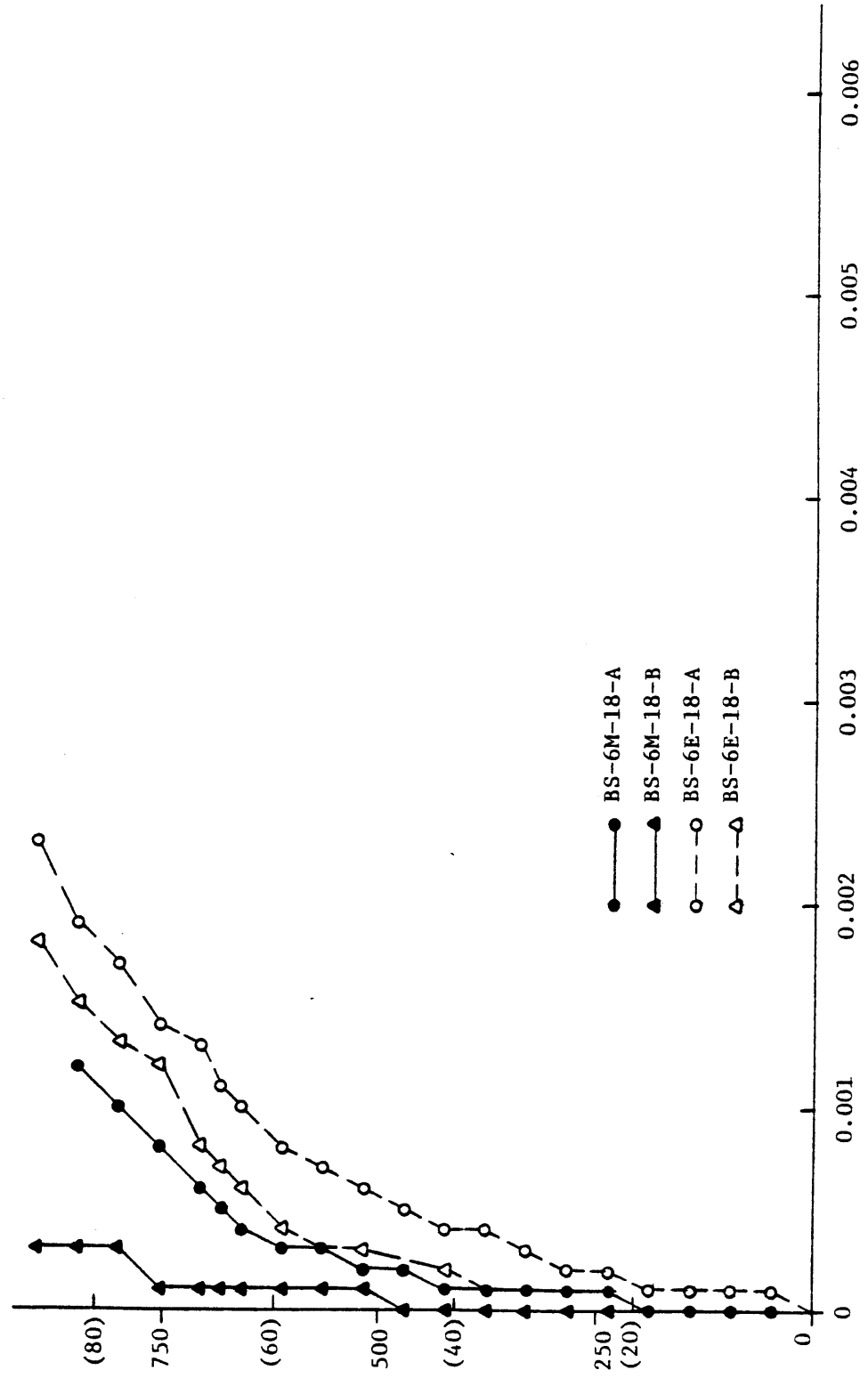

Figure 5.6 Bond Stress versus Free End Slip for Series BS-6x-18

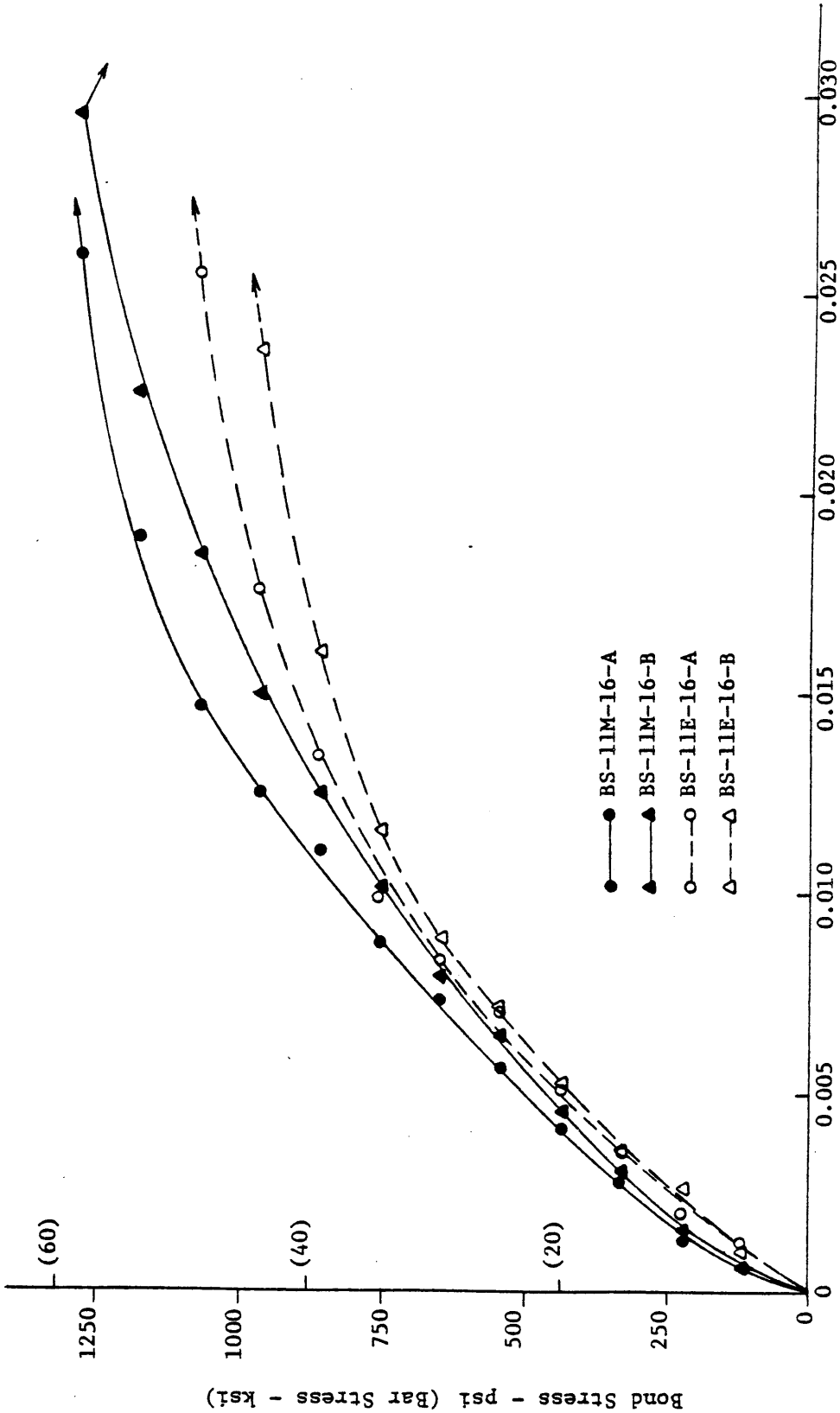

Figure 5.7 Bond Stress versus Loaded End Slip for Series BS-11x-16

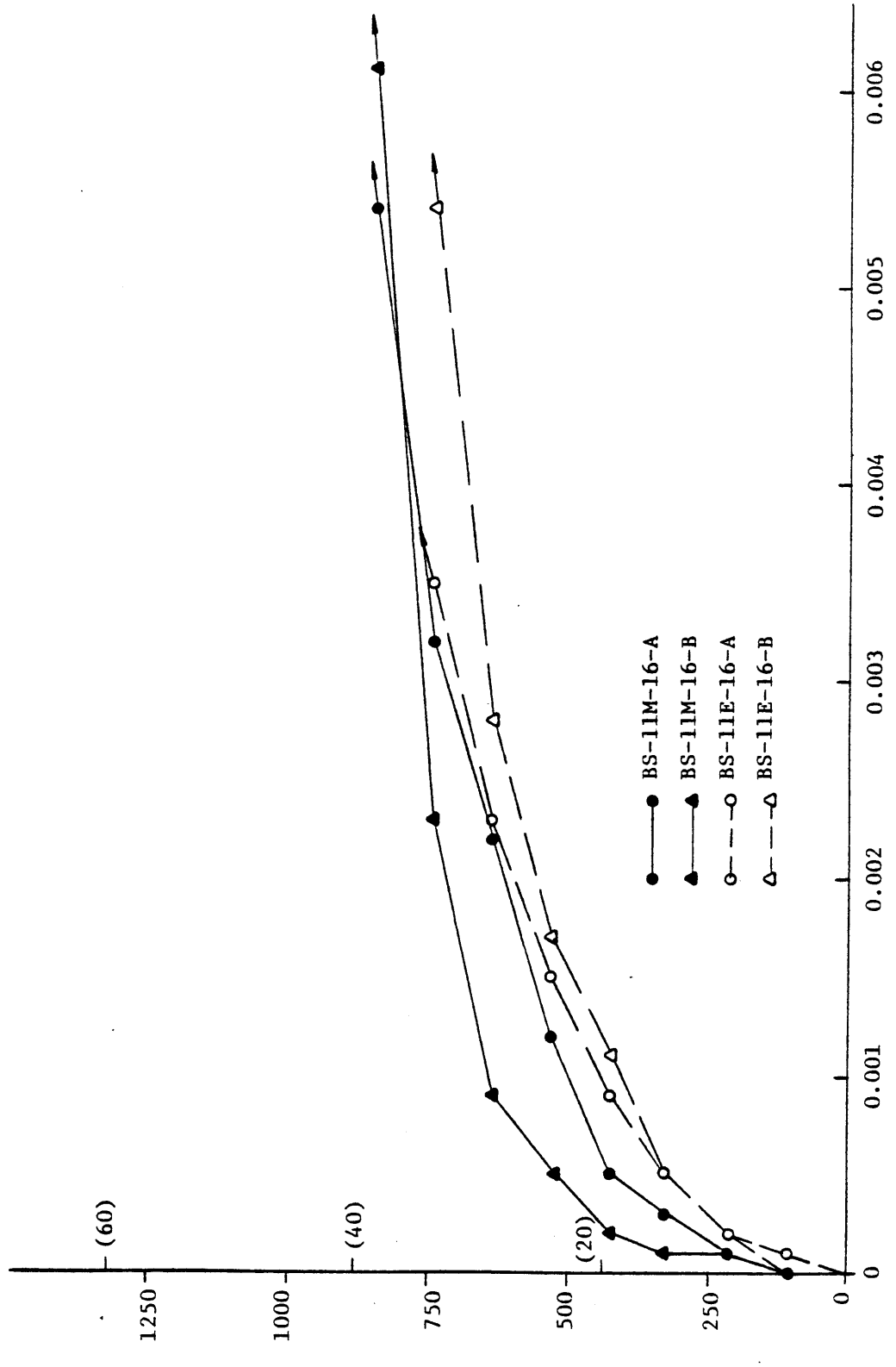

Figure 5.8 Bond Stress versus Free End Slip for Series BS-11x-16

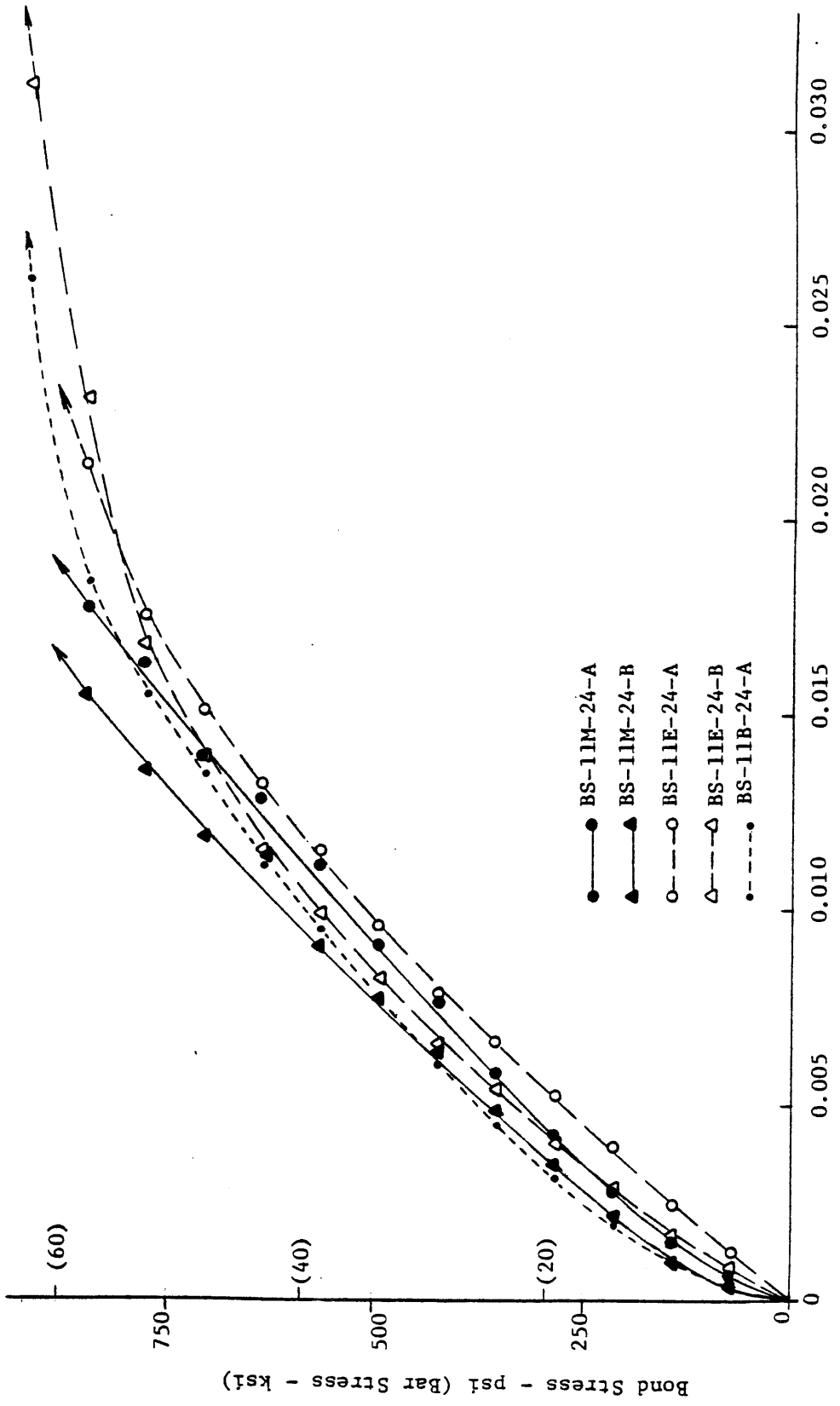

Figure 5.9 Bond Stress versus Loaded End Slip for Series BS-11x-24

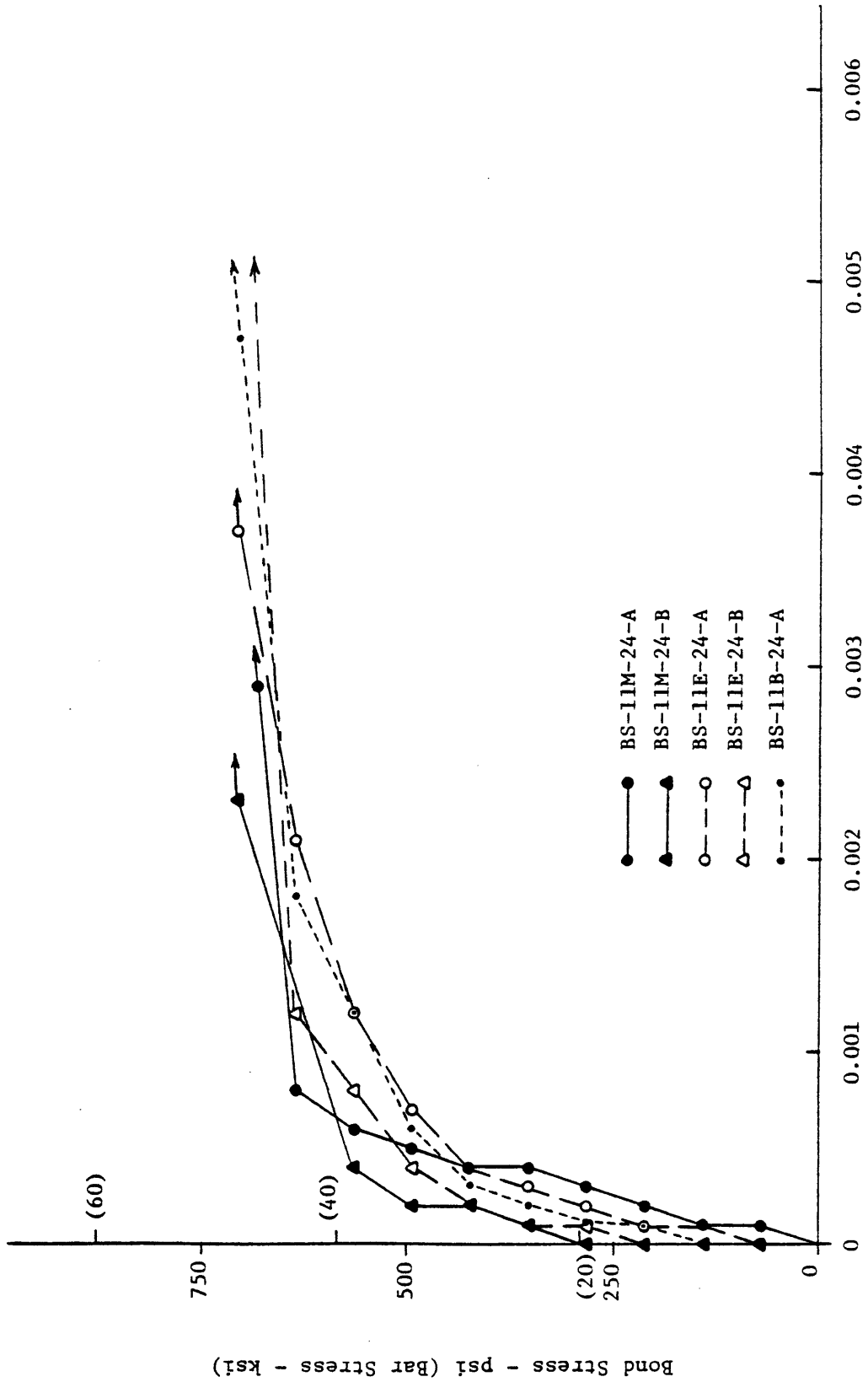

Figure 5.10 Bond Stress versus Free End Slip for Series BS-11x-24

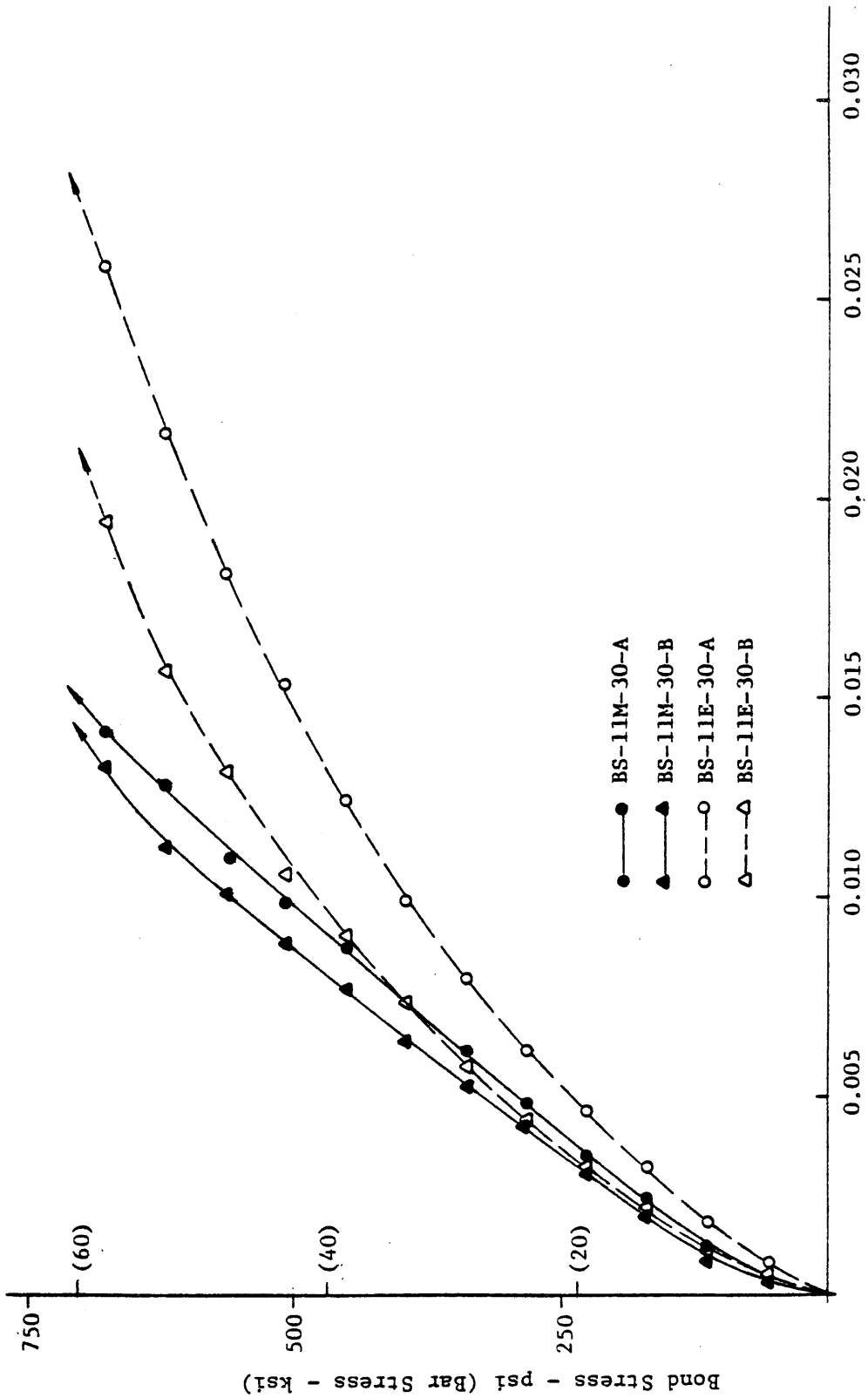

Figure 5.11 Bond Stress versus Loaded End Slip for Series BS-11x-30

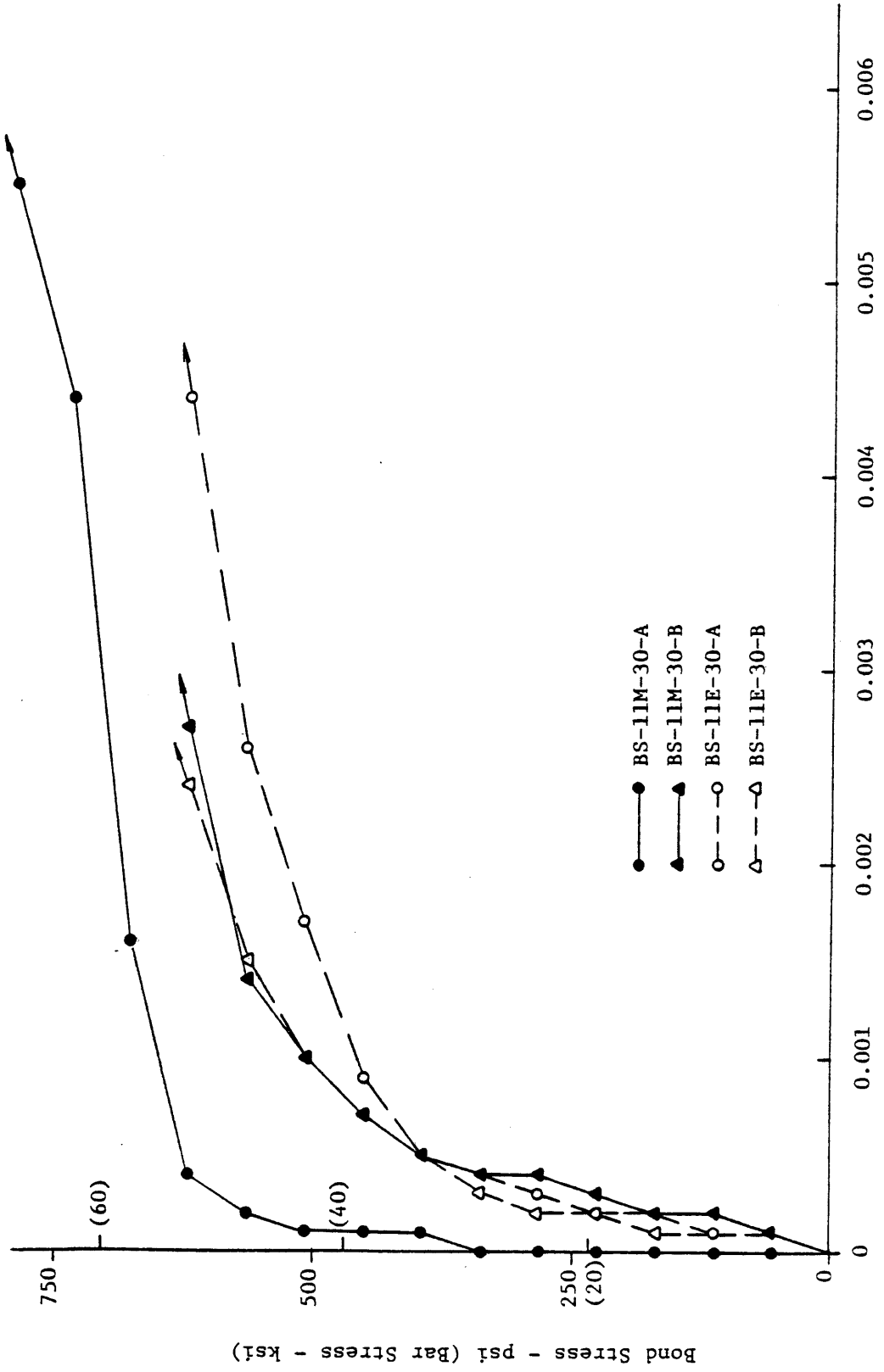

Figure 5.12 Bond Stress versus Free End Slip for Series BS-11x-30

adhesion and interlock are active in varying degrees along the embedded length. The third phase was marked by a significant increase in the rate of slip. Comparison of the curves with the splitting loads in Table 5.2 indicates that onset of higher slip rates in the third phase was usually related to the start of splitting. Yielding of the steel and the corresponding exaggeration of the Poisson effect also appeared to contribute to an increase in the rate of slip.

A comparison of average loaded end slips for various bar stress levels is presented in Table 5.3 for later discussion. The stress levels presented correspond approximately to particular load increments during the test and represent conditions at service loads, just prior to yield and post yield. It should be noted that loaded end slip measurements at the 73 ksi level are considered to be approximate. Since post-yield plastic bar elongation is variable, the calculated post-yield net loaded end slips are subject to some error.

Free end slip general behavior was more varied, but in most tests little if any slip was recorded under low loads, as shown in Figures 5.2, 4, 6, 8, 10 and 12. As loading increased and splitting occurred, free end slip increased significantly. A comparison of free end slips for various bar stress levels is presented in Table 5.4.

5.3.2 Effect of Blast Cleaning

The effect of blast cleaning on load-slip behavior is illustrated in Figures 5.3, 5.4, 5.9 and 5.10. Two blast cleaned specimens were tested, BS-6B-13-A and BS-11B-24-A. These can be compared with mill scale specimens BS-6M-13-A & B and BS-11M-24-A & B, respectively. The

Table 5.3 Comparison of Loaded End Slip at Various Stress Levels for BS Specimens

Specimen	Average Loaded End Slip at Bar Stress Level											
	At 28 ksi			At 45 ksi			At 59 ksi			At 73 ksi		
	Slip δ (in.)	$\frac{\delta_{E,B}}{\delta_M}$	$\delta_{E,B}-\delta_M$ (in. x 10^{-4})	Slip δ (in.)	$\frac{\delta_{E,B}}{\delta_M}$	$\delta_{E,B}-\delta_M$ (in. x 10^{-4})	Slip δ (in.)	$\frac{\delta_{E,B}}{\delta_M}$	$\delta_{E,B}-\delta_M$ (in. x 10^{-4})	Slip δ (in.)	$\frac{\delta_{E,B}}{\delta_M}$	$\delta_{E,B}-\delta_M$ (in. x 10^{-4})
BS-6M-8-A,B	0.0036	2.06	+38	0.0082	1.69	+56	0.0125	1.75	+95	0.0493	-	-
BS-6E-8-A,B	0.0074			0.0138			0.0220			*		
BS-6M-13-A,B	0.0032	1.54	+18	0.0067	1.37	+25	0.0095	1.29	+27	0.247	0.94	-17
BS-6E-13-A,B	0.0050			0.0092			0.0122			0.231		
BS-6B-13-A	0.0036	1.11	+4	0.0077	1.14	+10	0.0112	1.18	+17	0.0281	1.14	+33
BS-6M-18-A,B	0.0042	1.29	+13	0.0088	1.14	+12	0.0121	1.11	+13	0.0351	0.86	-50
BS-6E-18-A,B	0.0055			0.0100			0.0134			0.0301		
BS-11M-16-A,B	0.0082	1.09	+7	0.0155	1.87	+136	0.0280	-	-	*	-	-
BS-11E-16-A,B	0.0089			0.0291			*			*		
BS-11M-24-A,B	0.0076	1.00	0	0.0128	1.07	+9	0.0172	1.31	+53	0.0655	1.44	+269
BS-11E-24-A,B	0.0076			0.0137			0.0225			0.0924		
BS-11B-24-A	0.0066	0.87	-10	0.0130	1.01	+2	0.0190	1.10	+18	0.0757	1.16	+102
BS-11M-30-A,B	0.0062	1.18	+11	0.0104	1.42	+43	0.0142	1.63	+89	0.0463	1.78	+363
BS-11E-30-A,B	0.0073			0.0147			0.0231			0.0826		
Avg. E vs M		1.36	+14		1.34	+47		>1.42	>+55		-	-
Avg. B vs M		0.99	-3		1.07	+6		1.14	+17		1.15	+67

* Pullout below stress level indicated

Table 5.4 Comparison of Free End Slip at Various Stress Levels for BS Specimens

Specimen	Average Free End Slip at Bar Stress Level								
	At 45 ksi			At 59 ksi			At 73 ksi		
	Slip δ (in.)	$\frac{\delta_{E,B}}{\delta_M}$	$\delta_{E,B}-\delta_M$ (in. x 10^{-4})	Slip δ (in.)	$\frac{\delta_{E,B}}{\delta_M}$	$\delta_{E,B}-\delta_M$ (in. x 10^{-4})	Slip δ (in.)	$\frac{\delta_{E,B}}{\delta_M}$	$\delta_{E,B}-\delta_M$ (in. x 10^{-4})
BS-6M-8-A,B	0.0027	2.93	+52	0.0058	2.62	+94	>0.0082	-	-
BS-6E-8-A,B	0.0079			0.0152			*		
BS-6M-13-A,B	0.0003	3.33	+7	0.0005	3.55	+14	0.0010	3.65	+26
BS-6E-13-A,B	0.0010			0.0019			0.0036		
BS-6B-13-A	0.0003	1.00	0	0.0012	2.18	+7	0.0035	3.50	+25
BS-6M-18-A,B	0.0001	4.00	+3	0.0002	3.00	+4	0.0005	2.64	+9
BS-6E-18-A,B	0.0004			0.0006			0.0014		
BS-11M-16-A,B	0.0132	2.26	+167	0.0420	-	-	*	-	-
BS-11E-16-A,B	0.0299			*			*		
BS-11M-24-A,B	0.0017	1.91	+16	0.0116	1.56	+65	0.0292	>1.95	>+220
BS-11E-24-A,B	0.0033			0.0181			>0.0473		
BS-11B-24-A,B	0.0067	3.83	+49	0.0122	1.05	+6	0.0349	1.38	+96
BS-11M-30-A,B	0.0007	2.62	+10	0.0050	1.67	+34	0.0140	2.27	+177
BS-11E-30-A,B	0.0017			0.0084			0.0317		
Avg. E vs M		2.84	+42		2.48	+42		>2.85	>+108
Avg. B vs M		2.41	+24		1.62	+6		2.44	+60

*Pullout failure approximately at or below stress level indicated

No. 6 blast cleaned specimen had slightly more loaded and free end slip than the No. 6 mill scale specimen, but slightly less than the epoxy coated specimen. Below a bar stress of 30 ksi, the No. 11 blast cleaned specimen had slightly less loaded and free end slip than the mill scale or epoxy coated specimens. However, at higher bar stress levels, the No. 11 blast cleaned bar had slightly greater slip.

5.3.3 Effect of Epoxy Coating

The effect of epoxy coating on the load-slip relationship is an increase in both loaded end slip and free end slip when compared to mill scale bars, as shown in Figures 5.1 through 5.12. For the stress levels tabulated in Table 5.3, loaded end slips for the epoxy coated bars averaged 1.4 times those for the mill scale bars. This average ratio was fairly constant at the different bar stress levels but individual ratios for different embedment lengths varied from 1.0 to 2.0. Larger slip differences were noted for very short embedment lengths and high stress levels.

For the stress levels tabulated in Table 5.4, free end slips for the epoxy coated bars averaged 2.7 times those for the mill scale bars. Again, the average ratio was fairly constant at the different bar stress levels tabulated, but individual ratios varied widely. Also, larger slip differences were noted for very short embedment lengths and post-yield bar stress levels.

5.3.4 Effect of Embedment Length

In general, the effect of embedment length on the bond-slip relationship of epoxy coated bars parallels the effect on mill scale bars. As

embedment length increased, the free end and loaded end slips corresponding to a given bar stress decreased. However, similar to mill scale bars, the loaded end slip of epoxy coated bars was affected less as the embedment length became longer since loaded end slip is primarily influenced by local conditions at the pulling end.

5.3.5 Effect of Bar Size

As indicated in Chapters 1 and 2, most previous research on epoxy coated reinforcing bar involved size No. 6 bars. One objective of this study was to determine if bar size has a significant influence on comparative performance in relation to mill scale bars. From the test results, it appears that the comparative bond-slip performance of the No. 11 bars parallels that of the No. 6 bars. Thus, there does not appear to be a size factor that is unique to epoxy coated bars.

5.4 Analysis Based upon Failure Criteria

5.4.1 Failure Criteria

As discussed in Chapter 2, several failure criteria have been utilized in bond research. ACI 318-77 (7) and AASHTO (8) design specifications require a specified development length to ensure yielding at the critical section. The basic development length equation,

$$\ell_{db} = 0.04 A_b f_y / \sqrt{f'_c} \geq 0.0004\, d_b f_y \qquad (5.1)$$

for #11 bars and smaller

was developed based upon a strength criteria that the bar stress must reach 1.25 f_y in order for the anchorage to perform satisfactorily. ASTM A 775-81, Standard Specification for Epoxy-Coated Reinforcing

Bars (6), bases acceptance on critical bond strength corresponding to slip criteria. The critical strength is the lesser of the stress corresponding to a free end slip of 0.002 in. or the stress corresponding to a loaded end slip of 0.010 in.

The slip and the strength failure criteria have been used in bond studies involving both pullout type specimens as well as beam end type specimens. Hence both slip and strength comparisons will be considered in analyzing the comparative performance of specimens in this study.

5.4.2 Slip Criteria Comparisons

Comparisons of mill scale, epoxy coated and blast cleaned specimens based upon the slip criteria are presented in Table 5.5. Bar stresses and bond stresses corresponding to a loaded end slip of 0.010 in. and a free end slip 0.002 in. are tabulated. Under each slip criteria, a ratio of the average critical bond stress for the mill scale bar, μ_M, to the average critical bond stress for the epoxy coated bar, μ_E, or the blast cleaned bar, μ_B, is also tabulated.

Free end slip controlled the strength of specimens with short embedment lengths, 8" for No. 6 and 16" for No. 11, while loaded end slip controlled the longer embedment lengths tested for each size. The free end critical slip was not reached by the termination of testing for specimens BS-6M-13-A, BS-6M-18-A, BS-6M-18-B and BS-6E-18-B at loads given in Table 5.1.

With the exception of No. 6 specimens having 8 in. embedment lengths, the critical slip ratios comparing mill scale to epoxy coated bars were fairly consistent, ranging from 1.06 to something above 1.29. The ratios

Table 5.5 Comparison of Beam Static (BS) Specimens based upon Slip Criteria and Pullout Strength

Specimen	At Loaded End Slip = 0.01 in.			At Free End Slip = 0.002 in.			At Bar Pullout		
	Bar Stress (ksi)	Bond Stress (psi)	$\frac{\mu_M}{\mu_{E,B}}$	Bar Stress (ksi)	Bond Stress (psi)	$\frac{\mu_M}{\mu_{E,B}}$	Bar Stress (ksi)	Bond Stress (psi)	$\frac{\mu_M}{\mu_{E,B}}$
BS- 6M- 8-A	52.6	1228		41.3	964		>75.0	>1750	
BS- 6M- 8-B	53.5	1249	1.49	42.2	985	2.16	76.1	1777	1.17
BS- 6E- 8-A	32.4	752		16.2	378		63.6	1485	
BS- 6E- 8-B	38.7	903		22.5	525		65.9	1538	
BS- 6M-13-A	61.6	885		>75	>1077		*		
BS- 6M-13-B	59.3	852	1.21	80.0	1149	>1.29	*		
BS- 6E-13-A	49.9	717		58.4	839		*		
BS- 6E-13-B	49.9	717		61.1	878		*		
BS- 6B-13-A	54.8	787	1.10	65.6	942	1.22	*		
BS- 6M-18-A	44.9	466		*			*		
BS- 6M-18-B	57.5	597	1.12	*			*		
BS- 6E-18-A	51.2	531		82.7	858		*		
BS- 6E-18-B	40.5	420		*			*		
BS-11M-16-A	36.9	812		27.5	605		64.0	1408	
BS-11M-16-B	33.7	742	1.08	31.9	702	1.15	62.5	1376	1.17
BS-11E-16-A	33.7	742		26.6	585		56.7	1248	
BS-11E-16-B	31.6	695		25.0	550		51.3	1129	
BS-11M-24-A	35.0	513		45.1	662		*		
BS-11M-24-B	41.3	606	1.06	46.5	682	1.06	*		
BS-11E-24-A	33.7	494		42.9	629		*		
BS-11E-24-B	38.1	559		43.9	644		70.5	1034	
BS-11B-24-A	39.4	578	0.97	44.0	645	1.05	76.9	1128	
BS-11M-30-A	42.8	502		58.0	681		*		
BS-11M-30-B	47.2	554	1.22	50.3	590	1.14	*		
BS-11E-30-A	33.4	392		44.7	524		*		
BS-11E-30-B	40.6	477		50.3	590		*		

*Test terminated at 1.25 f_y or greater without reaching indicated criteria

for the No. 6 bars having 8 in. embedment length were much larger (1.49 and 2.16) and some cause for concern; however, this is tempered by code requirements for a minimum development length of 12 in. Again, with exception of No. 6 specimens with 8 in. embedment, the critical slip ratios, μ_M/μ_E, of the No. 6 and the No. 11 specimens were similar. Thus, bar size does not appear to be a significant factor in comparing mill scale to epoxy coated bars.

Overall, the average ratio of controlling critical bond strength comparing mill scale to epoxy coated bars based upon slip criteria was 1.32. If the No. 6 specimens with 8 in. embedments are excluded, the average was 1.15. Thus, while some variation was noted, the bond strength of epoxy coated bars is somewhat less than that of mill scale bars.

Also as indicated in Table 5.5, the blast cleaned bars had an average critical bond strength less than the mill scale bars but greater than the epoxy coated bars. The ratio of critical bond strength comparing mill scale bars to blast cleaned bars ranged from 0.97 to 1.22 and averaged 1.08.

5.4.3 Ultimate Strength Comparisons

A comparison of mill scale versus epoxy coated specimens based upon ultimate pullout strength is also presented in Table 5.5. Pullout generally occurred only in cases of specimens having very short embedment lengths, i.e. No. 6 specimens with 8 in. and No. 11 with 16 in. embedments. Thus, in these cases where comparisons can be made, the ratio of mill scale to epoxy coated specimen strengths was 1.17 for both No. 6 bars and No. 11 bars.

Note that the test of specimen BS-6M-8-A was terminated due to equipment problems at a bar stress of 75 ksi. Thus the ratio of 1.17 was arrived at largely on the basis of the failure strength of specimen BS-6M-8-B. The actual ratio may have varied somewhat; however, the load slip relationships shown in Figures 5.1 and 5.2 indicate that the two mill scale specimens were behaving very similarly.

Two other specimens, BS-11E-24-B and BS-11B-24-A, had pullout failures at bar stresses of 70.5 and 76.9 ksi, respectively. However, since the mill scale specimens had not failed up to test termination at 76 ksi, comparative ratios cannot be calculated. Nevertheless, the somewhat lower pullout strength of BS-11E-24-B is consistent with lower strengths of epoxy coated specimens in comparison to mill scale specimens determined for No. 6 bars with 8 in. and No. 11 bar with 16 in. embedments.

5.4.4 Comparison to Design Specification Requirements

As noted in Chapter 2, neither ACI nor AASHTO has special provisions for development of epoxy coated reinforcing bars. Nevertheless, it is meaningful to consider the test results in relation to current and proposed development length provisions for normal mill scale bars.

Calculation of development length for the bar sizes, bar strength, and concrete strength of the specimens is outlined in Table 5.6, based upon ACI 318-77 (7) and AASHTO (8) requirements. For Grade 60 steel, the intent of the requirements is to provide a length which will develop the reinforcement to 1.25 f_y or 75 ksi. The resulting development length, ℓ_d, can be compared to the test results presented in Table 5.1.

Table 5.6 Development Length Based upon ACI (7) and AASHTO (8) Requirements

Parameter	Bar Size		Units
	No. 6	No. 11	
d_b	0.75	1.41	in
A_b	0.44	1.56	in^2
f'_c	6500	6500	psi
f_y	60000	60000	psi
$\ell_{db} = 0.04A_b f_y/\sqrt{f'_c}$	13.1	46.4	in
$\ell_{db} = 0.0004 d_b f_y$ [12 in. min.]	18.0	33.8	in
ℓ_{db} [controlling]	18.0	46.4	in
Spacing modification factor	0.8	0.8	-
$\ell_d = 0.8\ell_{db}$ [12 in. min.]	14.4	37.1	in

For the No. 6 bar, the calculated requirement from Table 5.6 is 14.4 inches while all No. 6 test specimens (mill scale, epoxy coated and blast cleaned) with 13 in. embedment attained 1.25 f_y without failure. For the No. 11 bar, the calculated requirement is 37.1 inches while all No. 11 test specimens (mill scale and epoxy coated) with 30 in. embedment also attained 1.25 f_y without failure.

Calculation of development length using the approach suggested by the ACI Committee 408 report (9) is outlined in Table 5.7. The approach adds direct consideration of cover thickness and transverse reinforcement. Introduction of a capacity reduction factor, $\phi = 0.8$, in the denominator is again intended to assure a length which will develop the reinforcement to 1.25 f_y or 75 ksi for Grade 60 steel. The calculated lengths of 16.7 inches for the No. 6 and 32.4 inches for the No. 11 can be compared to test results in Table 5.1. Again, both mill scale and epoxy coated specimens having less embedment than needed by calculation attained the desired 1.25 f_y stress level without failure.

Top bar effect modification was not included in the calculated development lengths in order to make the comparison more severe. Furthermore, studies by Jirsa and Breen (16) indicate little actual top bar effect for mixes with slump less than 4 inches.

Thus, even though test results show that epoxy coated bars have less slip resistance and less bond strength than mill scale bars, the specimen bond strengths were still adequate to meet the intent of current ACI and AASHTO specifications and suggested provisions reported by ACI

Table 5.7 Development Length Based upon ACI Committee 408 Report (9)

Parameter	Bar Size		Units
	No. 6	No. 11	
d_b	0.75	1.41	in
A_b	0.44	1.56	in^2
C_c	2.70	2.70	in
A_{tr}	0.11	0.11	in^2
f_{yt}	60000	60000	psi
f'_c	6500	6500	psi
s	6.0	3.0	in
$K_{tr} = A_{tr}f_{yt}/(1500s) \leq d_b$	0.73	1.41	in
$K = C_c + K_{tr} \leq 3d_b$	2.25	4.11	in
$\phi\ell_{db} = 5500A_b/(K\sqrt{f'_c})$	13.3	25.9	in
ϕ	0.8	0.8	-
$\ell_{db} = 5500A_b/(\phi K\sqrt{f'_c})$	16.7	32.4	in
ℓ_d [controlling, 12 in. min.]	16.7	32.4	in

Committee 408 for mill scale bars. Nevertheless, in view of the difference encountered, modification of development lengths for epoxy coated bars appears desirable to provide comparable performance to normal mill scale bars.

A comparison of the failure criteria ratios versus development length is presented in Figure 5.13. The strength criteria ratios averaged 1.17, and controlling slip criteria ratios averaged 1.32 overall and 1.15 excluding specimens with less than 12 in. embedment length. As a criteria for acceptance, ASTM A 775-81 requires that the mean critical bond strength of epoxy coated bars shall not be less than 80% of the mean critical strength of uncoated bars. This 0.80 ratio, when inverted, would imply a mean upper bound modification factor of 1.25. Based upon the test results and consideration of the ASTM requirement, a modification factor of 1.15 is proposed to increase the basic development length of epoxy coated reinforcing bars by 15% in comparison to mill scale bars.

5.5 Conclusions from Beam End Static Tests

The following conclusions can be made based upon comparative flexural bond static tests of mill scale, epoxy coated and blast cleaned reinforcing.

1. Epoxy coated reinforcing has less slip resistance than normal mill scale reinforcing. Bond strength based on critical slip for the mill scale bars averaged 32% greater than for epoxy coated bars. For development lengths greater than 12 in., mill scale bar critical slip strength was 15% greater than for epoxy coated bars.

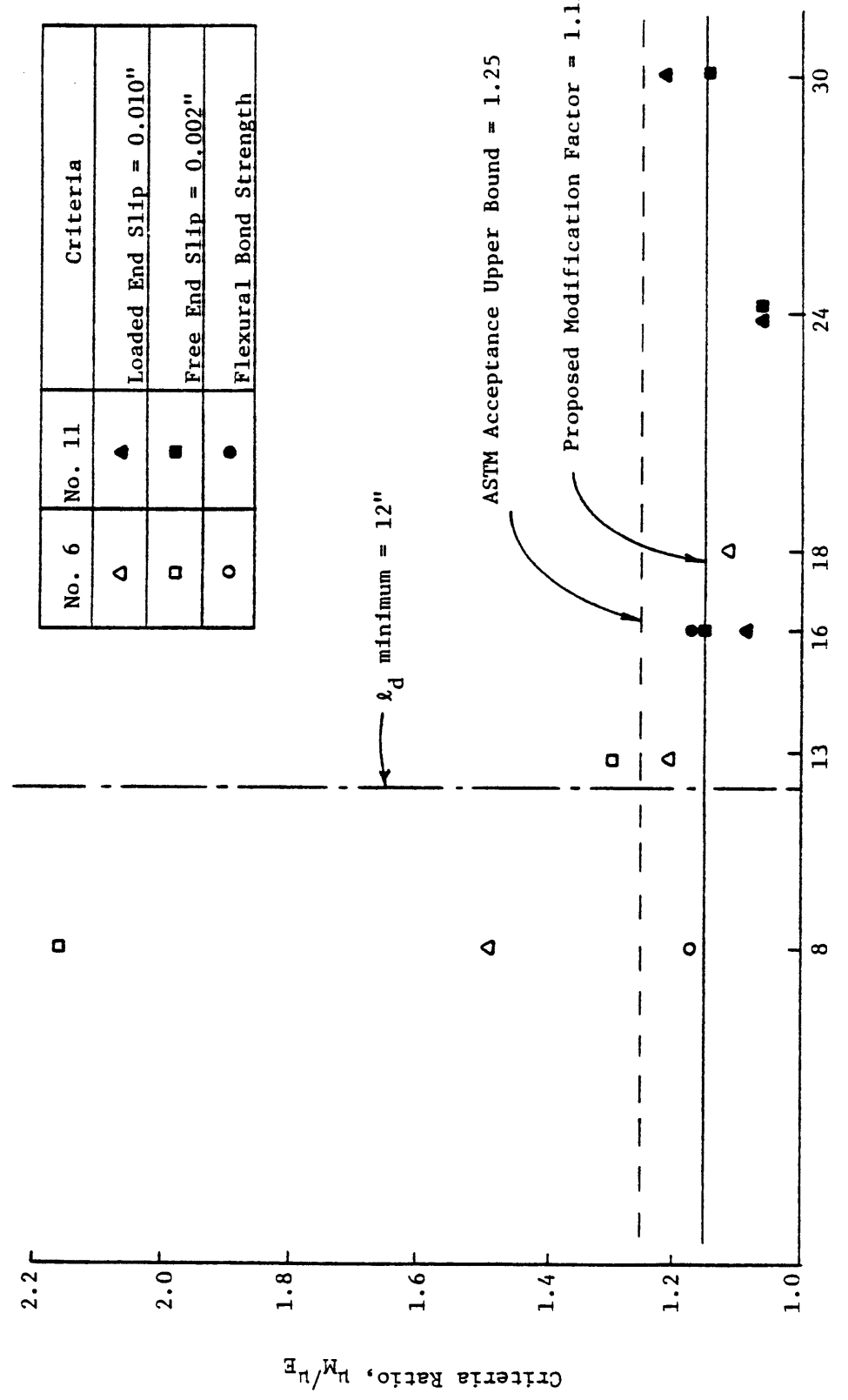

Figure 5.13 Failure Criteria Ratio Comparison versus Development Length

2. Epoxy coated reinforcing has less bond strength than mill scale reinforcing. The mill scale bars had 17% greater pullout strength.
3. Bond splitting cracks initiated at lower loads in the epoxy coated bar specimens.
4. The comparative performance of the No. 11 bars paralleled the comparative performance of the No. 6 bars. There does not appear to be a size factor unique to epoxy coated bars.
5. Epoxy coated No. 6 bars with 8 in embedment lengths had much higher slip ratios than encountered in other specimens with longer embedments. However, the pullout strength ratios were similar to both pullout strength and critical slip ratios of other sets of specimens.
6. Bond of the blast cleaned bars was generally somewhat lower than the mill scale and somewhat greater than the epoxy coated bars.
7. For the particular specimens tested, the epoxy coated bars attained stress levels compatible with current ACI and AASHTO development requirements.
8. In order to provide comparable performance with mill scale bars, a basic development length modification factor of 1.15 is proposed for epoxy coated bars.

6. PRESENTATION AND ANALYSIS OF RESULTS FOR BEAM END FATIGUE TESTS

6.1 Introduction

In this chapter, results of the beam end specimen bond fatigue tests (Series BF) are presented and analyzed. The objectives of this series of tests were as follows:

1. To determine whether the bond-slip performance of epoxy coated reinforcement is significantly different from that of normal mill scale bars when subjected to numerous cycles of loading in a working stress range.
2. To determine whether the bond strength of epoxy coated reinforcement is significantly different from that of normal mill scale bars after being subjected to numerous cycles of loading in a working stress range.

The principal variables in the BF series were bar surface condition (mill scale, epoxy coated or blast cleaned), embedment length and bar size (No. 6 or No. 11). Neither epoxy coating type nor thickness were intended variables. While companion specimens were of essentially the same concrete strength and age, the strength and age of the No. 11 specimens was slightly greater than for the No. 6 specimens, as noted in Section 3.6. The age and strength correspond to cylinder tests made midway through the fatigue test.

A listing of beam end fatigue specimens is presented in Table 6.1. The number of cycles of loading and the minimum and maximum bar stress and bond stress in each cycle are also listed. Selection of the bond stress range was based upon consideration of the fatigue provisions

Table 6.1 Cycle and Stress Ranges for Beam End Fatigue Specimens (Series BF)

Specimen	Cycle Range	Minimum Stress		Maximum Stress	
		Bar Stress (ksi)	Bond Stress (psi)	Bar Stress (ksi)	Bond Stress (psi)
BF- 6M- 8-A	0-1,400,000	1,777	41.5	10,666	249
BF- 6E- 8-A	0-1,400,000	1,777	41.5	10,666	249
BF- 6M-13-A	0-1,400,000	2,888	41.5	17,332	249
BF- 6E-13-A	0-1,400,000	2,888	41.5	17,332	249
BF- 6B-13-A	0-1,400,000	2,888	41.5	17,332	249
BF- 6M-18-A	0-1,400,000	4,000	41.5	24,000	249
BF- 6E-18-A	0-1,400,000	4,000	41.5	24,000	249
BF-11M-16-A	0-1,400,000	2,133	46.9	12,800	282
BF-11E-16-A	0-1,400,000	2,133	46.9	12,800	282
BF-11M-24-A	0-313,000	3,200	46.9	19,200	282
	313,000-323,000	3,200	46.9	25,600	375
BF-11E-24-A	0-10,000	3,200	46.9	19,200	282
	10,000-20,000	3,200	46.9	25,600	375
BF-11B-24-A	0-10,000	3,200	46.9	19,200	282
	10,000-20,000	3,200	46.9	25,600	375
BF-11M-30-A	0-10,000	4,000	46.9	24,000	282
	10,000-20,000	4,000	46.9	32,000	375
BF-11E-30-A	0-10,000	4,000	46.9	24,000	282
	10,000-20,000	4,000	46.9	32,000	375

discussed in Chapter 2. Initially, the maximum bar stress level was set at 24 ksi to correspond with AASHTO (8) allowable tension stress limits for Grade 60 reinforcement. It was considered desirable to evaluate bond fatigue performance over a range that would approximate the maximum bar stress range allowed. From Equation 2.6 with f_{min} = 4 ksi and r/h = 0.3, the AASHTO range limit would be approximately 22 ksi. Hawkins (5) suggested 21 ksi and ACI 215 (11) suggested 20 ksi. Thus, the maximum bar stress range was set at 20 ksi. The maximum bar stress level, 24 ksi, and range, 20 ksi, was then to be associated with the longest embedment lengths for each bar size. For shorter embedment lengths, the minimum and maximum bond stress was maintained constant while the minimum and maximum bar stress was adjusted accordingly. Hence, for the No. 6 specimens, the bond stress was to range from 41.5 to 249 psi and for the No. 11 specimens from 46.9 to 282 psi. It was decided to load the specimens through 1,400,000 cycles, assuming premature fatigue failures did not occur, as a reasonable approximation of long life.

This approach was used for all No. 6 bar specimens and the No. 11 bar specimens with 16 inch embedment length. However, as indicated in Table 6.1, the approach was changed for the No. 11 bar specimens with 24 and 30 in. embedments. The larger bar forces associated the longer embedment lengths combined with fatigue caused wear of the bar in the grip. During the test of specimen BF-11M-24-A, the grip slipped loose several times after approximately 313,000 cycles of loading. The problem was not due to the gripping device.

The grip had been capable of transferring much higher loads in the static tests. Rather, the rebar ends had been machined to a diameter that was slightly too small for fatigue loading. With the limited grip area on the remains of the deformations (see Figure 3.11), a somewhat small diameter, and a rebar material having lower strength than prestressing steel, the teeth wore some bar material away under cyclic load. Since all specimens had been fabricated, an alternate loading approach was necessary for the remaining specimens.

If the grip wedges were split, the bars could withstand a lower number of cycles at higher loads. This provided an opportunity to examine the effect of a limited number of overload cycles on comparative bond strength. Thus, the remaining specimens, BF-11E-24-A, BF-11B-24-A, BF-11M-30-A and BF-11E-30-A were first loaded 10,000 cycles at the original bond stress levels followed by 10,000 cycles at a 40% increase in stress range. For specimen BF-11M-24-A, the 10,000 cycles of higher stress range were immediately following the initial 313,000 cycles.

Operating 24 hours per day, accumulation of 1,400,000 cycles at 2.5 to 2.7 cycles per second plus time to take readings required approximately 7 days. The tests involving only 20,000 cycles were usually completed within 3 hours. After completion of the cyclic loadings, each specimen was unloaded and then subjected to a static (monotonic) load test.

6.2 Fatigue Test Results

6.2.1 Loaded End Slip

The bond fatigue test results are presented in Figures 6.1 through 6.6. In each figure, the loaded end net slips corresponding to both the minimum stress and the maximum stress are plotted versus the log of the number of loading cycles.

Upon application of load in the first cycle, the slips measured were generally consistent with those in the Series BS static tests. Where differences in magnitude were encountered, the epoxy coated bars had slightly more slip than the mill scale bars. As load was reduced to the minimum stress level before beginning the second cycle, much of the slip was recovered. However, due to breaking of bond at the higher load levels, the initial load slip relationship is less stiff after the first cycle. Thus the slip at minimum stress was always greater for the second cycle. This is illustrated in Figures 6.3, 6.4, 6.5 and 6.6 for those specimens where second cycle slips were recorded.

For any single specimen, there are occasional ups and downs in the recorded slip measurements. Some of these variations can be attributed to the non-homogeneous nature of concrete. Also, some variations can be attributed to measurements taken by different individuals at different times, occasional automatic test shutdowns due to electro/mechanical problems, and vibration of instrumentation and mounts. However, it is the general trend of the slip data that provides meaningful information rather than small variations in a series of points.

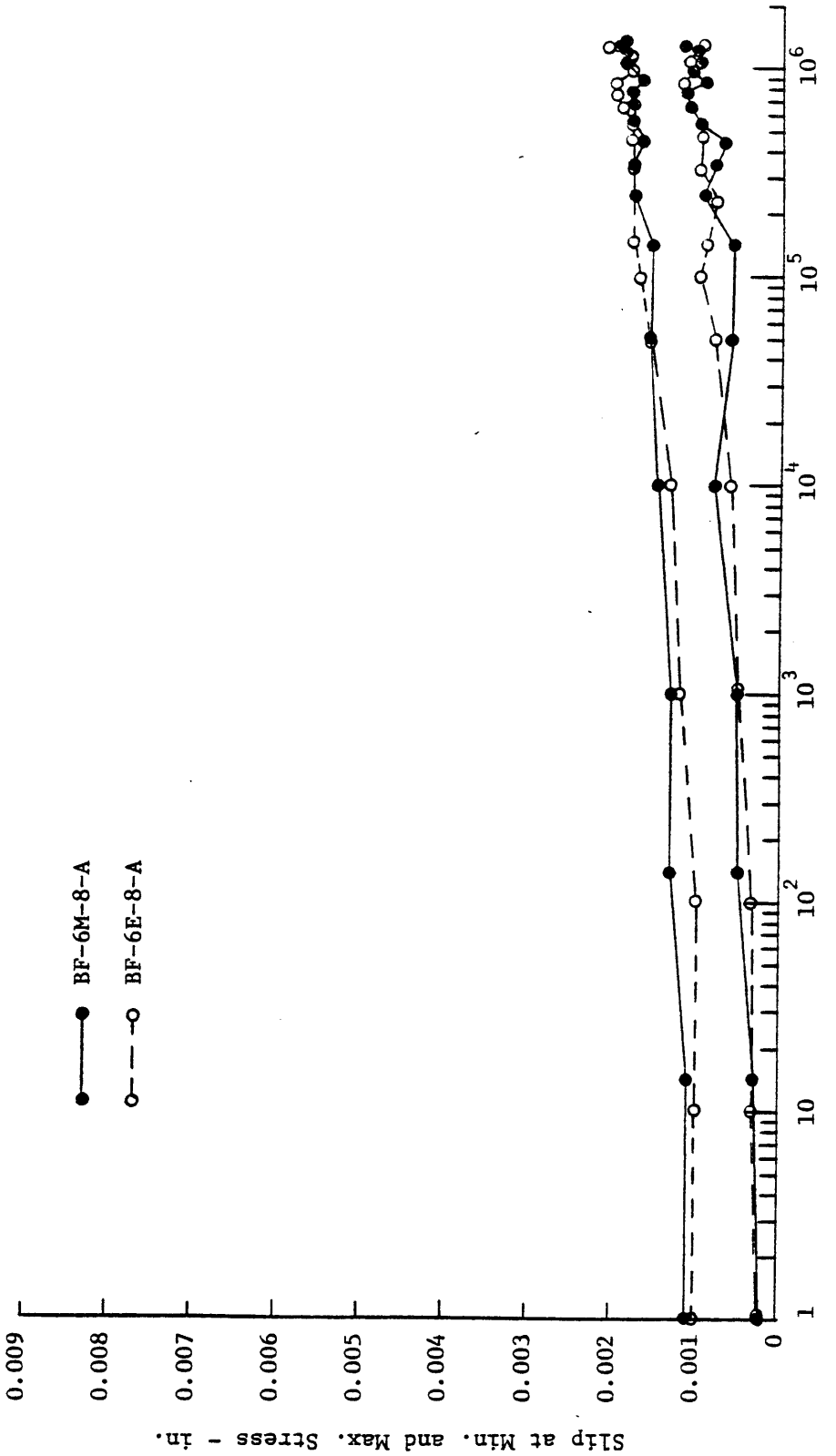

Figure 6.1 Loaded End Slip versus Cycles for Series BF-6x-8

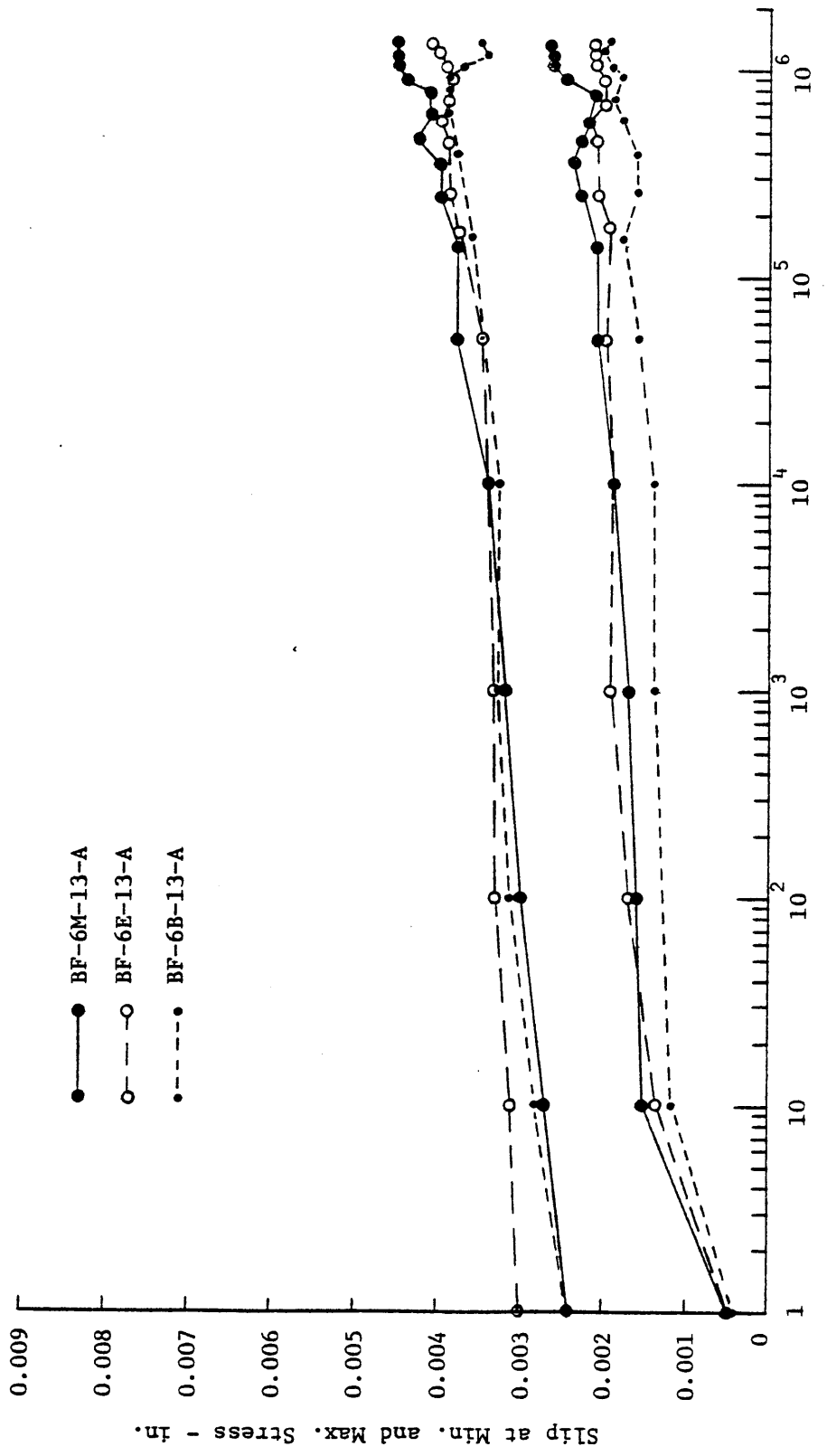

Figure 6.2 Loaded End Slip versus Cycles for Series BF-6x-13

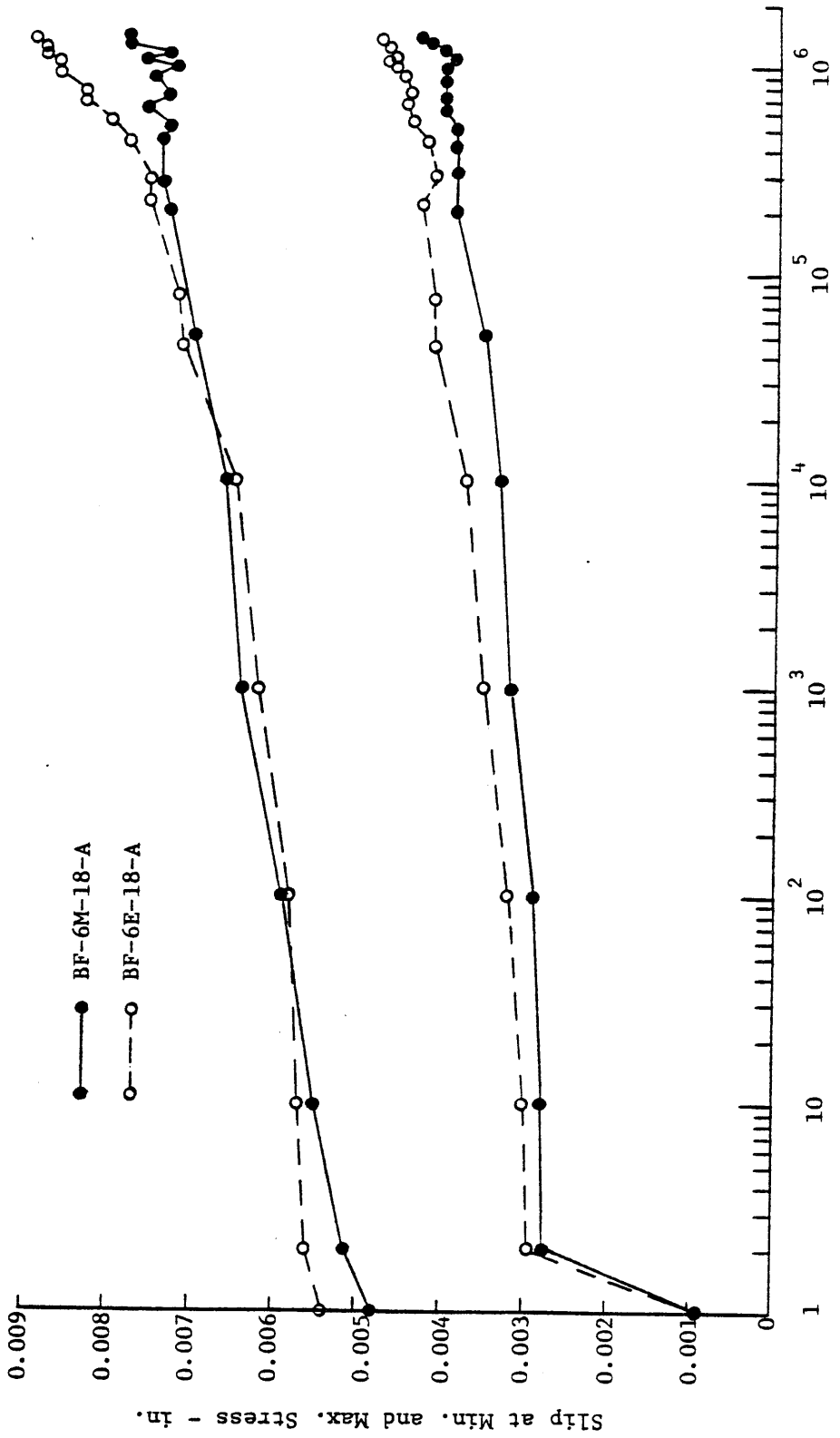

Figure 6.3 Loaded End Slip versus Cycles for Series BF-6x-18

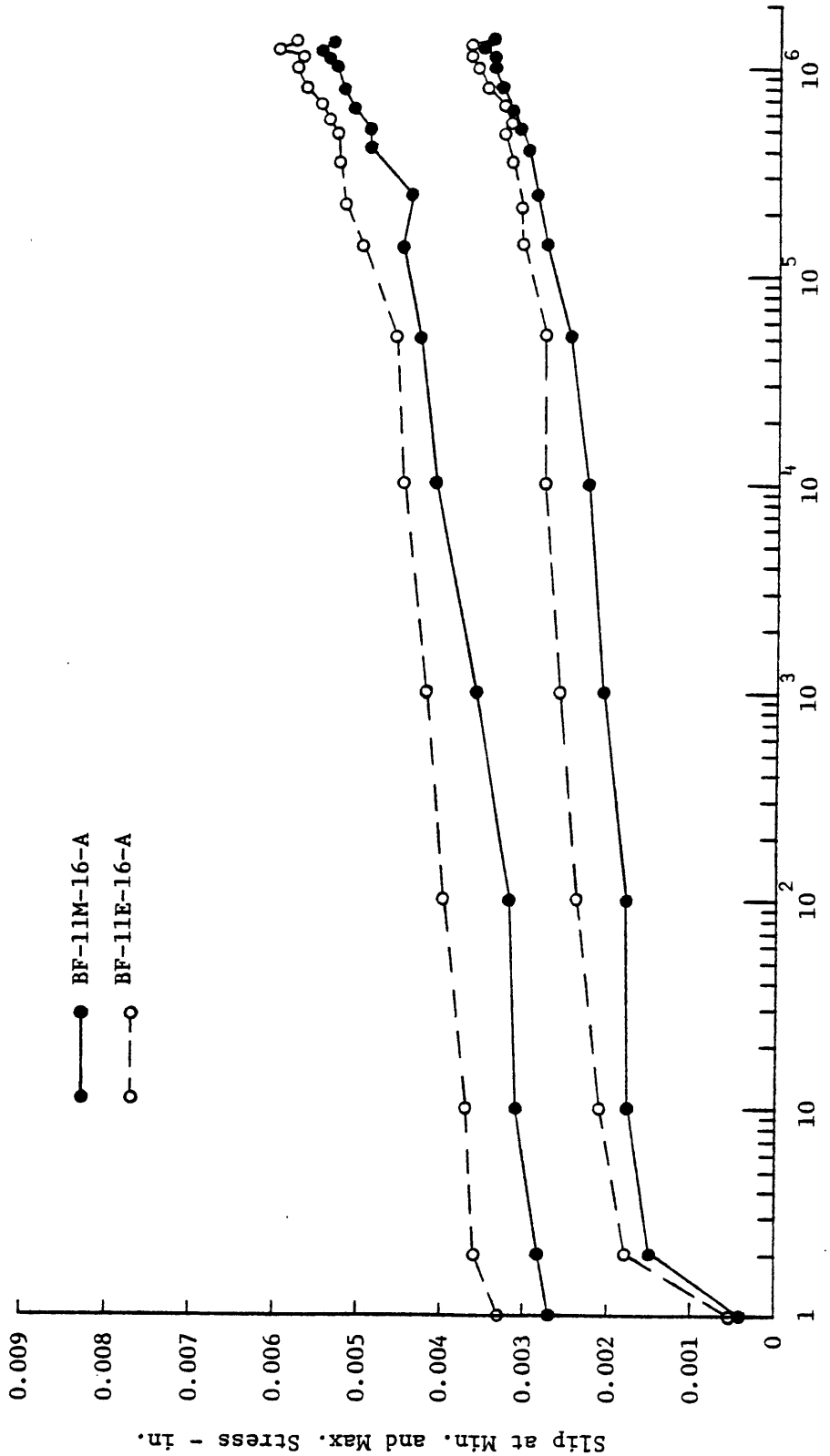

Figure 6.4 Loaded End Slip versus Cycles for Series BF-11x-16

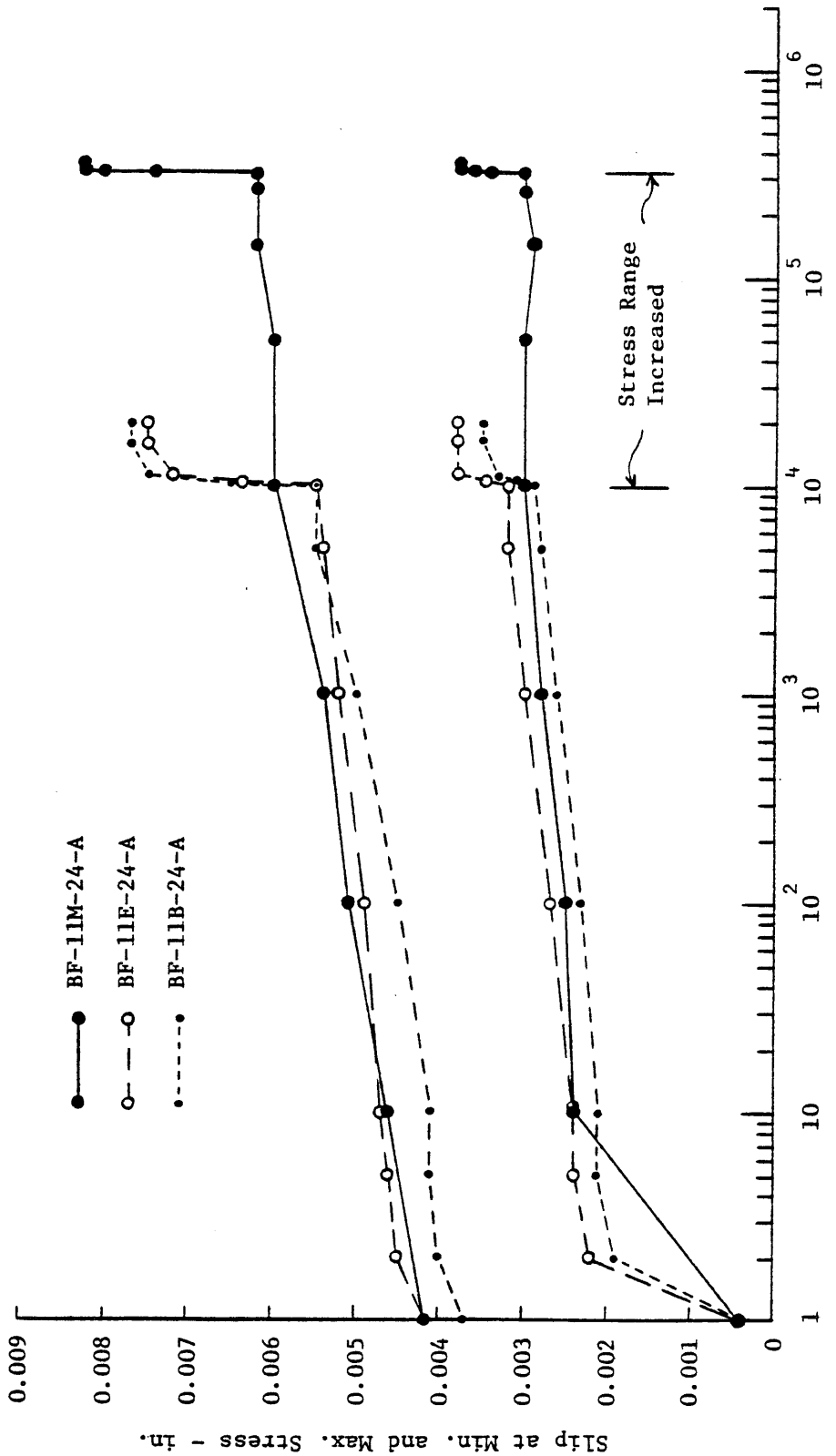

Figure 6.5 Loaded End Slip versus Cycles for Series BF-11x-24

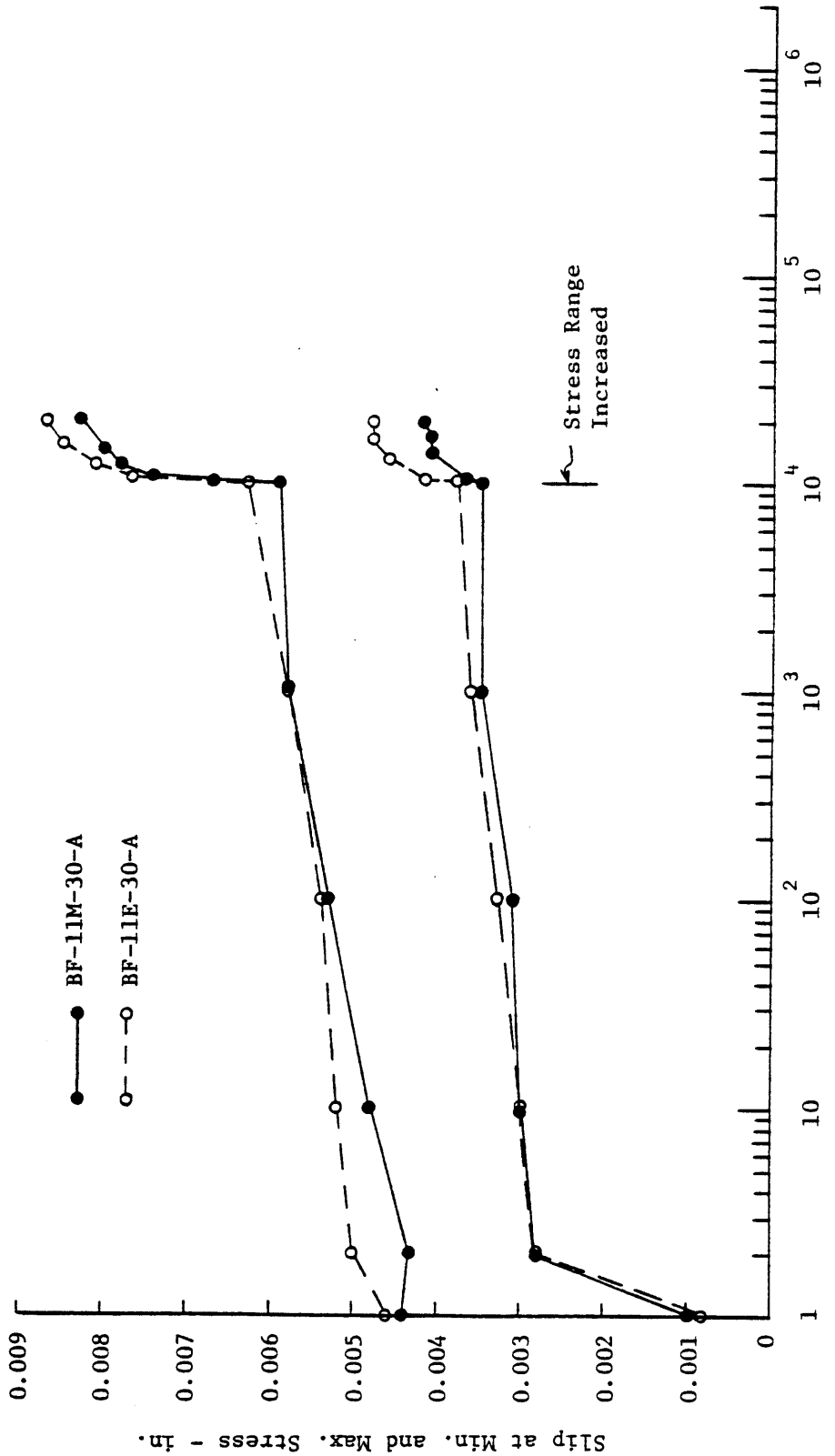

Figure 6.6 Loaded End Slip versus Cycles for Series BF-11x-30

As cycles accumulated, all specimens exhibited a gradual increase in loaded end slip. On a log scale, it appears linear, but on an arithmetic scale the rate of increase actually decreases. The added slip is to be expected due to effects of cyclic loading and bond creep. The magnitude of increase may have been slightly accentuated in these tests due to the non-symmetry of the specimen. As the magnitude of load varied in each cycle, there were very small deformations of the specimen and test frame. These small movements of the specimen relative to the bar pulling direction would also be expected to contribute to an increase in slip. Nevertheless, this action did not affect the objectives of the test since all specimens were subjected to the same conditions.

The effect of increasing the level of bond stress, as indicated in Table 6.1, is illustrated in Figures 6.5 and 6.6. Although the behavior is somewhat masked by the log scale, the behavior under the last 10,000 cycles at a higher load level essentially paralleled behavior at the lower bond stress level. The loaded end slip increased initially, but soon stabilized. One problem was noted in the loaded end slip measurements for specimens BF-11M-30-A (Figure 6.6). Some twisting of the gage mount occurred during the first cycle of load. Thus, the accuracy of the slip measurements for this specimen is uncertain.

Based upon a comparative analysis of the loaded end slip test results several observations can be made. First, in terms of general behavior, no major differences were noted between mill scale, epoxy coated and blast cleaned bars. Second, there is some indication, as

shown in Figures 6.2 through 6.6, that the difference in slip between epoxy coated bars and mill scale bars decreases with cyclic loading. The exact mechanism is not known, but if mill scale bars have a roughness and adhesion bond advantage, this might be reduced by cyclic loading. Third, no major differences in loaded end slip under cyclic load were noted on the basis of bar size or embedment length when comparing epoxy coated and mill scale bars.

6.2.2 Free End Slip

Due to the low level of load applied, the first cycle free end slip for all specimens was either zero or very small. Where initial slip was noted, it was generally similar in magnitude to that measured during the static test series at comparable loads.

During application of the cyclic loadings, little additional slip was recorded. The slips were small in comparison to the sensitivity of the gage. Furthermore, vibration of the specimen and gage mounts made the reliability of the small slip measurements less certain. Nevertheless, and perhaps most important, no particular pattern of free end slip difference was detected due to fatigue when comparing specimens on the basis of different bar surface conditions.

6.3 Specimen Cracking

During both the fatigue tests and static tests of the Series BF, the specimens were repeatedly examined for cracks. The bar tension load at which each crack became visible was marked adjacent to the crack and this process repeated to mark crack progress at each subsequent increment.

Concrete cracks were noted in only two specimens during the fatigue tests. Several flexural cracks became visible in specimens BF-11M-30A and BF-11E-30A at bar loads of 30 to 37 kips. No splitting cracks were detected in any of the Series BF specimens during the fatigue tests.

Cracking patterns for the beam end fatigue specimens (BF) after completion of the static test are shown in photographs compiled in Appendix Figures 10.2 and 10.35 through 10.48. The cracking patterns noted were similar to those previously discussed for the Series BS specimens. A comparison of the splitting and flexural cracking loads is presented in Table 6.2. Although the comparison is based on a limited number of specimens, the results tend to indicate a higher splitting strength for mill scale bars in comparison to epoxy coated bars. However, the flexural cracking occurred at lower loads for mill scale specimens in comparison to epoxy coated specimens. The results of the BF specimen cracking in Table 6.2 can be compared to results of the BS specimen cracking in Table 5.2. Overall, there was less cracking difference between mill scale and epoxy coated specimens in Series BF than in Series BS.

6.4 Static Test Results for BF Specimens

6.4.1 Ultimate Strength Comparisons

After completion of the cyclic loadings, each BF specimen was unloaded and then subjected to a static test. The load was gradually increased until either the bar began to pull out of the specimen or until the bar stress reached 1.25 to 1.40 times the yield stress, as

Table 6.2 Beam Fatigue Specimen Splitting and Flexural Cracking Loads

Specimen	Splitting Load				Flexural Cracking Load		
	Bar Force (k)	Bar Stress (ksi)	Bond Stress (psi)	$\frac{\mu_M}{\mu_{E,B}}$	Bar Force (k)	Bar Stress (ksi)	$\frac{T_M}{T_{E,B}}$
BF- 6M- 8-A	34.0	77.3	1803	1.13	26.0	59.1	0.92
BF- 6E- 8-A	30.0	68.2	1592		28.0	63.6	
BF- 6M-13-A	*	-	-	-	30.0	68.2	0.93
BF- 6E-13-A	*	-	-		32.0	72.7	
BF- 6B-13-A	*	-	-	-	30.0	68.2	1.00
BF- 6M-18-A	*	-	-	-	28.0	63.6	0.74
BF- 6E-18-A	*		-		38.0	86.4	
BF-11M-16-A	67.5	43.3	952	1.12	52.5	33.7	1.00
BF-11E-16-A	60.0	38.5	846		52.5	33.7	
BF-11M-24-A	82.5	52.9	776	1.22	37.5	24.0	1.00
BF-11E-24-A	67.5	43.3	635		37.5	24.0	
BF-11B-24-A	75.0	48.1	705	1.09	37.5	24.0	1.00
BF-11M-30-A	90.0	57.7	677	1.00	30.0	19.2	0.80
BF-11E-30-A	90.0	57.7	677		37.5	24.0	

*Indicates no cracking at termination of test ($T > 1.25\ f_y$)

indicated in Table 6.3. One exception was the test of specimen BF-11M-24-A which was terminated at a bar stress level of 66 ksi, or 1.1 f_y, due to equipment and grip problems.

Bar pullout occurred in five specimens, BF-6M-8-A, BF-6E-8-A, BF-11M-16-A, BF-11E-16-A and BF-11E-24-A. This distribution of failure, involving both epoxy coated and mill scale bars in the shortest embedments for each bar size and the No. 11 epoxy coated bar with 24 in. embedment, exactly paralleled the distribution results for the BS static series (Table 5.1). The ratio of mill scale bar bond stress to epoxy coated bar bond stress, μ_M/μ_E, was 1.15 for the No. 6 bars with 8 in. embedment. This was less than the 1.17 average ratio encountered in the BS series tests (Table 5.5). Similarly, the ratio of 1.07 for the No. 11 bars with 16 in. embedment in the BF series was less than the 1.17 ratio in the BS series tests. Furthermore, the loads corresponding to pullout in the BF specimens were of similar magnitude to those in the BS specimens. Series BF-6x-8 specimens pulled out at slightly higher loads than series BS-6x-8 specimens. Series BF-11x-16 specimens pulled out at slightly lower loads than series BS-11x-16 specimens.

Thus, the ultimate bond strength of the epoxy coated specimens was still lower than that of mill scale specimens after being subjected to approximately 1.4 million cycles of bond stress in a service load range. However, the effect of cyclic loading did not increase the difference, rather the difference was slightly decreased.

Table 6.3 Comparison of Beam Fatigue Specimens based upon Static Tests

Specimen	At End of Test					At Free End Slip = 0.002 in.		
	Bar Force (k)	Bar Stress (ksi)	Bond Stress (psi)	Note*	$\frac{\mu_M}{\mu_{E,B}}$	Bar Stress (ksi)	Bond Stress (psi)	$\frac{\mu_M}{\mu_{E,B}}$
BF- 6M- 8-A	34.5	78.4	1830	P>Y	1.15	52.1	1214	1.35
BF- 6E- 8-A	30.0	68.2	1592	P>Y		38.5	899	
BF- 6M-13-A	36.0	81.8	1175	t	-	74.5	1070	1.20
BF- 6E-13-A	38.0	86.4	1241	t		62.0	891	
BF- 6B-13-A	38.0	86.4	1241	t	-	58.0	833	1.28
BF- 6M-18-A	38.0	86.4	896	t	-	>86.4	-	-
BF- 6E-18-A	38.0	86.4	896	t		84.0	871	
BF-11M-16-A	87.0	55.8	1227	P<Y	1.07	30.0	660	1.09
BF-11E-16-A	81.0	51.9	1143	P<Y		27.5	605	
BF-11M-24-A	103.0	66.0	968	t	-	48.6	713	1.11
BF-11E-24-A	115.0	73.7	1082	P>Y		43.8	642	
BF-11B-24-A	120.0	76.9	1129	t	-	45.0	660	1.08
BF-11M-30-A	120.0	76.9	903	t	-	54.0	634	1.08
BF-11E-30-A	120.0	76.9	903	t		50.0	586	

*P<Y = Test ended when bar pulled out at load below yield.

P>Y = Test ended when bar pulled out at load above yield.

t = Test terminated at force and stresses indicated (Usually above 1.25 f_y except for BF-11M-24-A which was terminated due to equipment and grip problems at a lower stress).

6.4.2 Loaded End Slip

Although loaded end slip was recorded during the static test of the series BF specimens, the measurements are of limited value. After completion of the cyclic loadings, the specimens were unloaded completely in order to change hydraulic jacks. During the change-over process, the slip gage mountings were retightened without taking a final slip reading at zero load.

Upon unloading, the bar does not usually return to the original position of zero slip. This is due to a number of factors such as bond creep, free end slip, microcracking and accumulation of concrete fines behind the deformations. Due to the random nature of some of the factors, this unrecovered slip is variable.

Slip measurements taken during the static test of the BF specimens were relative to the new zero for each specimen. Without the unrecovered slip, the actual slips cannot be determined. The bond stress versus loaded end slip curves presented in Figures 6.7, 6.9, 6.11, 6.13, 6.15 and 6.17 are referenced to the new zero only. Thus, even within companion specimens, the slip magnitudes are not comparable and no conclusions can be accurately made comparing epoxy coated, mill scale and blast cleaned specimens based on the curves.

An attempt was made to estimate the unrecovered slip by translating the individual curves until each coincided with the point corresponding to the last slip measurement at maximum cyclic load. With this alignment of the curves, the difference in slip between epoxy coated, mill scale and blast cleaned specimens was generally smaller than that

encountered in the BS specimen tests. However, since approximations were involved, calculation of meaningful comparison ratios could not be justified.

The general shape of the load-slip curves is worth noting. Due to the effect of previous loading, the initial load-slip stiffness is much less upon re-loading. As can be seen by review of the figures, the load-slip stiffness reaches a maximum at a bond stress level which corresponds to the maximum cyclic load stress.

6.4.3 Free End Slip

Bond stress versus free end slip curves from the static tests of the beam and fatigue specimens are presented in Figures 6.8, 6.10, 6.12, 6.14, 6.16 and 6.18. Since virtually no free end slip occurred in the bond fatigue tests, the free end slips can be compared as an indicator of relative bond performance. Comparison of the load slip curves for the BF series with those of the BS series in Chapter 5 reveals essentially the same general behavior. Slip of the epoxy coated bars was generally greater than that for mill scale bars at corresponding load levels. The slip differences were more pronounced in the No. 6 bars than the No. 11 bars.

A comparison based on the critical bond stress corresponding to a free end slip of 0.002 in. is presented in Table 6.3. The critical bond stress ratios, $\mu_M/\mu_{E,B}$, were slightly greater for the No. 6 bars than for the No. 11 bars. The critical bond strength of the epoxy coated bars was less than that of the mill scale bars. For the blast cleaned bars, the critical bond strength was less than that of the

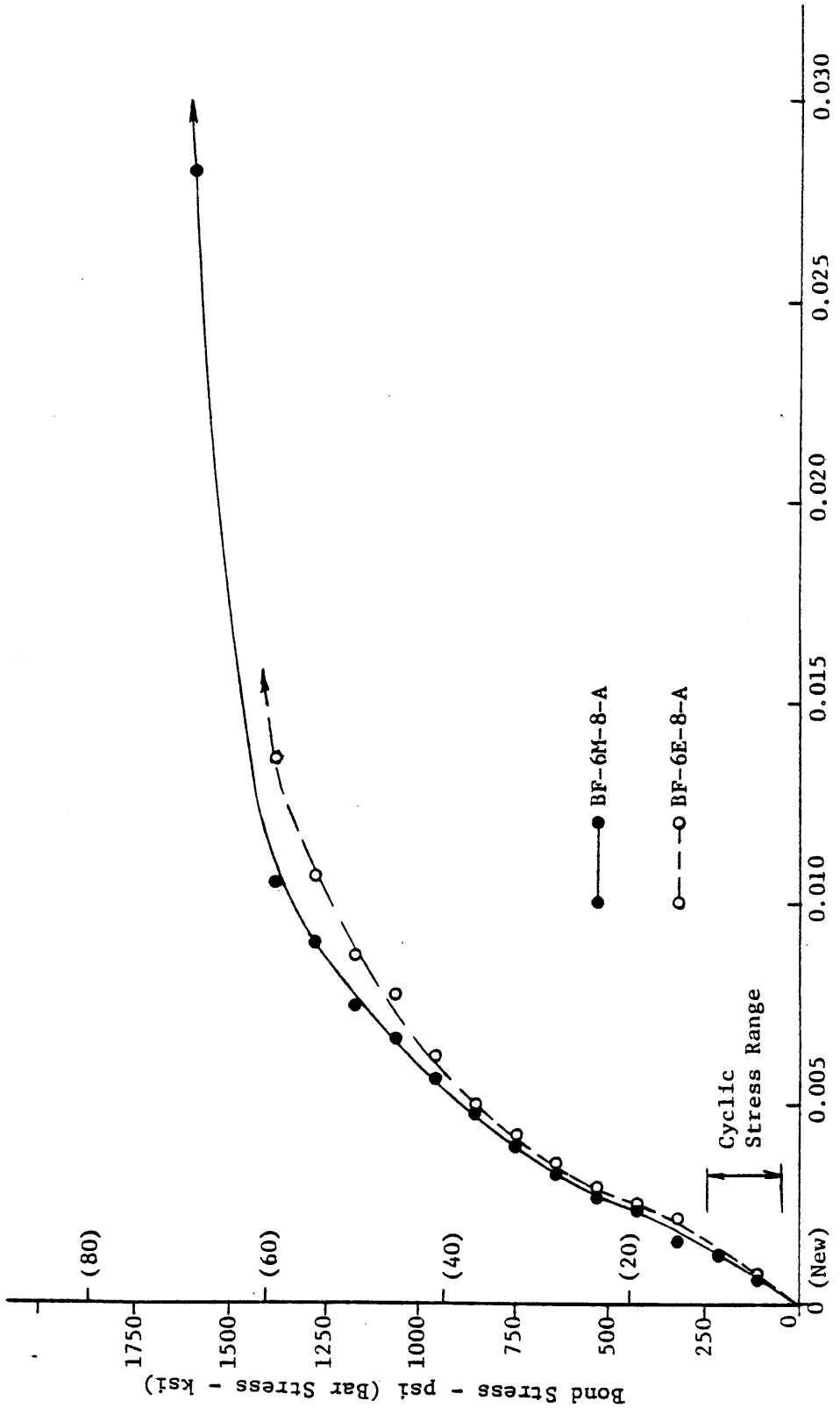

Figure 6.7 Bond Stress versus Loaded End Slip for Series BF-6x-8 Static Test

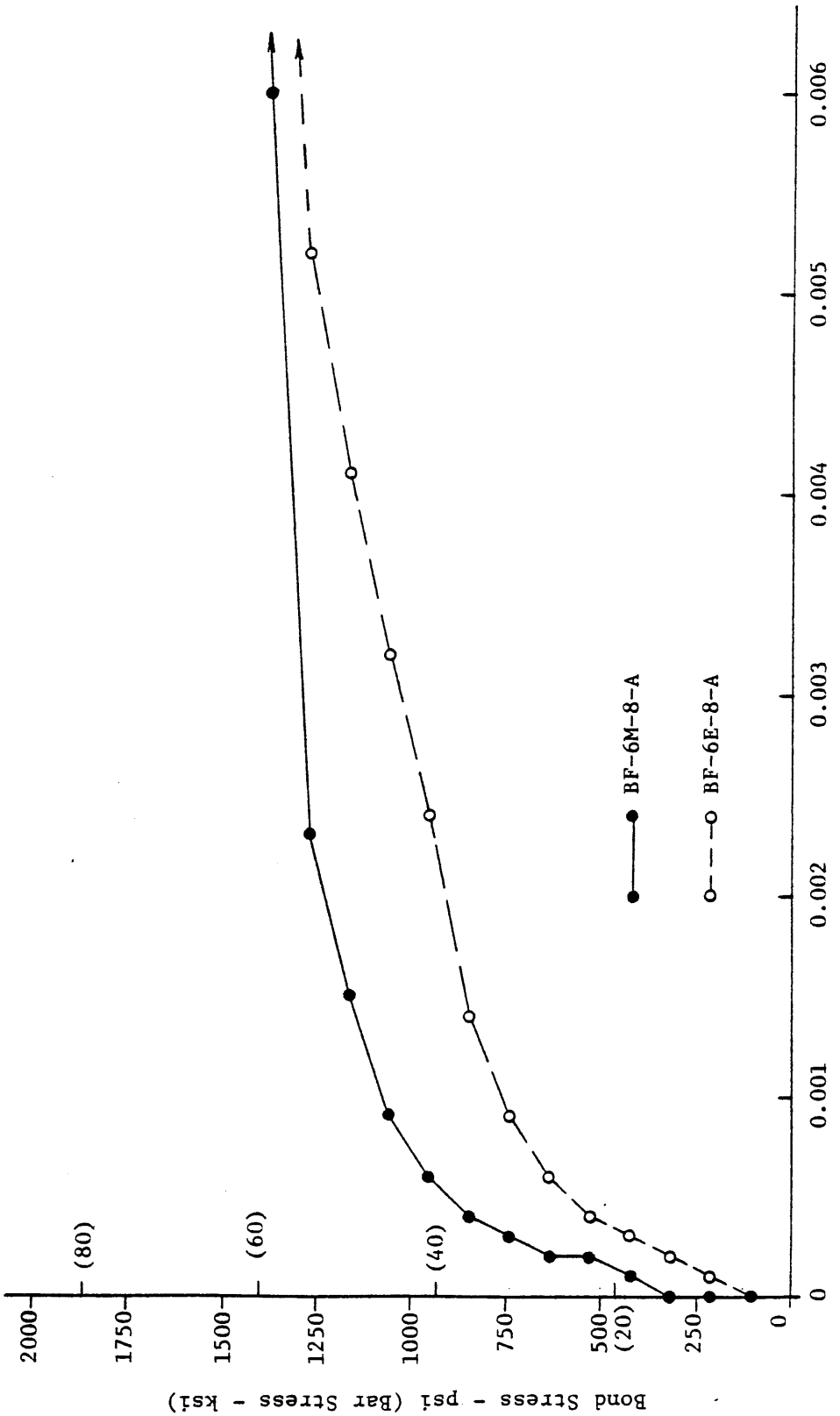

Figure 6.8 Bond Stress versus Free End Slip for Series BF-6x-8 Static Test

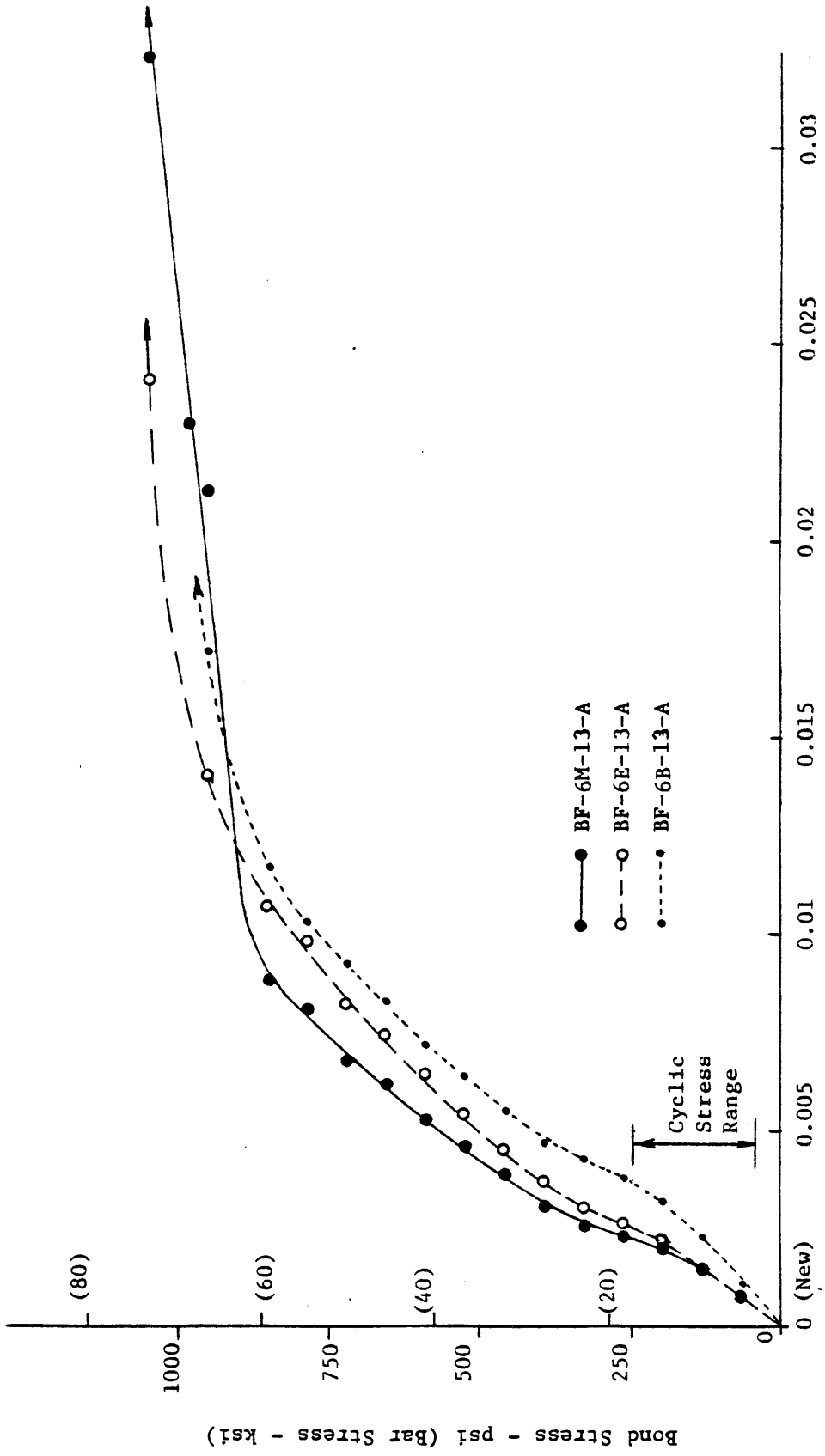

Figure 6.9 Bond Stress versus Loaded End Slip for Series BF-6x-13 Static Test

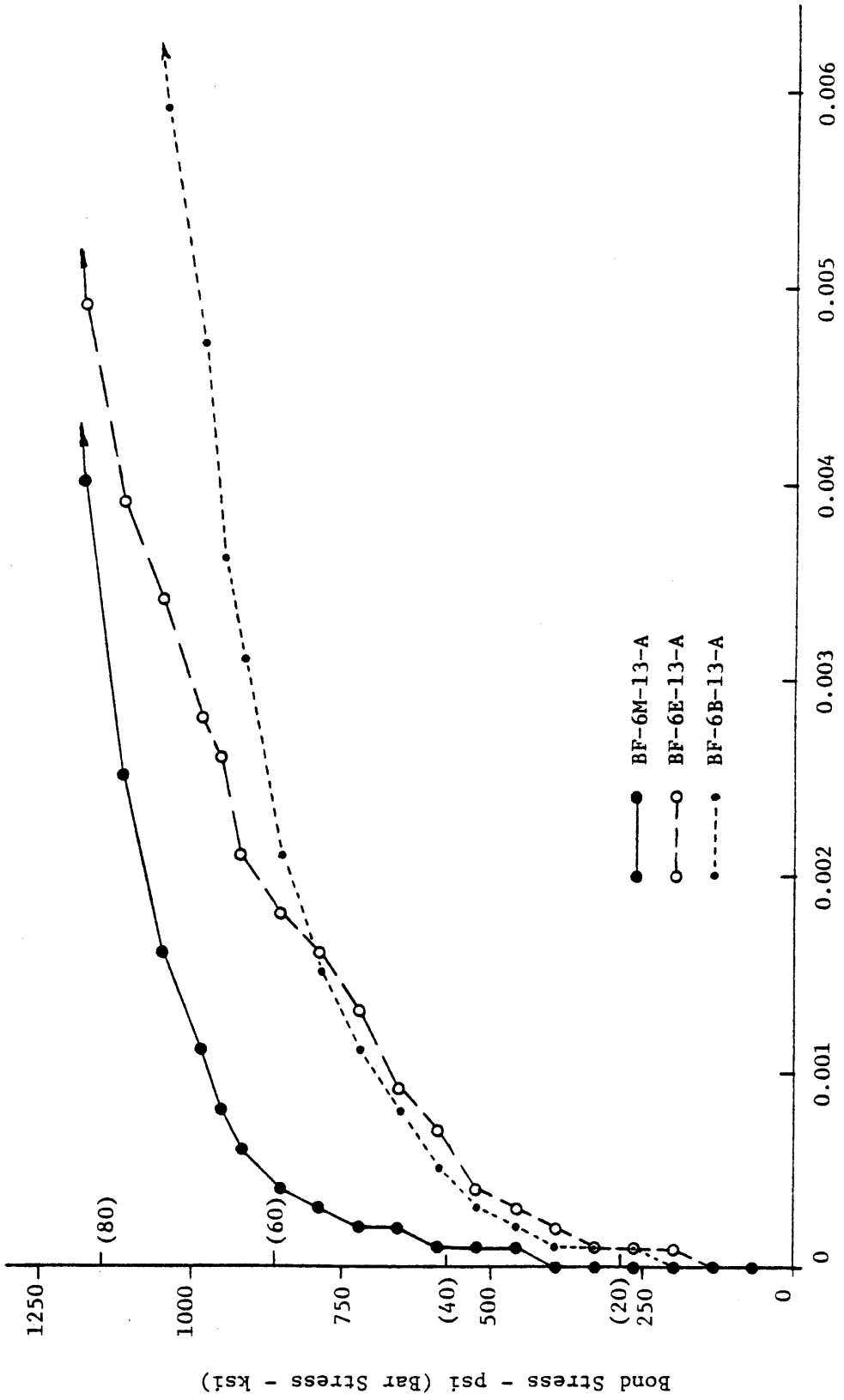

Figure 6.10 Bond Stress versus Free End Slip for Series BF-6x-13 Static Test

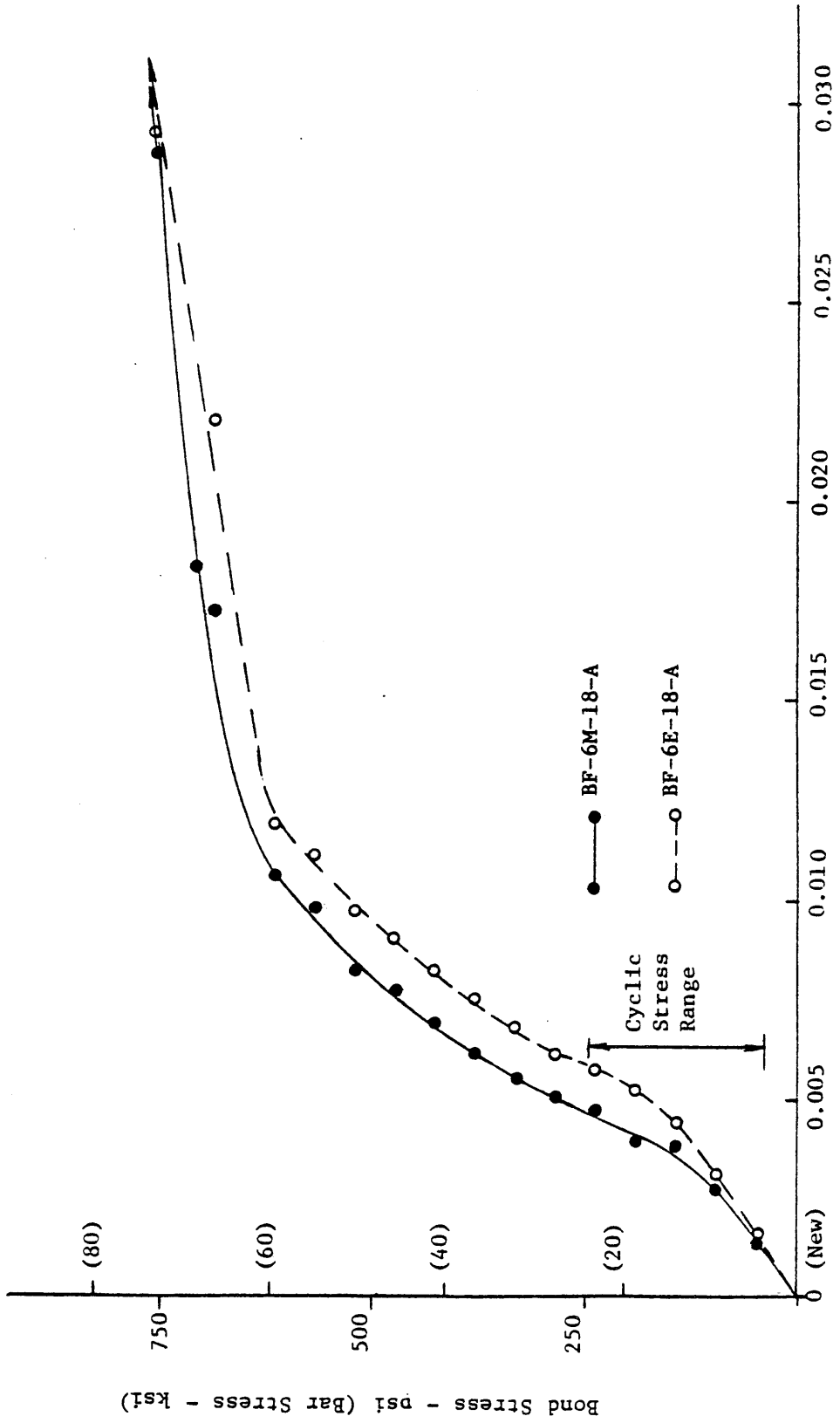

Figure 6.11 Bond Stress versus Loaded End Slip for Series BF-6x-18 Static Test

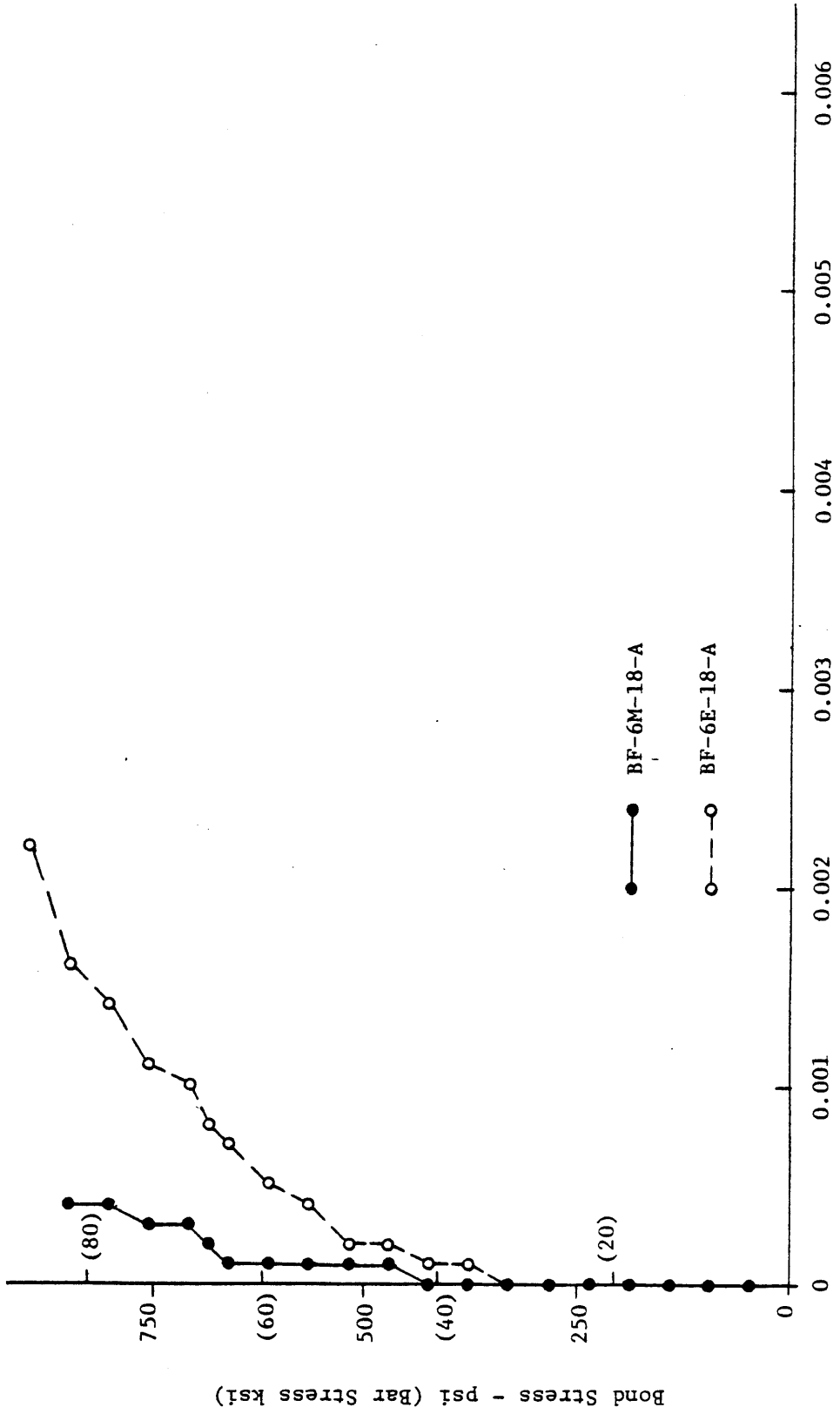

Figure 6.12 Bond Stress versus Free End Slip for Series BF-6x-18 Static Test

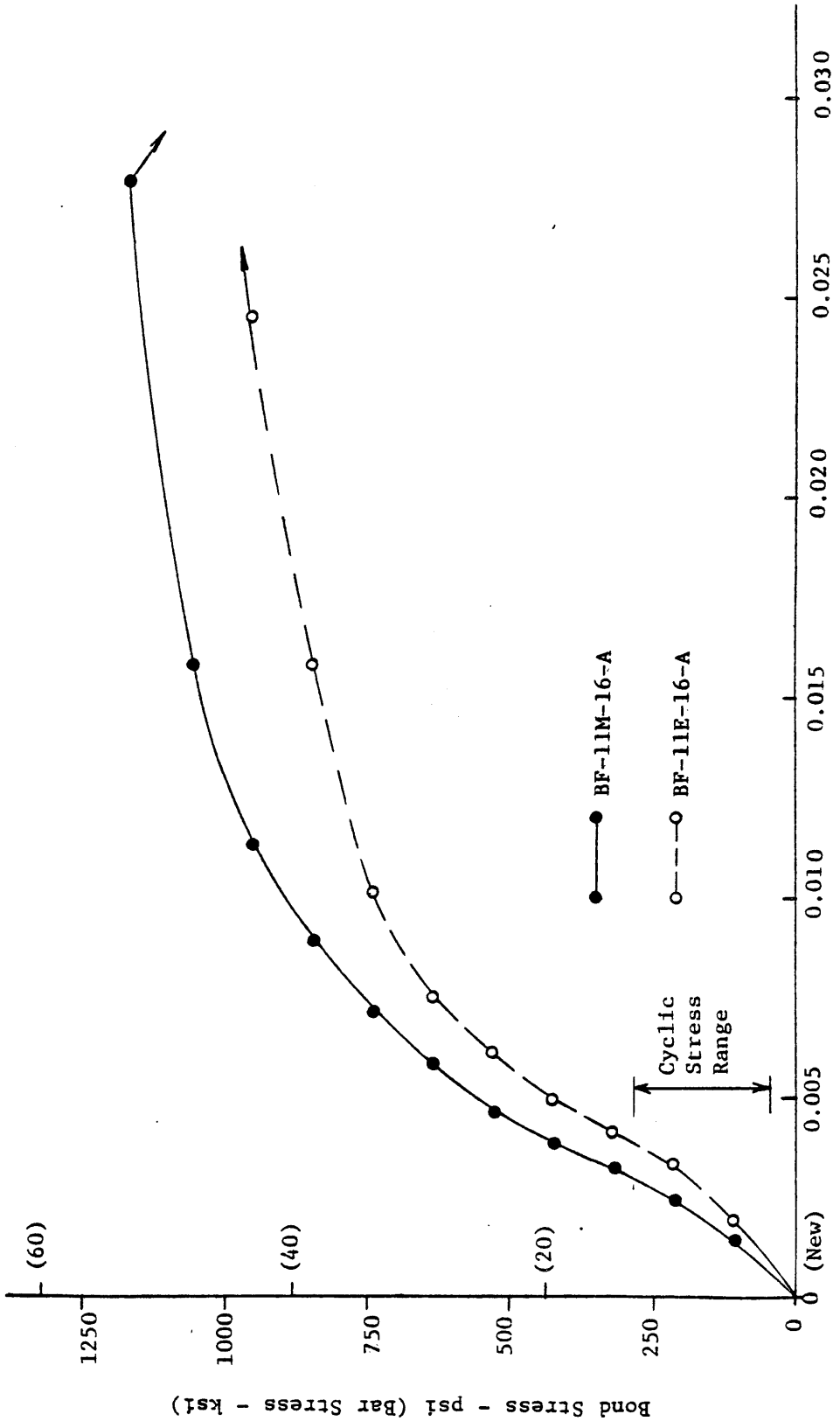

Figure 6.13 Bond Stress versus Loaded End Slip for Series BF-11x-16 Static Test

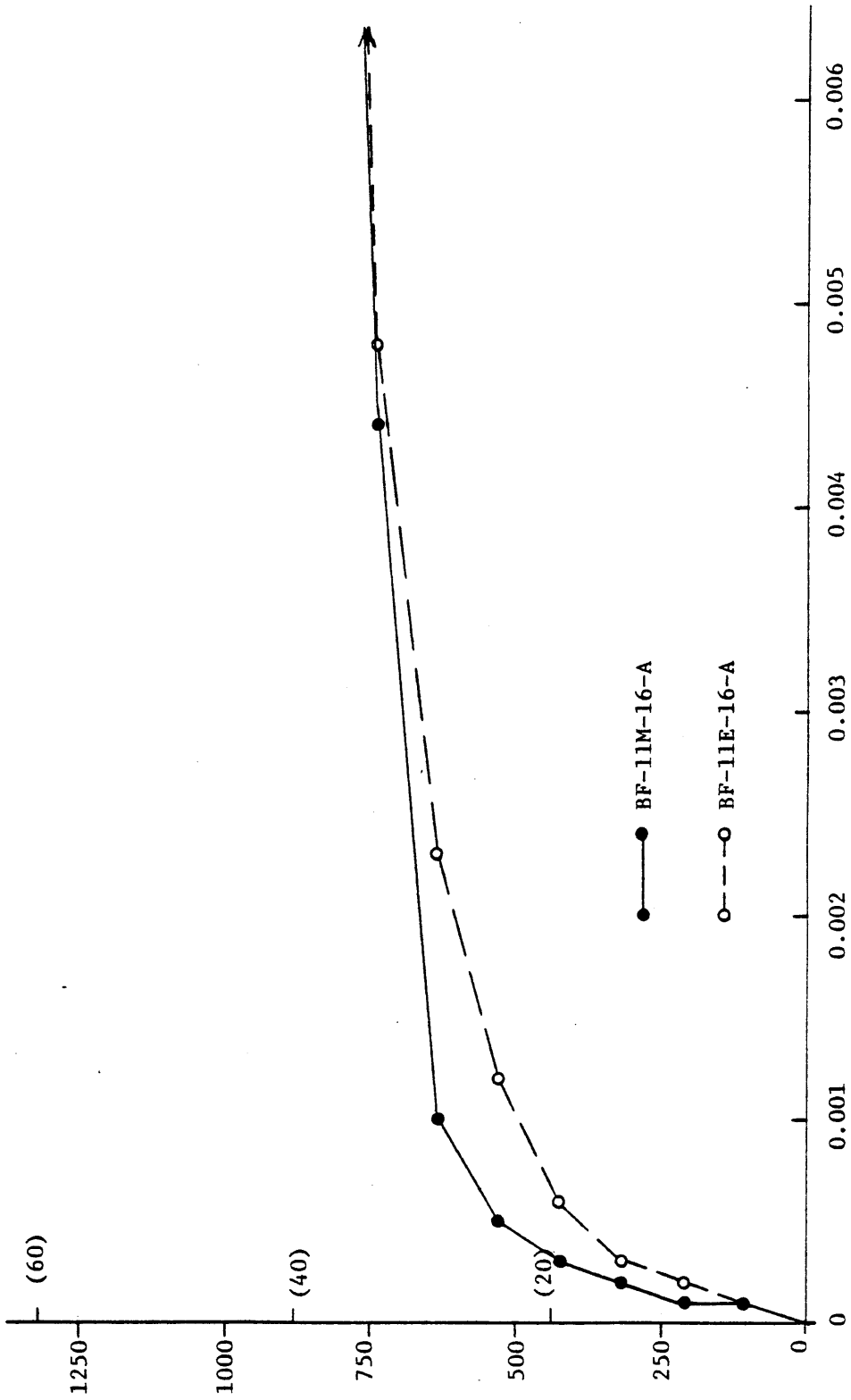

Figure 6.14 Bond Stress versus Free End Slip for Series BF-11x-16 Static Test

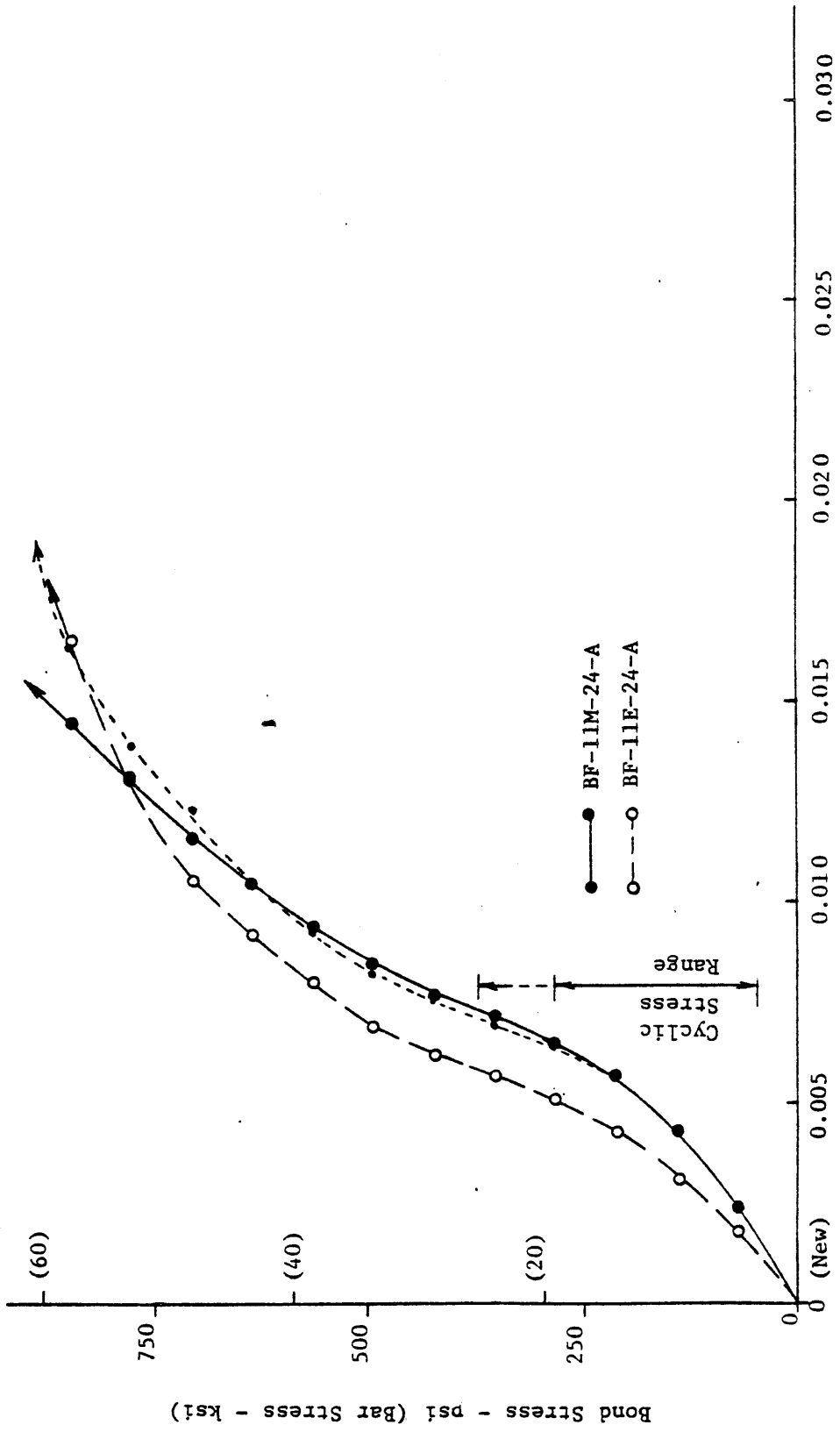

Figure 6.15 Bond Stress versus Loaded End Slip for Series BF-11x-24 Static Test

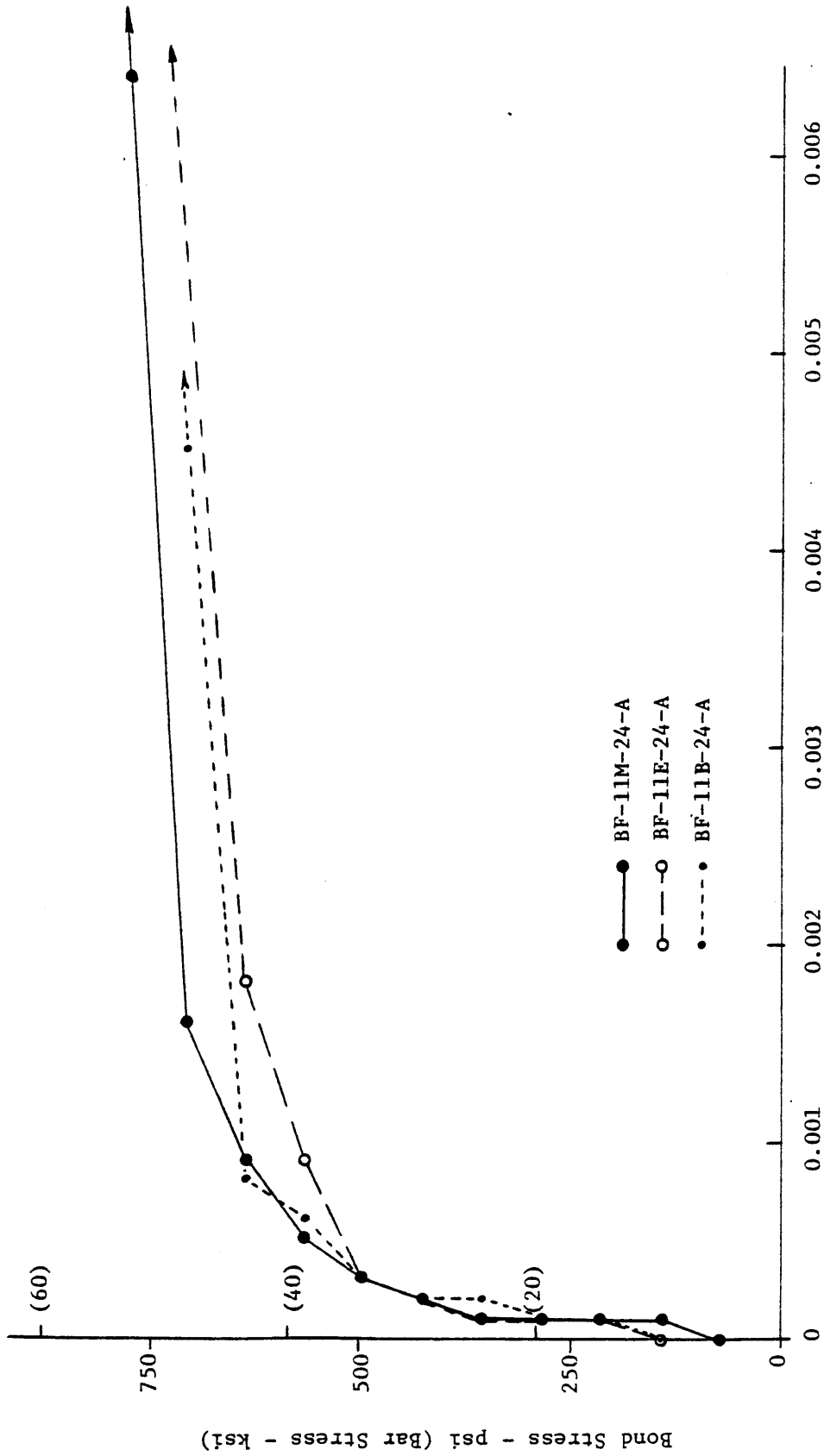

Figure 6.16 Bond Stress versus Free End Slip for Series BF-11x-24 Static Test

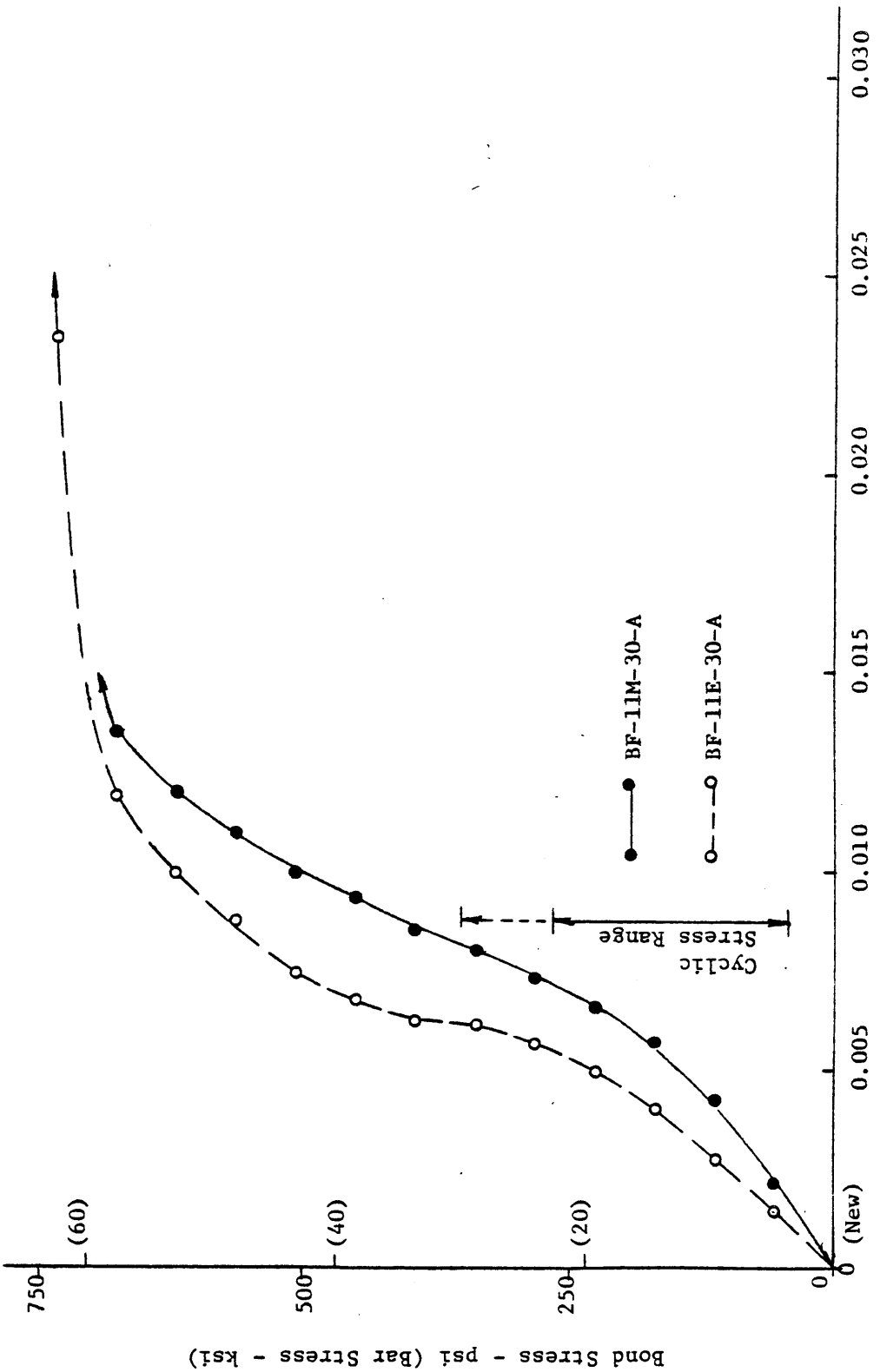

Figure 6.17 Bond Stress versus Loaded End Slip for Series BF-11x-30 Static Test

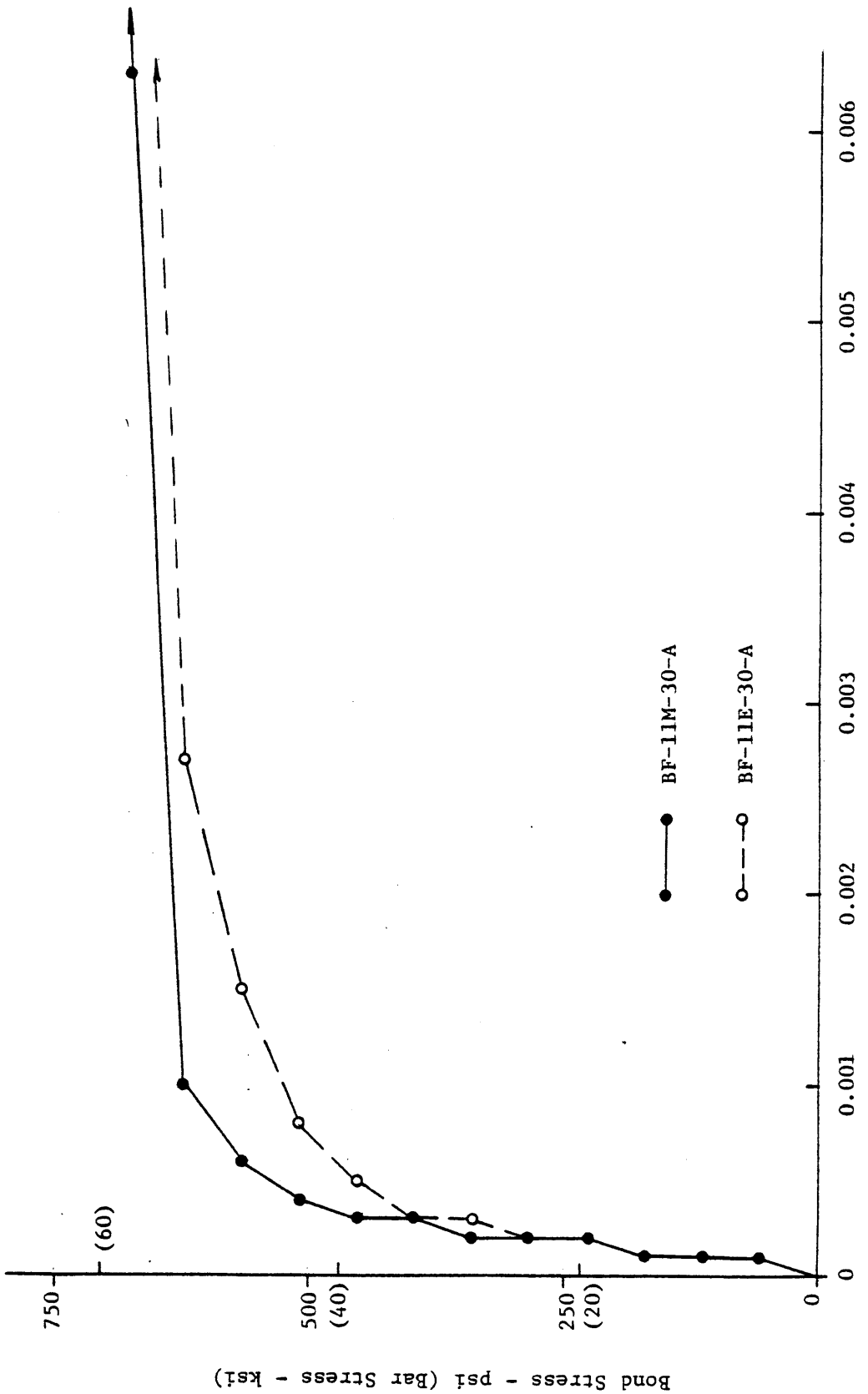

Figure 6.18 Bond Stress versus Free End Slip for Series BF-11x-30 Static Test

mill scale bars but slightly greater than that for the epoxy coated bars.

A comparison between the Series BF specimens and the series BS specimens can be made on the basis of the free end slip critical stresses and stress ratios in Tables 6.3 and 5.5. The critical stress levels of the Series BF specimens were generally about the same magnitude as those for the companion specimens of the BS series. The principal exception was for the No. 6 bar specimens with 8 in. embedment where critical stresses were higher for the BF specimens than the BS specimens. Comparing blast cleaned bars to mill scale bars, the critical stress ratio, μ_M/μ_B, averaged 1.18 for Series BF specimens and 1.14 for Series BS specimens. Comparing epoxy coated No. 11 bars to mill scale No. 11 bars, the critical stress ratio, μ_M/μ_E, averaged 1.09 for Series BF and 1.12 for Series BS. Comparing epoxy coated No. 6 bars to mill scale No. 6 bars the critical stress ratio averaged 1.28 for Series BF and greater than 1.72 for Series BS. However, the principal difference for the No. 6 comparison is for the 8 in. embedment length specimens.

Thus, it can be concluded that free end slip of the epoxy coated bars in comparison to mill scale bars was not adversely affected by bond fatigue. If anything the static strength difference as measured by free end slip criteria was somewhat less after the fatigue loading.

6.5 Conclusions from Beam End Fatigue Tests

The following conclusions can be made based upon comparative bond fatigue tests of mill scale, epoxy coated and blast cleaned reinforcing.

1. Under bond fatigue loading in a working stress range, the slip behavior of the mill scale, epoxy coated and blast cleaned bars is essentially similar.
2. First cycle differences in loaded end slip, where epoxy coated bar slip was greater than mill scale bar slip, often diminished somewhat as the number of cycles increased.
3. The bond strength of epoxy coated bars in comparison to mill scale bars is not adversely affected by up to 1.4 million cycles of loading in a working stress range. The relative difference based upon both flexural bond pullout strength and slip criteria was actually slightly less after the cyclic loadings.

7. CONCLUSIONS AND RECOMMENDATIONS

7.1 Conclusions

A. For specimens and loadings representative of concrete bridge deck slabs, the following comparative conclusions can be made between mill scale and epoxy coated reinforcing:

1. No difference was found in terms of crack spacing for the short span specimens.
2. At working stress levels and even up to yield of the reinforcement, little difference was noted in terms of deflection or crack widths. Deflection and crack widths of the epoxy coated bar specimens may have been slightly but not significantly larger.
3. At post yield load levels, the epoxy coated bar specimens exhibited greater deflection and larger crack widths.
4. The mill scale bar specimens failed at a load level averaging 4% higher than the epoxy coated bar specimens.

B. The following conclusions can be made based upon comparative flexural bond static tests of mill scale, epoxy coated and blast cleaned reinforcing.

1. Epoxy coated reinforcing has less slip resistance than normal mill scale reinforcing. Bond strength based on critical slip for the mill scale bars averaged 32% greater than for epoxy coated bars. For development lengths greater than 12 in., mill scale bar critical slip strength was 15% greater than for epoxy coated bars.

2. Epoxy coated reinforcing has less bond strength than mill scale reinforcing. The mill scale bars had 17% greater flexural bond pullout strength.
3. Bond splitting cracks initiated at lower loads in the epoxy coated bar specimens.
4. The comparative performance of the No. 11 bars paralleled the comparative performance of the No. 6 bars. There does not appear to be a size factor unique to epoxy coated bars.
5. Epoxy coated No. 6 bars with 8 in. embedment lengths had much higher slip ratios than encountered in other specimens with longer embedments. However, the flexural bond pullout strength ratios were similar to both pullout strength and critical slip ratios of other sets of specimens.
6. Bond of the blast cleaned bars was generally somewhat lower than the mill scale and somewhat greater than the epoxy coated bars.
7. For the particular specimens tested, the epoxy coated bars attained stress levels compatible with current ACI and AASHTO development requirements.

C. The following conclusions can be made based upon comparative bond fatigue tests of mill scale, epoxy coated and blast cleaned reinforcing.

1. Under bond fatigue loading in a working stress range, the slip behavior of the mill scale, epoxy coated and blast cleaned bars is essentially similar.

2. First cycle differences in loaded end slip, where epoxy coated bar slip was greater than mill scale bar slip, often diminished somewhat as the number of cycles increased.
3. The bond strength of epoxy coated bars in comparison to mill scale bars is not adversely affected by up to 1.4 million cycles of loading in a working stress range. The relative difference based upon both flexural bond pullout strength and slip criteria was actually slightly less after the cyclic loadings.

7.2 Recommendations

In order to provide comparable performance with mill scale bars, a basic development length modification factor of 1.15 is proposed for epoxy coated bars. This recommendation is based upon three considerations.

1. The weighted average of the flexural bond pullout strength ratios was 4 comparisons at 1.17 from the BS Series tests plus one at 1.15 and one at 1.07 from the BF Series tests or $[(4 \times 1.17) + 1.15 + 1.07]/6 = 1.15$.
2. In the BS Series tests, critical bond strength ratios based upon loaded end and free end slips averaged 1.32 overall and 1.15 excluding specimens with less than 12 in. embedment. In the BF Series tests, critical bond strength ratios based upon free end slip averaged 1.17 overall and 1.12 excluding specimens with less than 12 in. embedment.

3. For coating acceptance, ASTM A 775-81 requires that the mean critical bond strength of epoxy coated bars based upon slip criteria shall not be less than 80% of the mean critical strength of uncoated (mill scale) bars. This 0.80 ratio, when inverted, would imply a mean upper bound critical bond strength ratio of 1.25.

8. RECOMMENDATIONS FOR FURTHER RESEARCH

This research has enabled recommendations to be developed based upon the scope of the tests undertaken. However, during the course of the study, many questions arose which were beyond the scope but still in need of answers. The following is a list of questions related to bond of epoxy coated reinforcement that need attention.

1. What is the bond behavior of epoxy coated bars under low-cycle/high-stress loadings typical of earthquakes.
2. What is the influence of field touch-up coatings (which are sometimes of significant thickness) on bond performance of epoxy coated bars.
3. What is actual field practice on touching up cut ends of epoxy coated bars and how does the thicker end coating influence anchorage of the bars.
4. For specimens with lower moment gradients and larger shear span to depth ratios, what is the influence of epoxy coated reinforcement on crack width and crack spacing.
5. What is the bond performance of epoxy coated and mill scale bars in conjunction with high strength concrete.
6. What is the bond performance of epoxy coated and mill scale bars in concrete with high slumps or with superplasticizer admixtures.
7. What is the influence of early loading on bond performance of epoxy coated and mill scale bars.

Obtaining answers to these questions would be highly desirable considering the increasing use of epoxy coated reinforcement in a variety of applications.

9. REFERENCES

1. Clifton, Jr., H. F. Beeghly and R. G. Mathey, "Nonmetallic Coatings for Concrete Reinforcing Bars," National Bureau of Standards, FHWA-RD-74-18, NTIS Catalog No. PB 236 424, Feb. 1974.

2. Mathey, R. G., and J. R. Clifton, "Bond of Coated Reinforcing Bars in Concrete," Journal of the Structural Division, ASCE, Vol. 102, No. ST 1, Proc. Paper 11855, Jan., 1976, pp. 215-229.

3. Clifton, J. R., R. G. Mathey and E. D. Anderson, "Creep of Coated Reinforcing Bars in Concrete," Journal of the Structural Division, ASCE, Vol. 105, No. ST10, Proc. Paper 14911, Oct. 1979, pp. 1935-1947.

4. Clifton, J. R., H. F. Beeghly and R. G. Mathey, "Protecting Reinforcing Bars from Corrosion with Epoxy Coatings," Corrosion of Metals in Concrete, ACI SP 49-10, pp. 115-133.

5. Hawkins, N. M., "Fatigue Design Considerations for Reinforcement in Concrete Bridge Decks," Journal of the American Concrete Institute, Vol. 73, No. 2, Feb. 1976, pp. 104-115.

6. "Standard Specification for Epoxy-Coated Reinforcing Bars," ASTM Designation: A 775-81, American Society for Testing and Materials, Philadelphia, 1981.

7. ACI Committee 318, "Building Code Requirements for Reinforced Concrete," ACI Standard 318-77, American Concrete Institute, Detroit, 1977.

8. Standard Specifications for Highway Bridges, 12th ed., American Association of State Highway and Transportation Officials, Washington, D. C., 1977.

9. ACI Committee 408, "Suggested Development, Splice and Standard Hook Provisions for Deformed Bars in Tension," Concrete International, Vol. 1, No. 7, July, 1979, pp. 44-46.

10. Jirsa, J. O., L. A. Lutz and P. Gergely, "Rationale for Suggested Development, Splice and Standard Hook Provisions for Deformed Bars in Tension," Concrete International, Vol. 1, No. 7, July 1979, pp. 47-61.

11. ACI Committee 215, "Considerations for Design of Concrete Structures Subjected to Fatigue Loading," Journal of the American Concrete Institute, Vol. 71, No. 3, March 1974, pp. 97-121.

12. Hawkins, N. M., "Fatigue Characteristics in Bond and Shear of Reinforced Concrete Beams," Abeles Symposium: Fatigue of Concrete, ACI SP-41-10, 1974, pp. 203-221.

13. Kemp, E. L. and W. J. Wilhelm, "An Investigation of the Parameters Influencing Bond Behavior with a View Towards Establishing Design Criteria," Department of Civil Engineering, West Virginia Univ., Report WVaDH 46-2, Nov., 1977.

14. U. S. Bureau of Reclamation, A Manual for the Control of Concrete Construction, U. S. Department of Interior, Bureau of Reclamation, 6th Ed., 1956.

15. Kemp, E. L., F. S. Brezny and J. A. Unterspan, "Effect of Rust and Scale on the Bond Characteristics of Deformed Reinforcing Bars," Journal of the American Concrete Institute, Vol. 65, No. 9, Sept. 1968, pp. 743-756.

16. Jirsa, J. O., and J. E. Breen, "Influence of Casting Position and Shear on Development and Splice Length - Design Recommendations," Center for Transportation Research, The University of Texas at Austin, Res. Report 242-3F, November 1981.

10. APPENDIX

Photographs of Tested Specimens

After test of each specimen, photographs were taken of the three principal faces where cracking occurred. The three views were assembled into a composite developed surface, as illustrated graphically in Figure 10.1 for the slab specimens and Figure 10.2 for the beam end specimens. The orientation of the photographs was maintained in all cases to be consistent with the loading arrangements shown in Figures 10.1 and 10.2.

Photographs of the slab specimens are shown in Figure 10.3 through 10.8. To facilitate comparison, the mill scale bar specimens are arbitrarily paired with epoxy coated bar specimens based upon the specimen letter designation. Only the 4 foot section between supports is shown in the photograph. The lines at the edges of the photographs indicate the centerlines of the supports. A gridwork of lines at 2 inch centers (drawn on the top surface before testing) as well as the Whittemore gage points are visible in the photographs. In the case of the slabs, the cracks appear without any additional marking.

Photographs of the beam end specimens are shown in Figures 10.9 through 10.48. To facilitate comparison, the mill scale bar specimens are paired with the companion epoxy coated bar specimens. To aid visibility, the crack edges are marked with ink. The bar tension load increment (kips) at which each crack became visible is marked adjacent to the crack. For reference, yield occurred at approximately 28 kips (63.6 ksi) for the #6 bar specimens and at approximately 98 kips (63.0 ksi) for the #11 bar specimens.

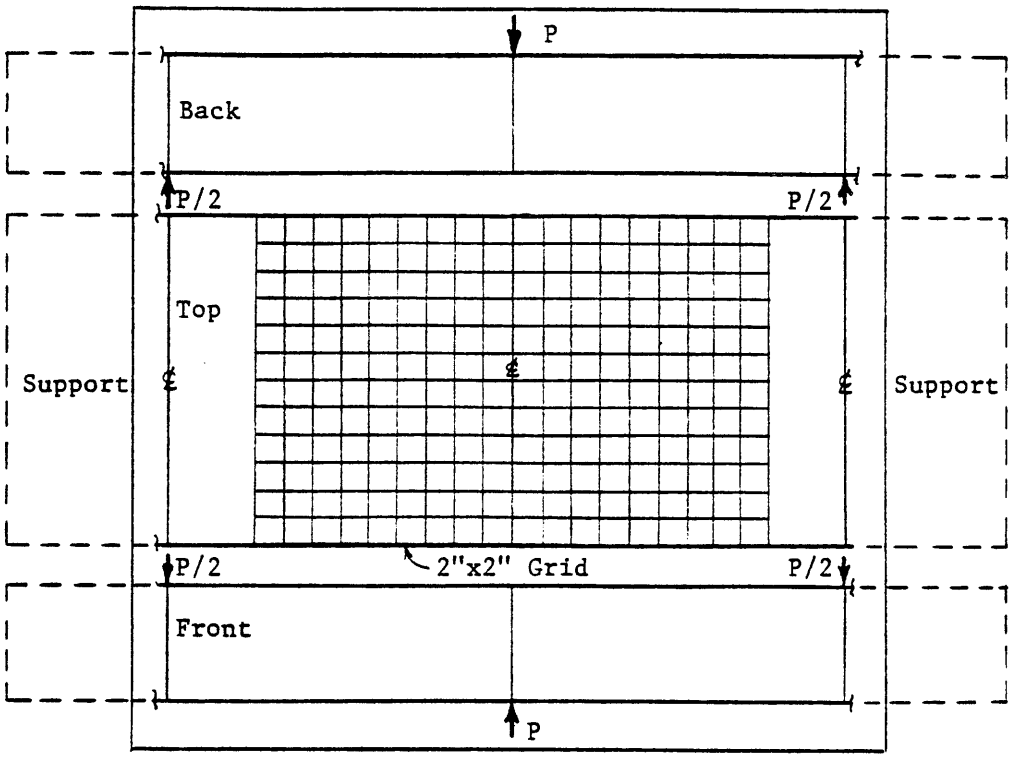

Figure 10.1 Developed Surface of Slab Specimens.

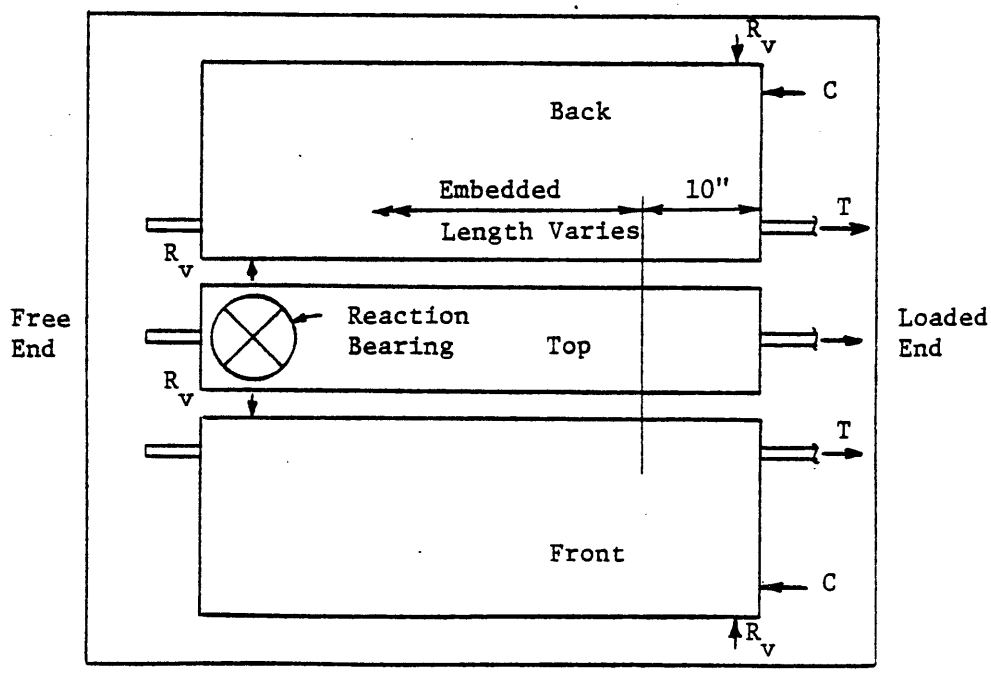

Figure 10.2 Developed Surface of Beam End Specimens.

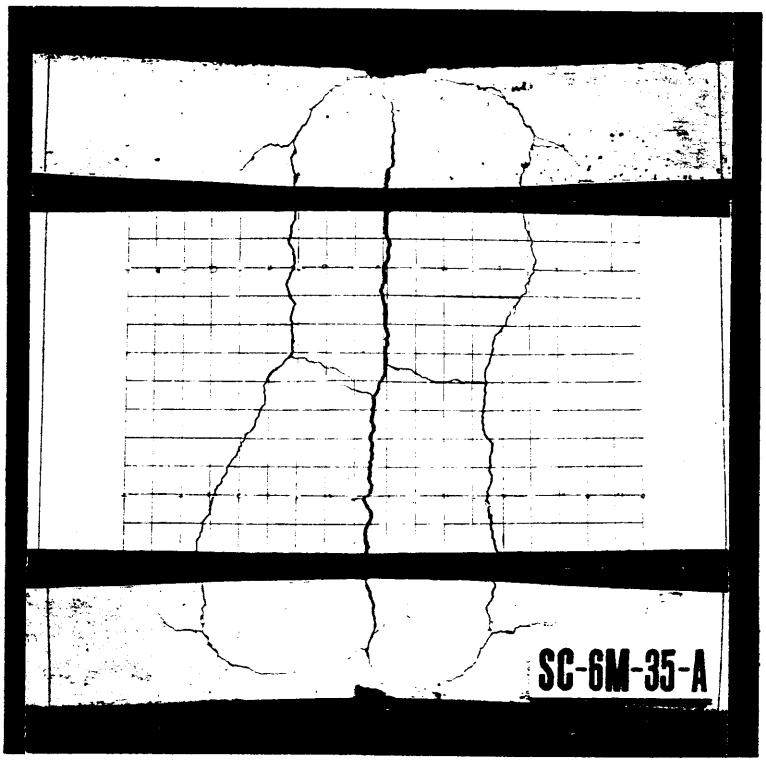

Figure 10.3 Specimen SC-6M-35-A after Test

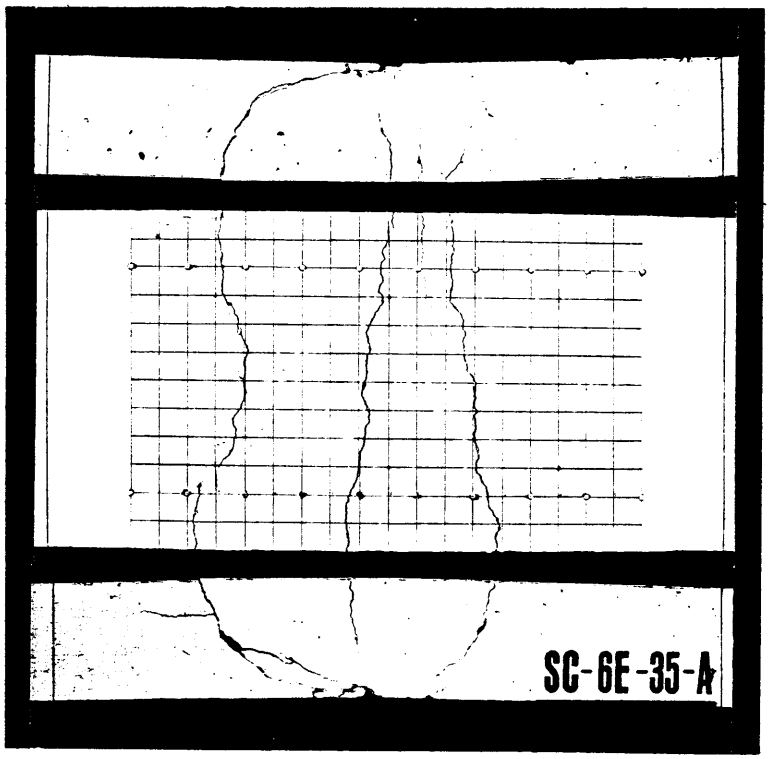

Figure 10.4 Specimen SC-6E-35-A after Test

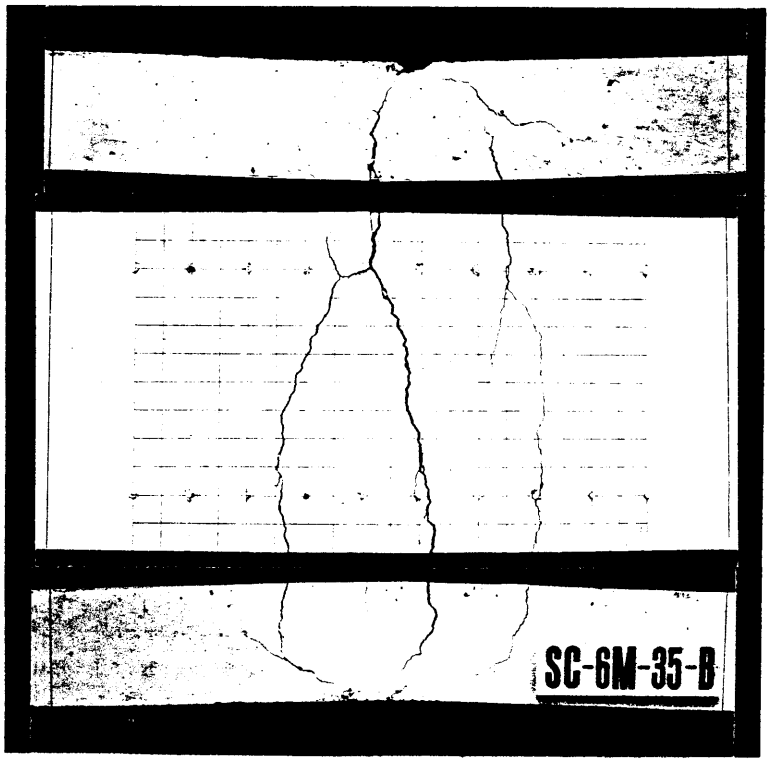

Figure 10.5 Specimen SC-6M-35-B after Test

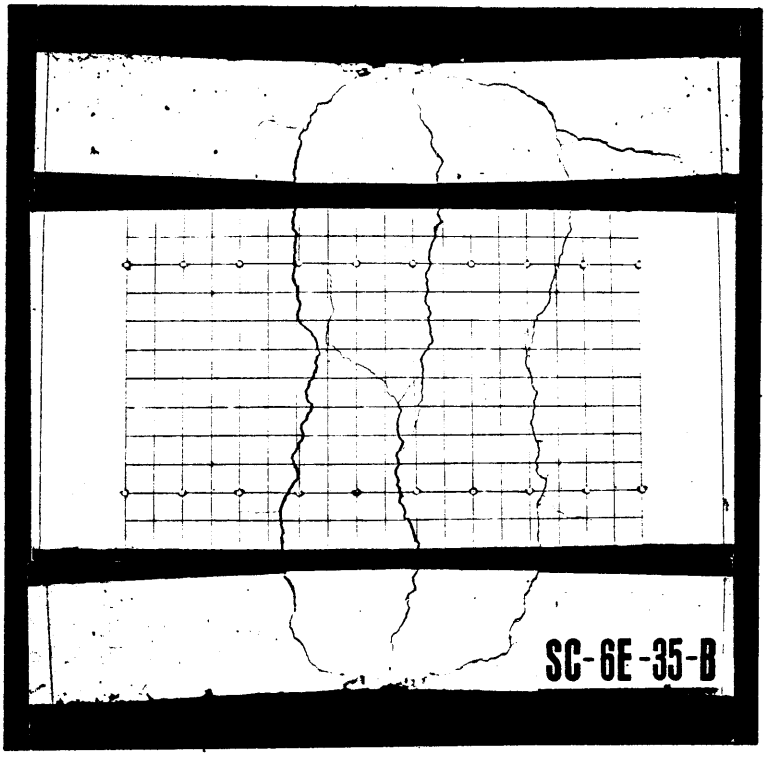

Figure 10.6 Specimen SC 6E-35-B after Test

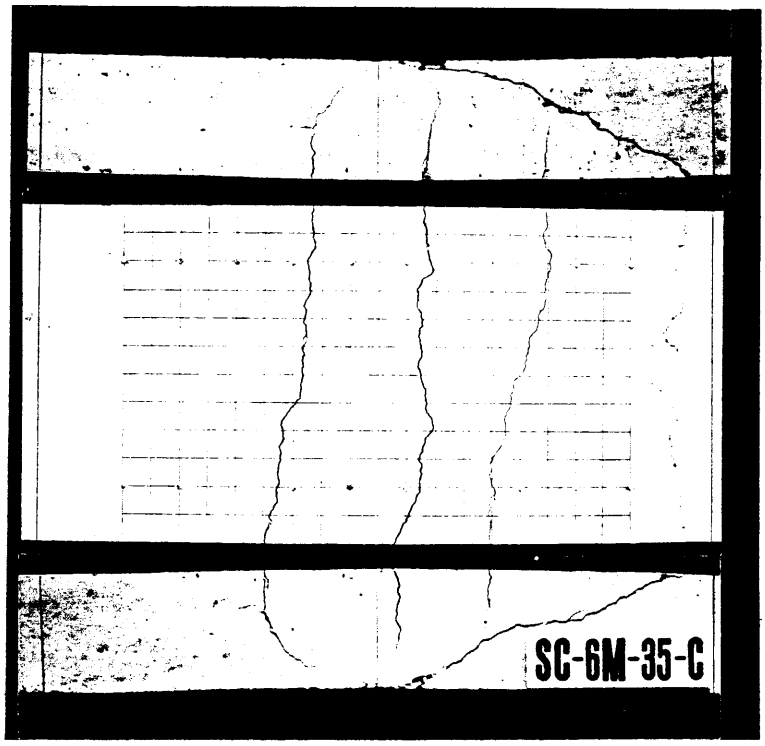

Figure 10.7 Specimen SC-6M-35-C after Test

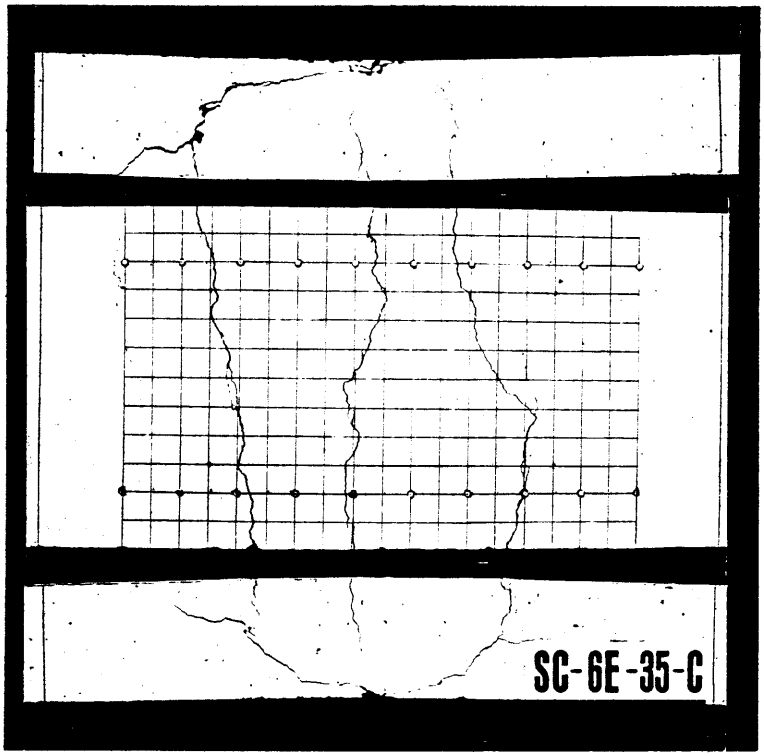

Figure 10.8 Specimen SC-6E-35-C after Test

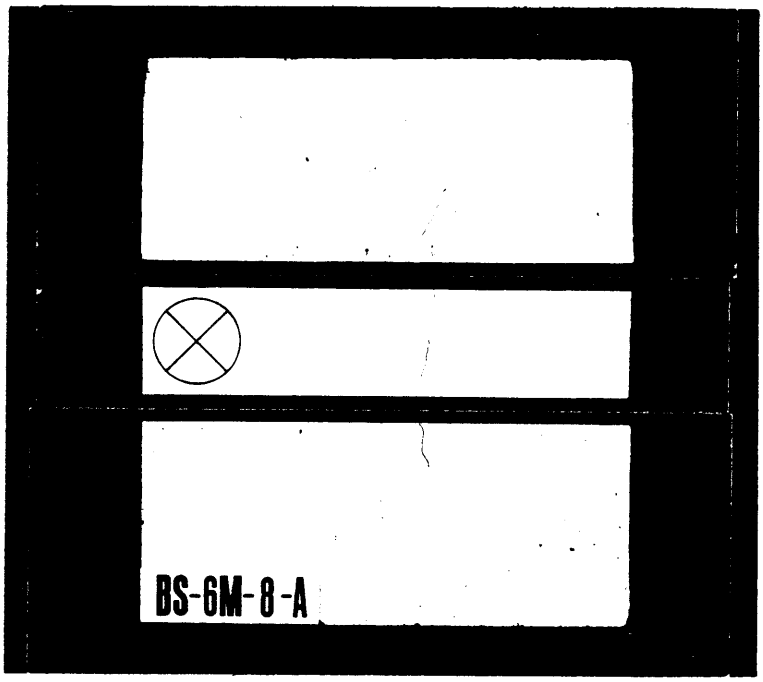

Figure 10.9 Specimen BS-6M-8-A after Test

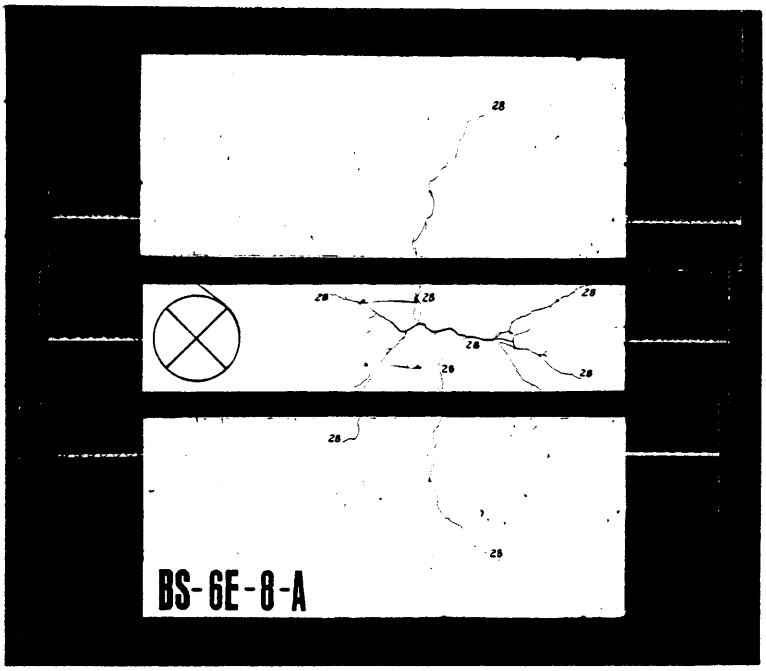

Figure 10.10 Specimen BS-6E-8-A after Test

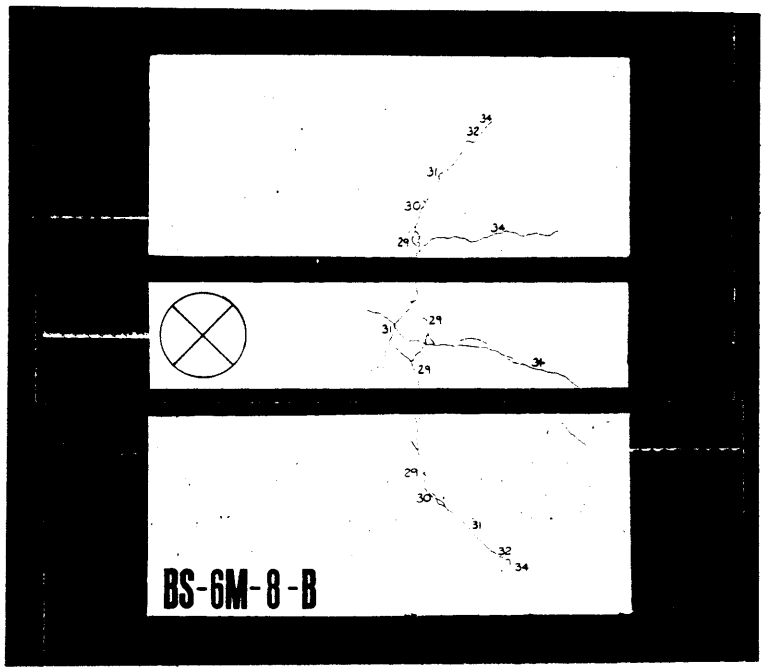

Figure 10.11 Specimen BS-6M-8-B after Test

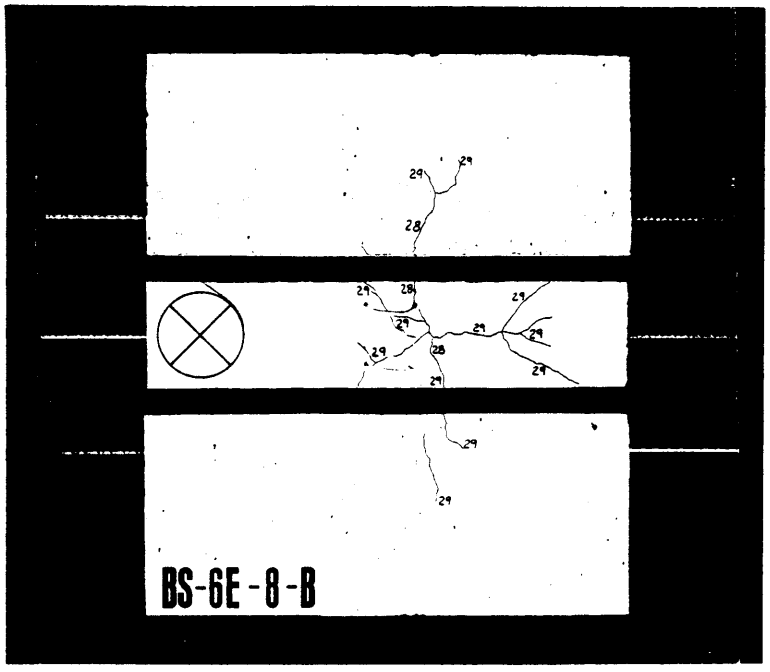

Figure 10.12 Specimen BS-6E-8-B after Test

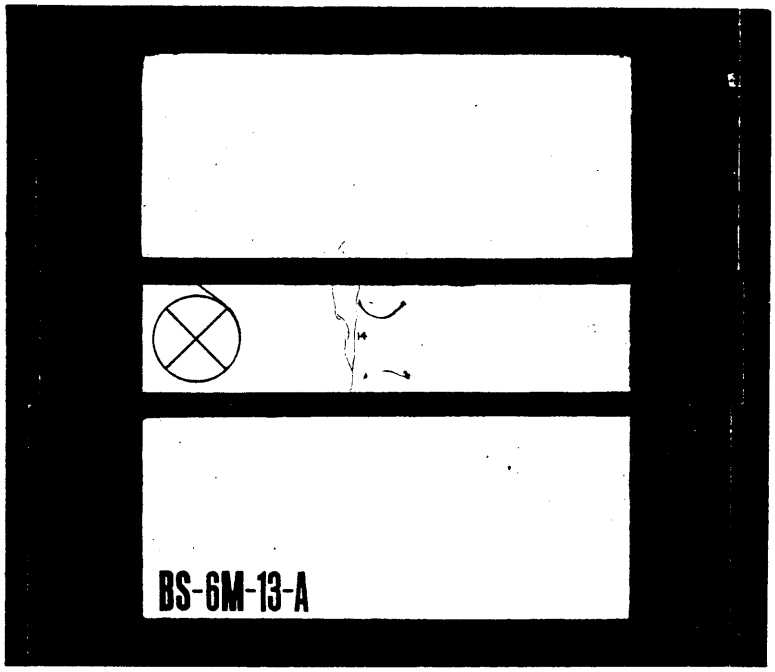

Figure 10.13 Specimen BS-6M-13-A after Test

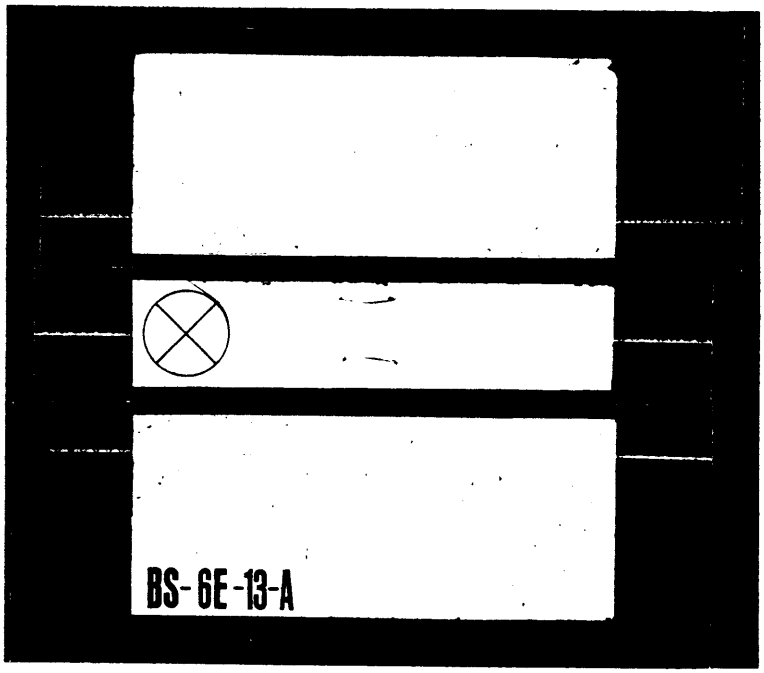

Figure 10.14 Specimen BS-6E-13-A after Test

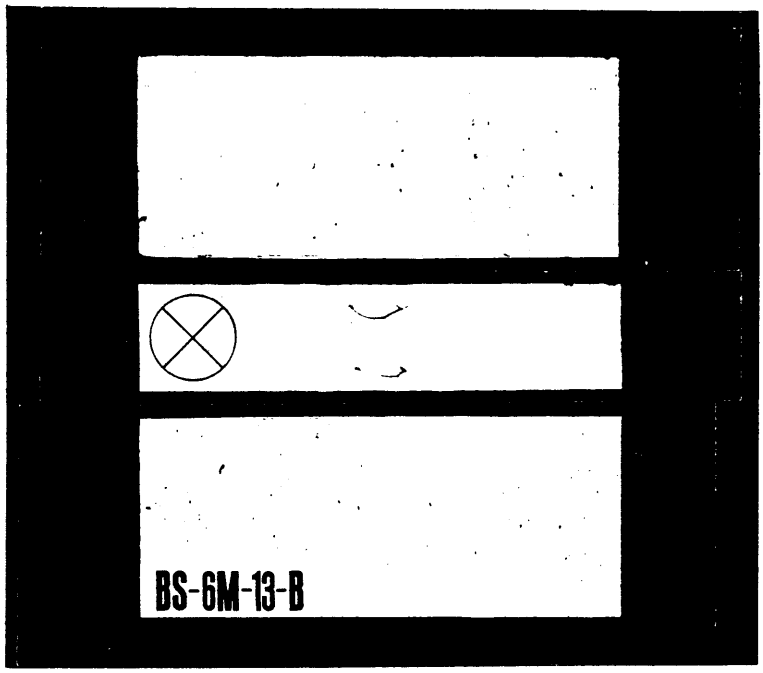

Figure 10.15 Specimen BS-6M-13-B after Test

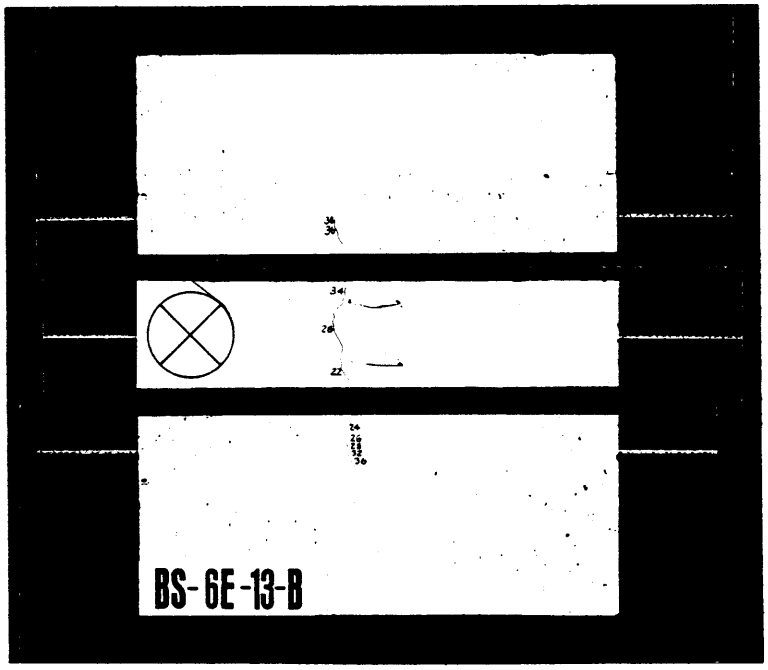

Figure 10.16 Specimen BS-6E-13-B after Test

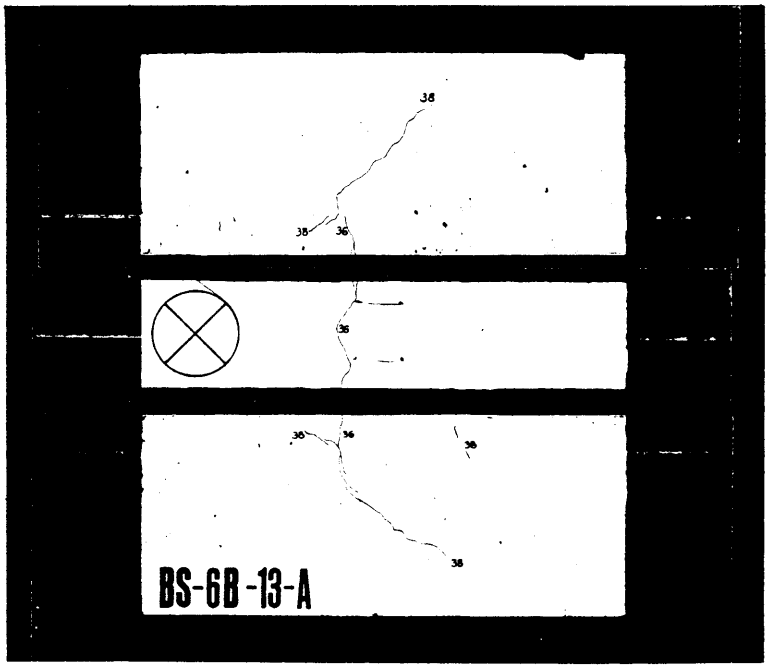

Figure 10.17 Specimen BS-6B-13-A after Test

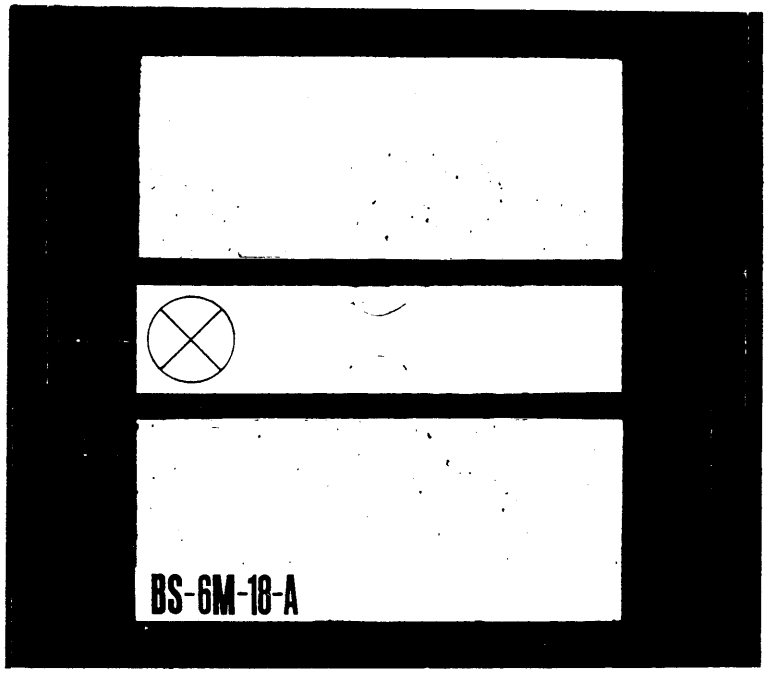

Figure 10.18 Specimen BS-6M-18-A after Test

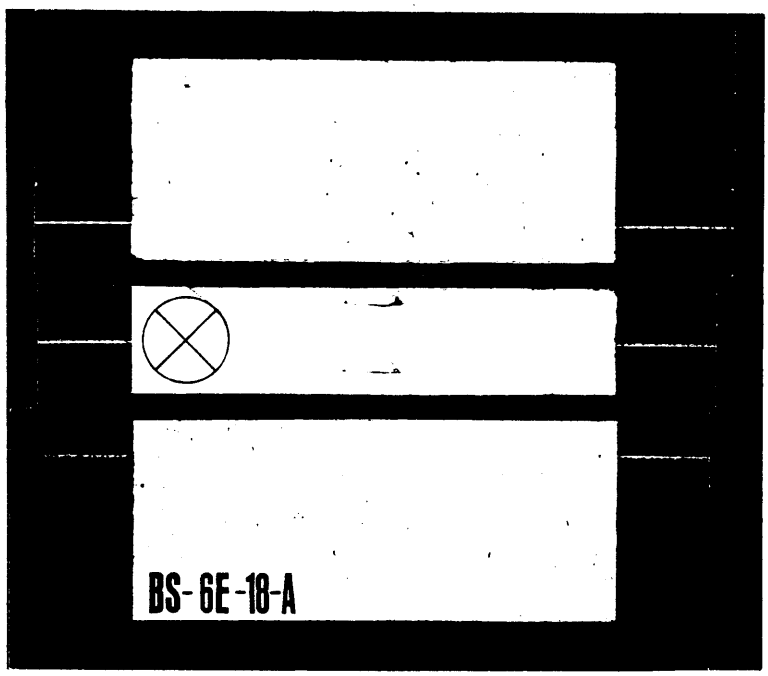

Figure 10.19 Specimen BS-6E-18-A after Test

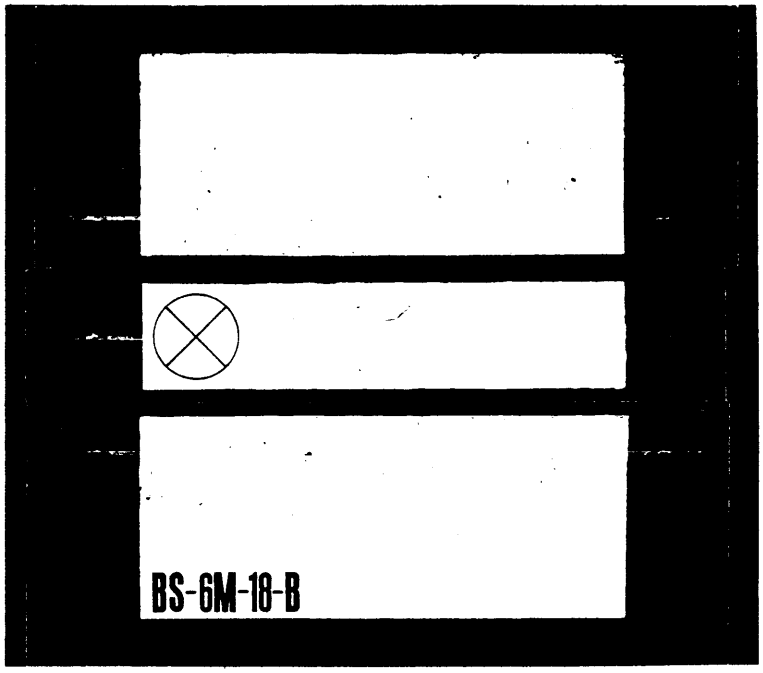

Figure 10.20 Specimen BS-6M-18-B after Test

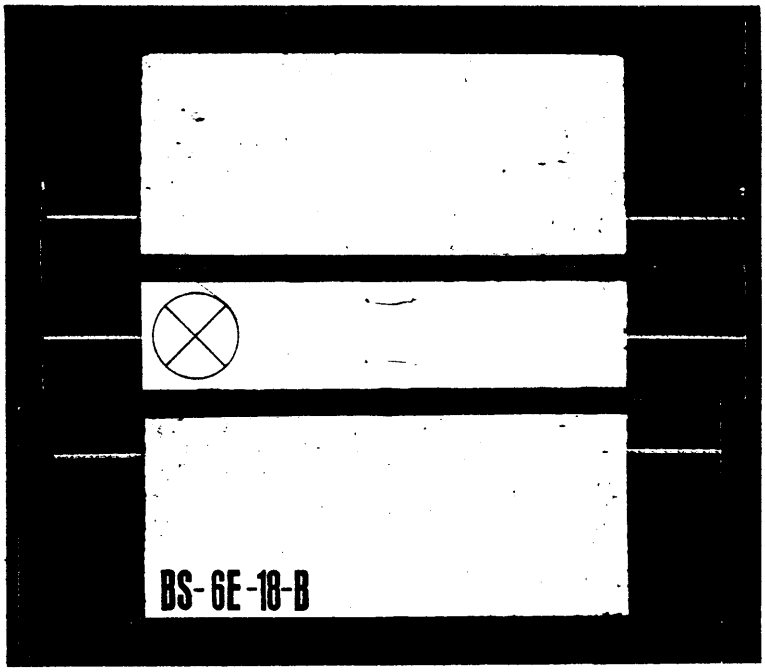

Figure 10.21 Specimen BS-6E-18-B after Test

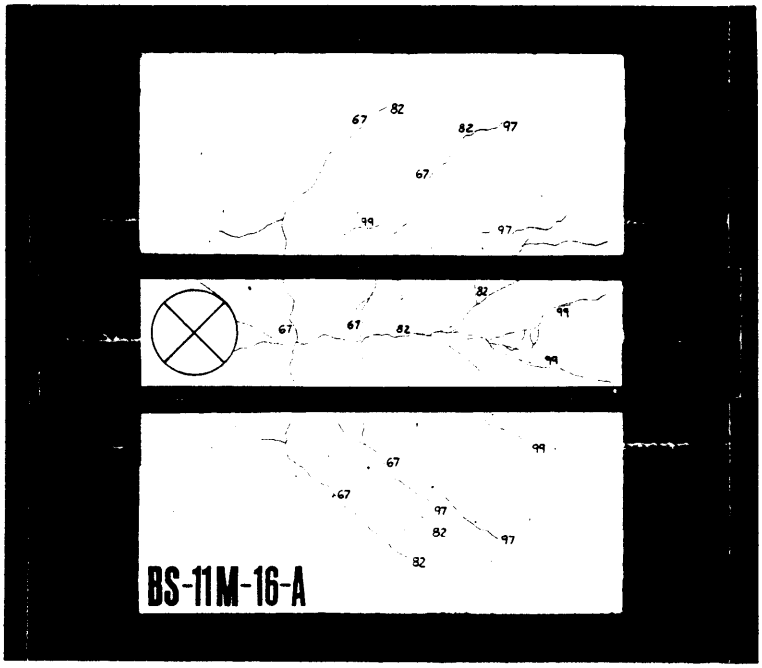

Figure 10.22 Specimen BS-11M-16-A after Test

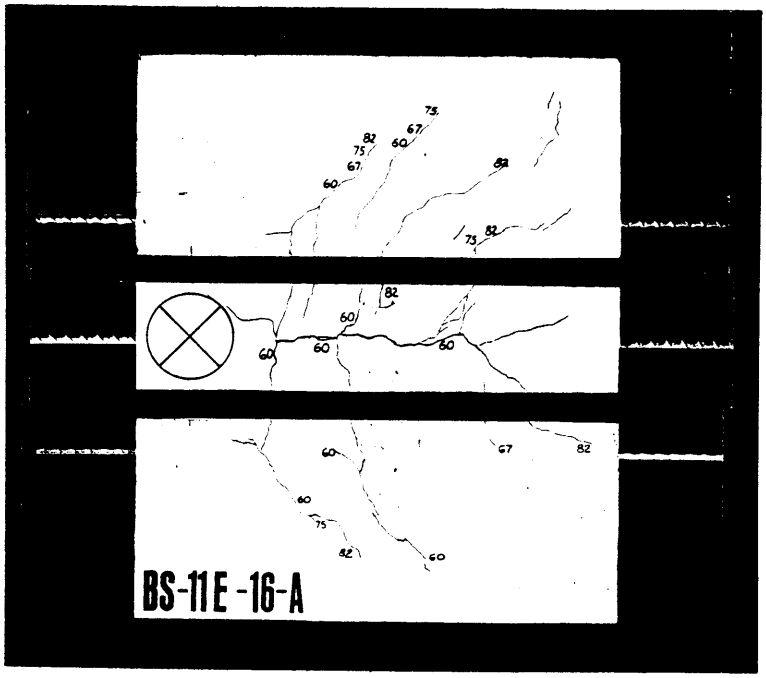

Figure 10.23 Specimen BS-11E-16-A after Test

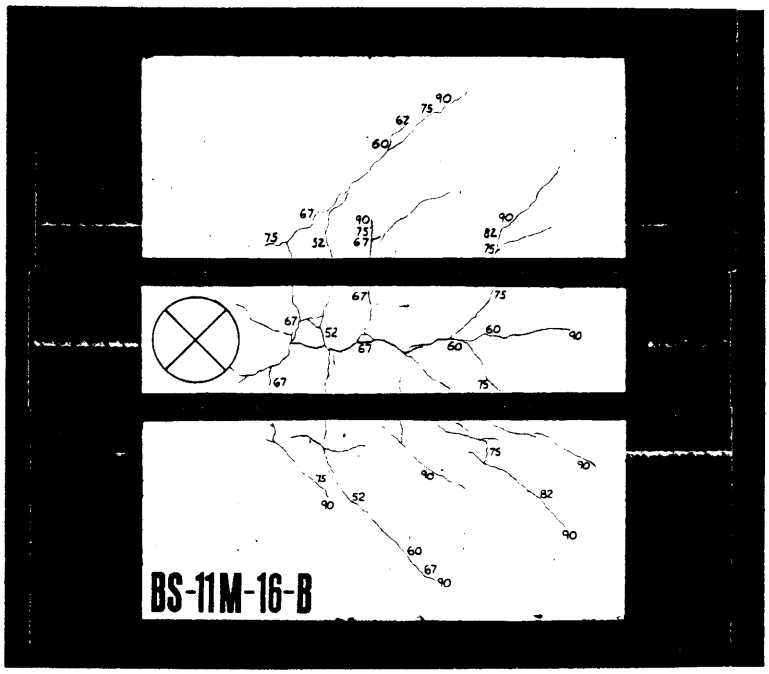

Figure 10.24 Specimen BS-11M-16-B after Test

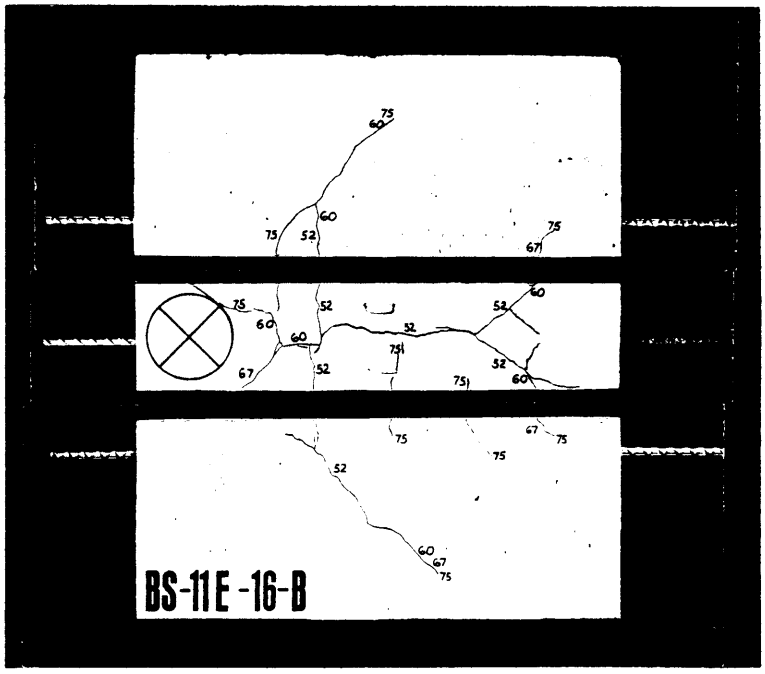

Figure 10.25 Specimen BS-11E-16-B after Test

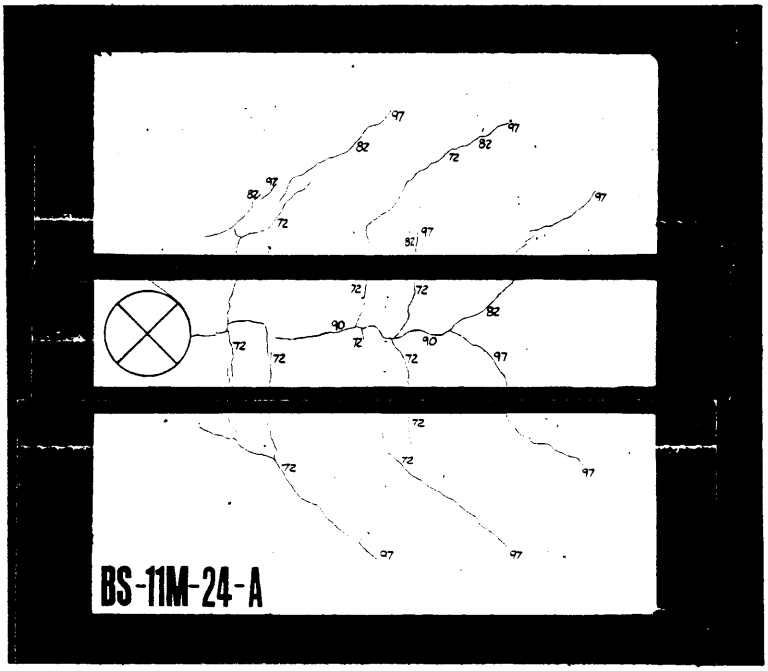

Figure 10.26 Specimen BS-11M-24-A after Test

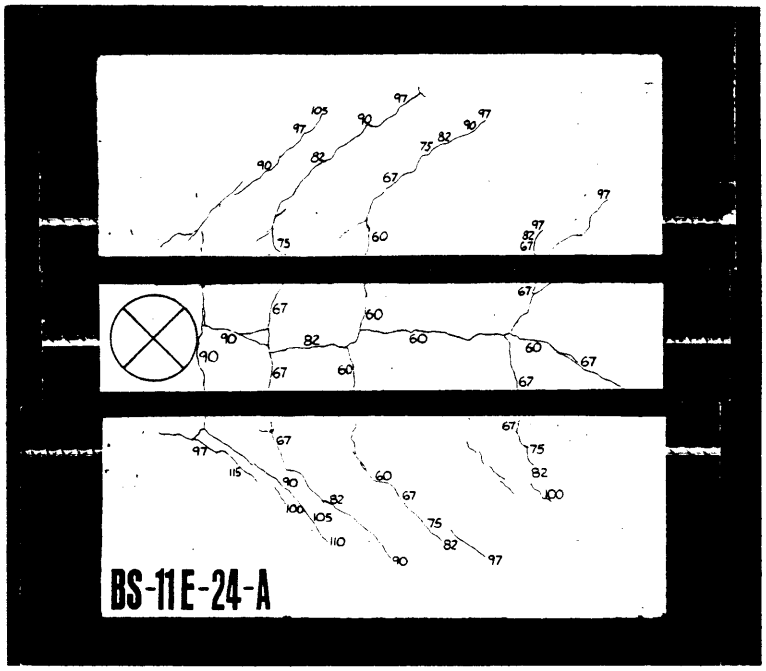

Figure 10.27 Specimen BS-11E-24-A after Test

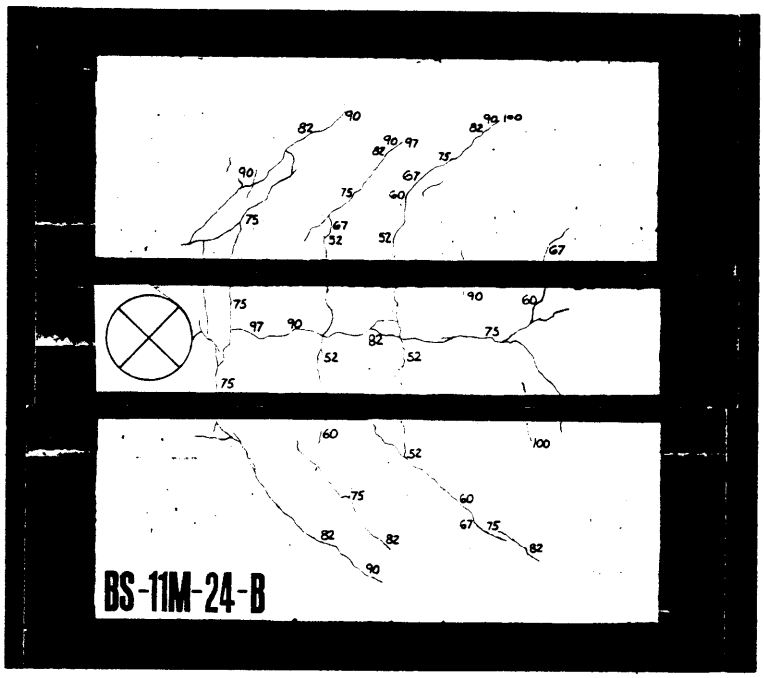

Figure 10.28 Specimen BS-11M-24-B after Test

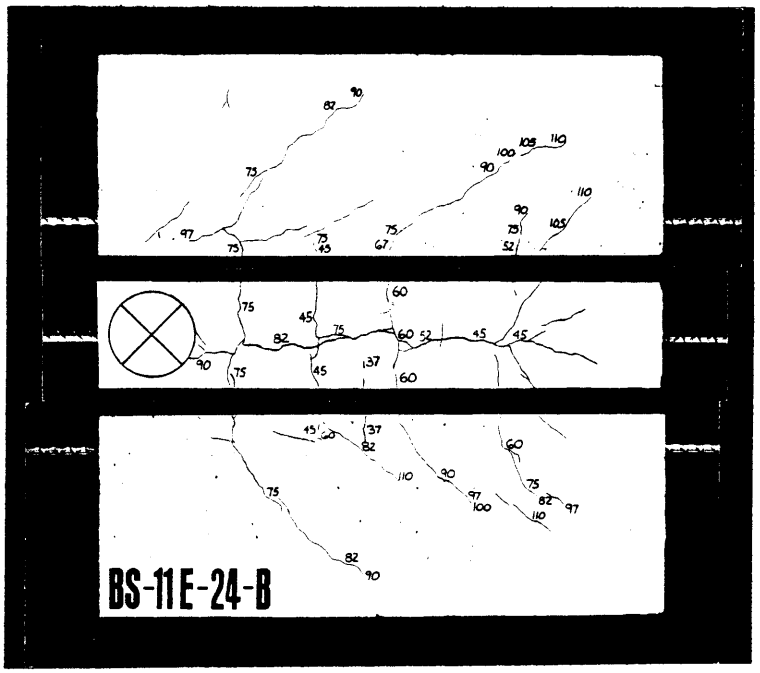

Figure 10.29 Specimen BS-11E-24-B after Test

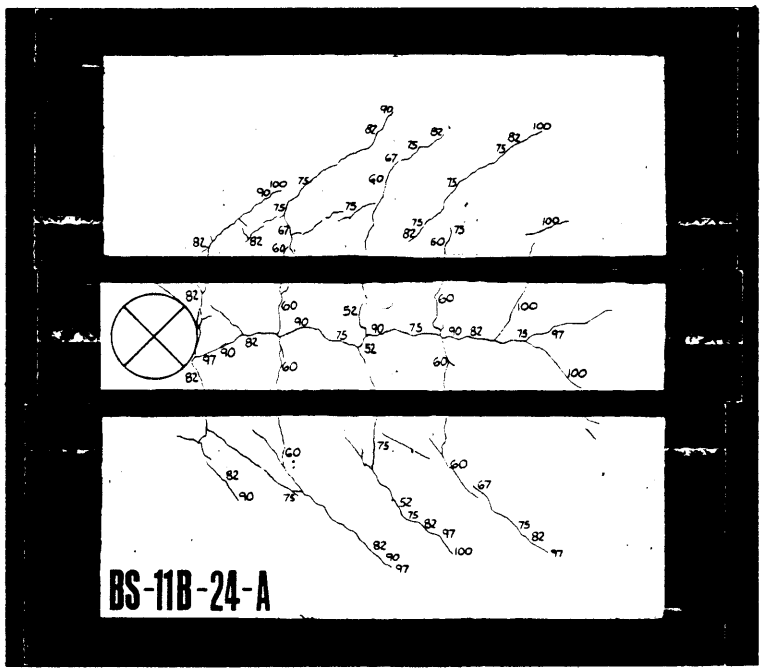

Figure 10.30 Specimen BS-11B-24-A after Test

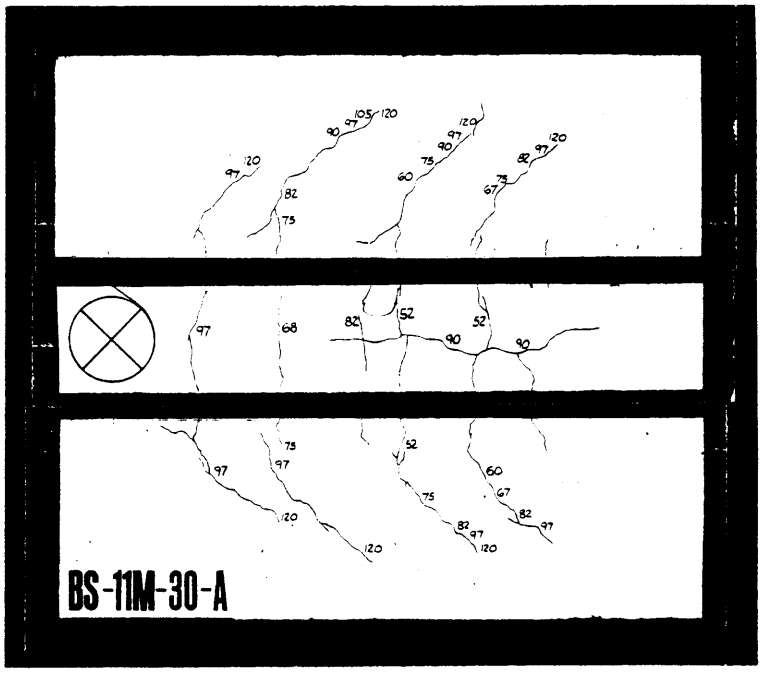

Figure 10.31 Specimen BS-11M-30-A after Test

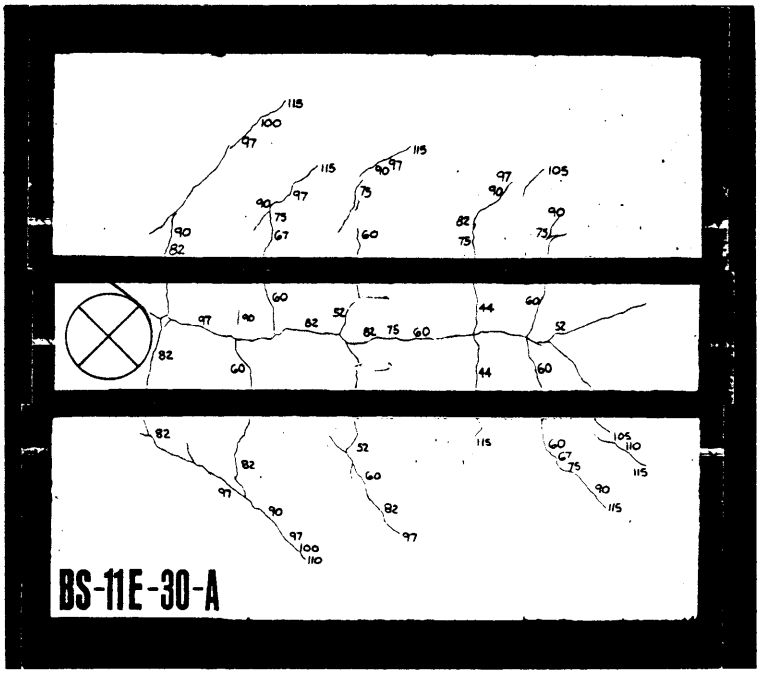

Figure 10.32 Specimen BS-11E-30-A after Test

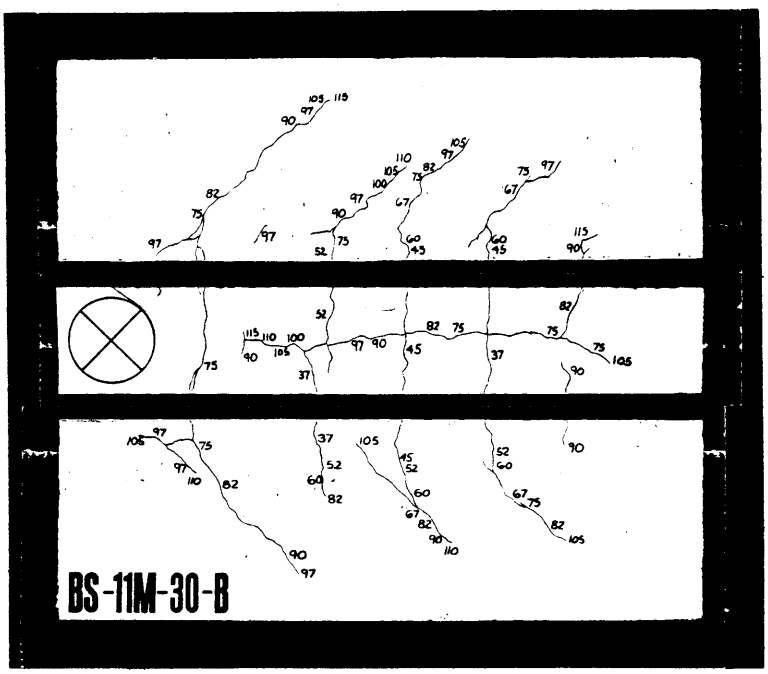

Figure 10.33 Specimen BS-11M-30-B after Test

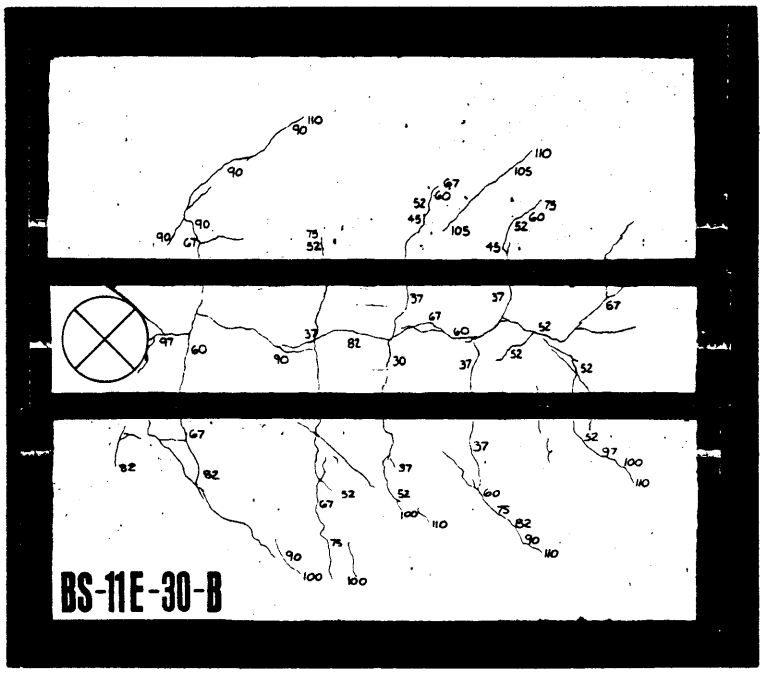

Figure 10.34 Specimen BS-11E-30-B after Test

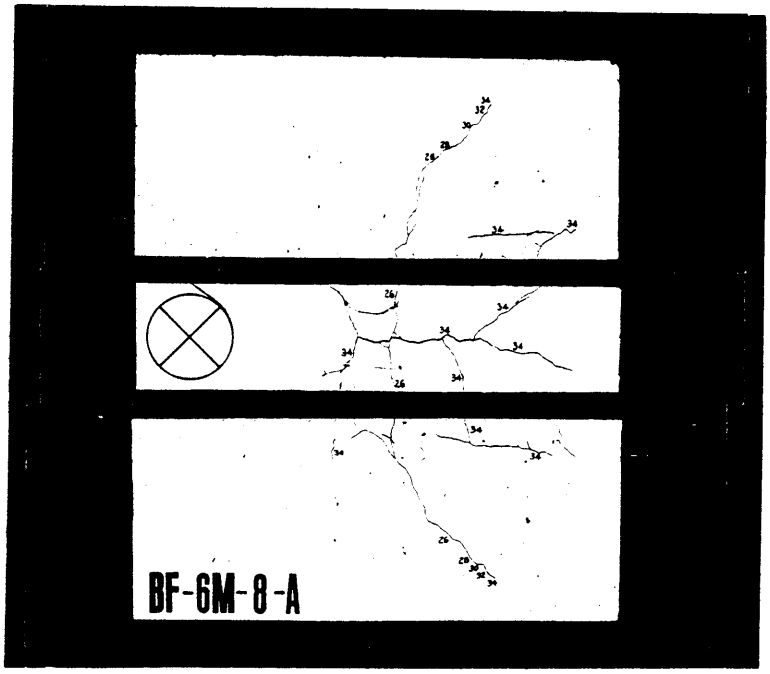

Figure 10.35 Specimen BF-6M-8-A after Test

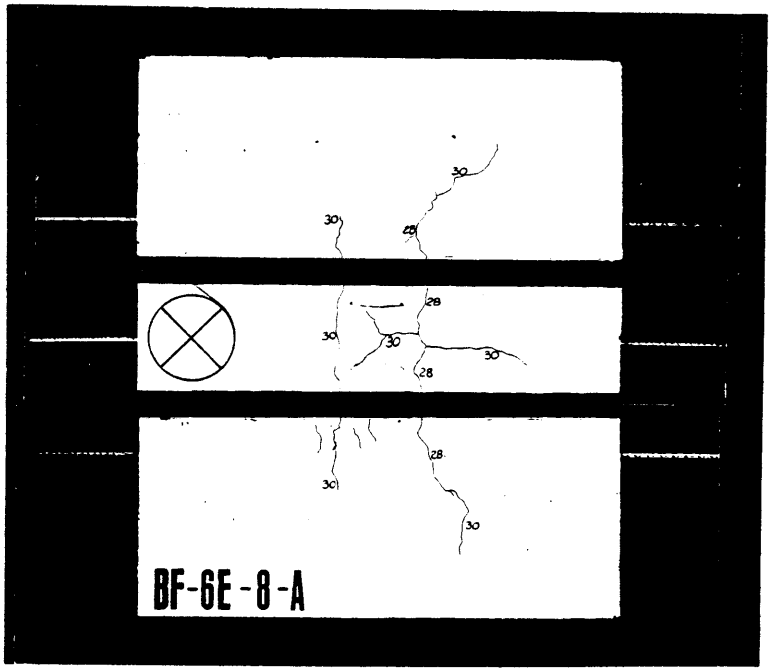

Figure 10.36 Specimen BF-6E-8-A after Test

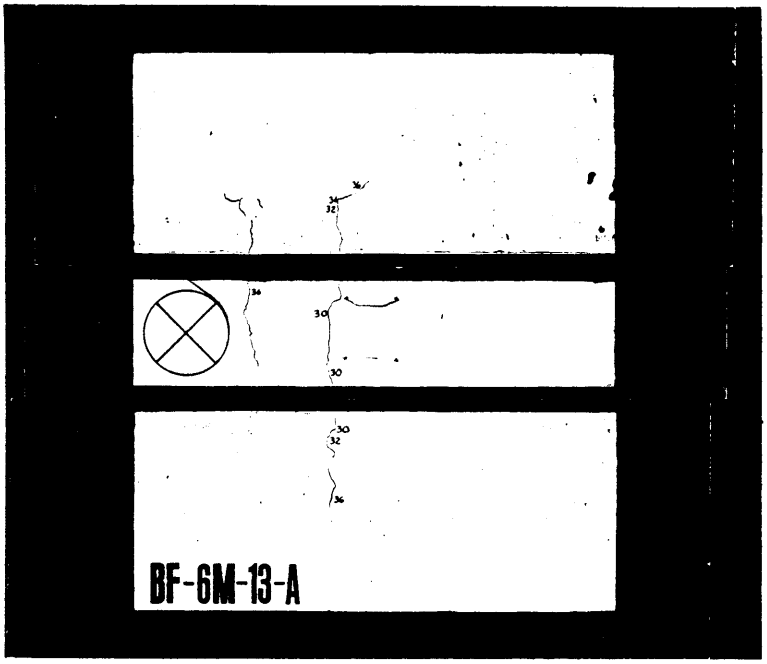

Figure 10.37 Specimen BF-6M-13-A after Test

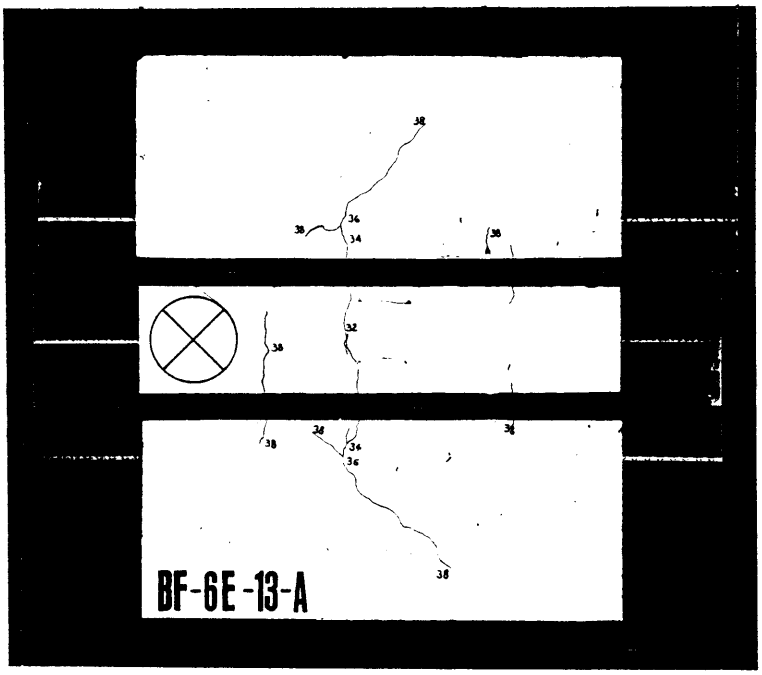

Figure 10.38 Specimen BF-6E-13-A after Test

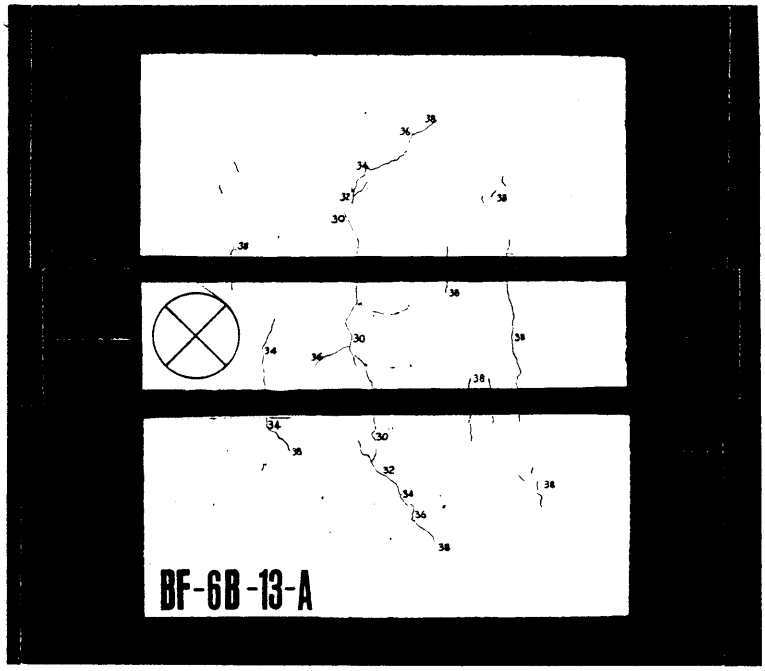

Figure 10.39 Specimen BF-6B-13-A after Test

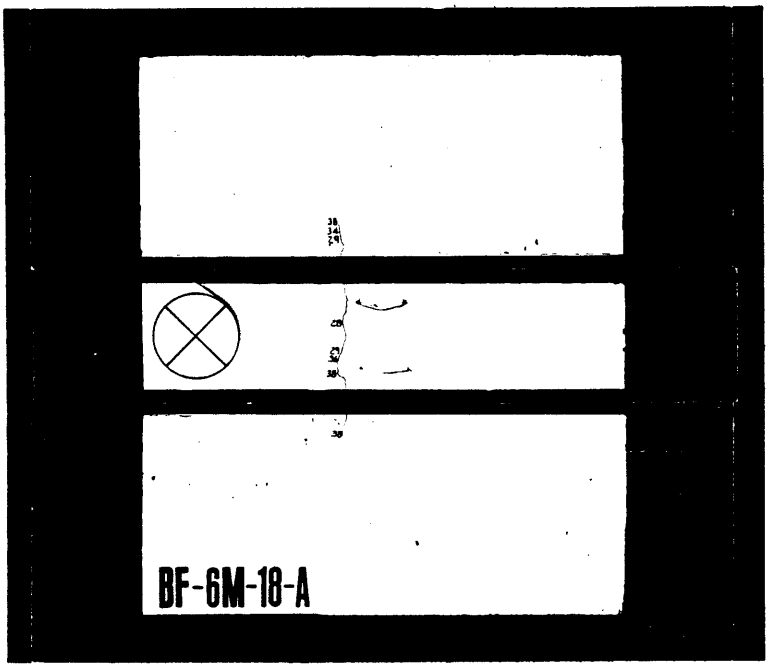

Figure 10.40 Specimen BF-6M-18-A after Test

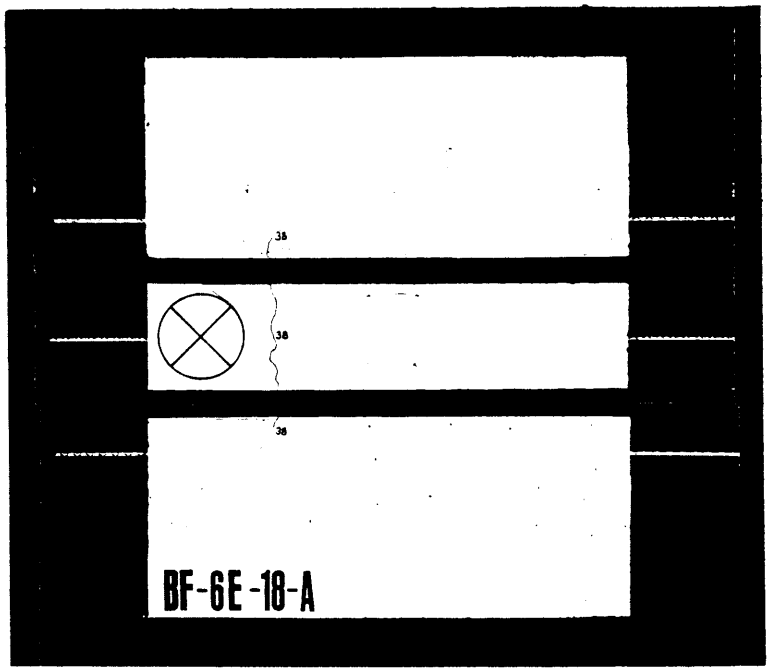

Figure 10.41 Specimen BF-6E-18-A after Test

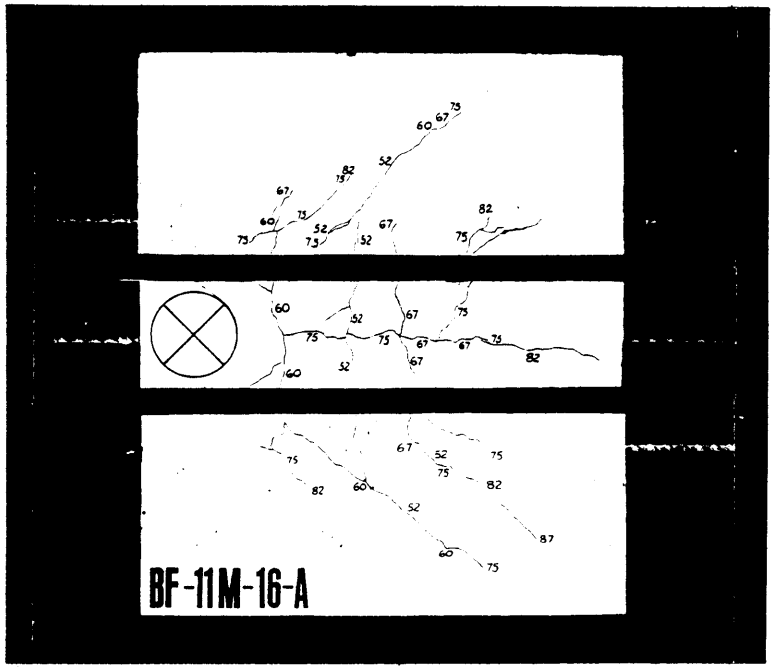

Figure 10.42 Specimen BF-11M-16-A after Test

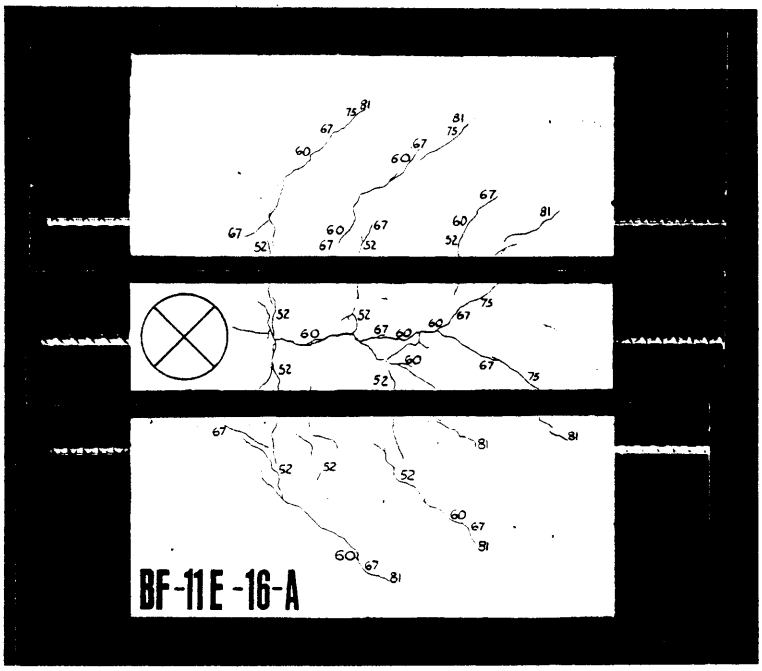

Figure 10.43 Specimen BF-11E-16-A after Test

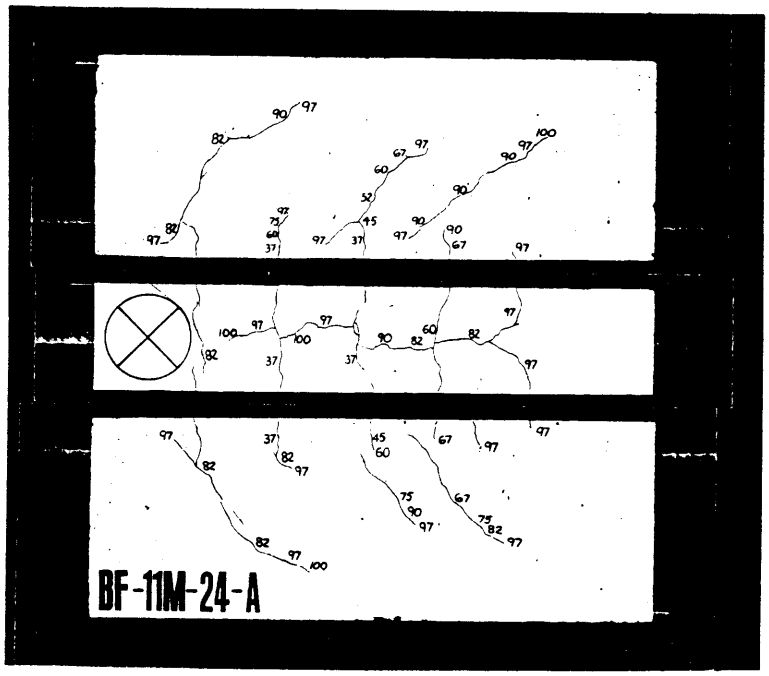

Figure 10.44 Specimen BF-11M-24-A after Test

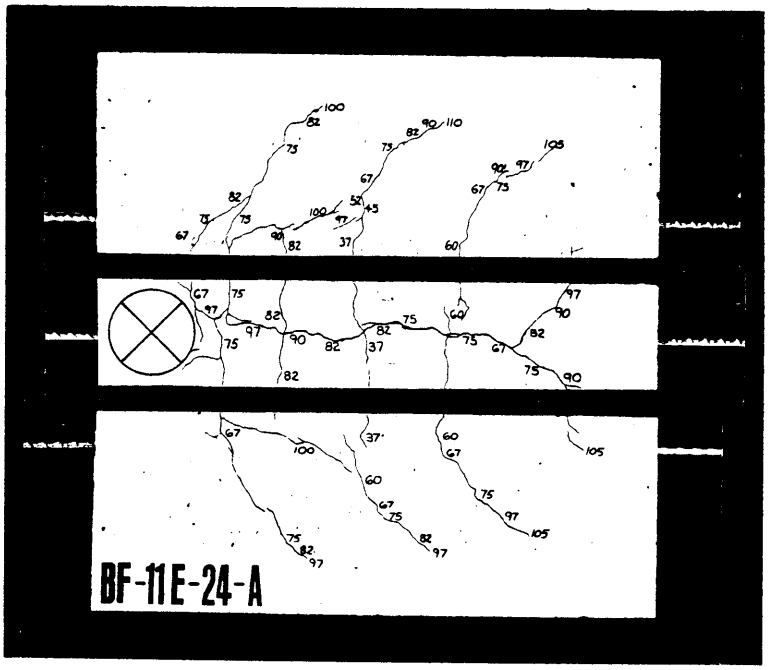

Figure 10.45 Specimen BF-11E-24-A after Test

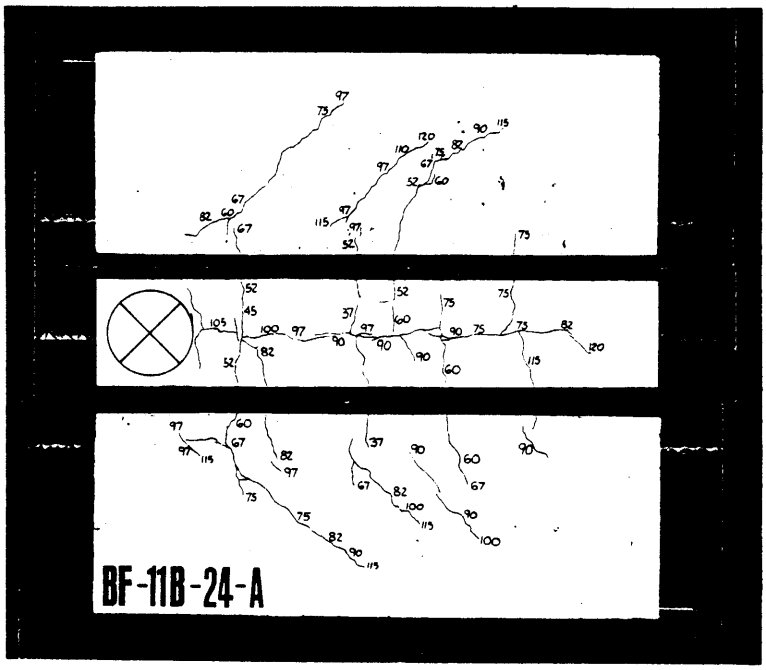

Figure 10.46 Specimen BF-11B-24-A after Test

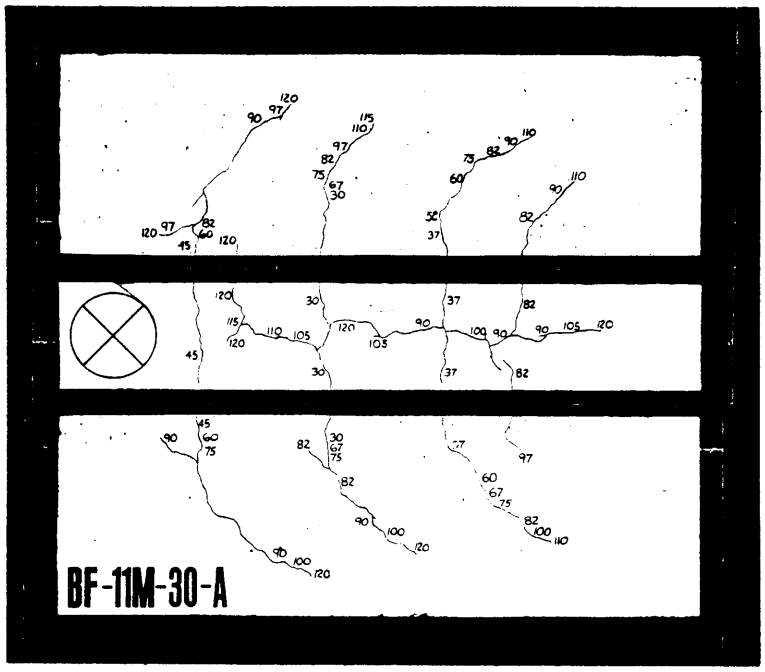

Figure 10.47 Specimen BF-11M-30-A after Test

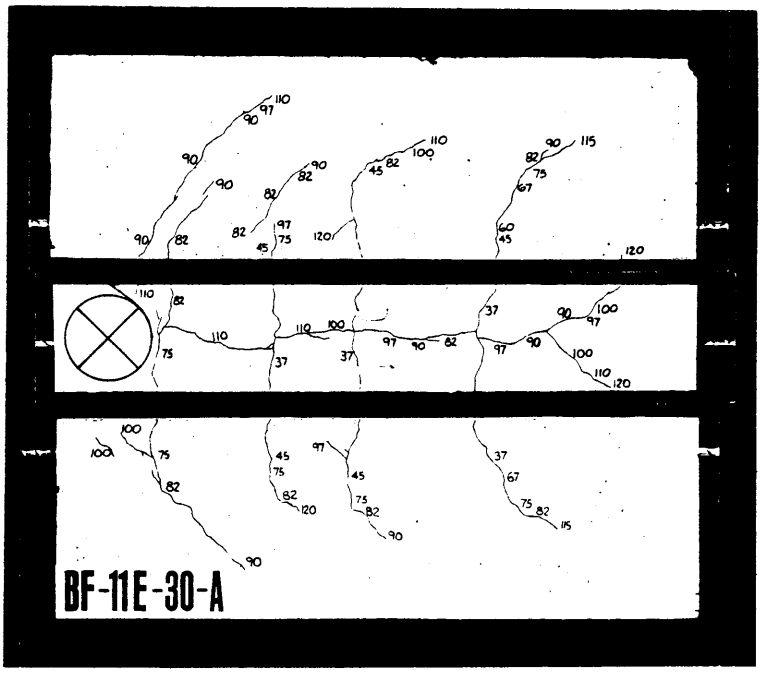

Figure 10.48 Specimen BF-11E-30-A after Test